AERMOD DESCRIPTION OF MODEL FORMULATION

draft document

Version: 98314 (AERMOD & AERMET)
98022 (AERMAP)
(December 15, 1998)

By:

Alan J. Cimorelli,	U. S. Environmental Protection Agency, Region 3
Steven G. Perry[1],	Atmospheric Sciences Modeling Division/Air Resources Laboratory/NOAA, MD-80, USEPA
Akula Venkatram,	College of Engineering, University of California at Riverside
Jeffrey C. Weil,	Cooperative Institute for Research in Environmental Sciences, University of Colorado
Robert J. Paine,	ENSR Corporation
Robert B. Wilson,	U. S. Environmental Protection Agency, Region 10
Russell F. Lee,	Trinity Consultants
Warren D. Peters,	U.S. Environmental Protection Agency, OAQPS

[1]On assignment to the Atmospheric Research and Exposure Assessment Laboratory, U. S. Environmental Protection Agency.

ACKNOWLEDGMENTS

The authors wish to recognize the insightfulness, and diligence of Mr. Roger Brode and Mr. James Paumier, of Pacific Environmental Services Inc., in transforming our ideas into the reality that is AERMOD. This project was made possible through the continued support of Mr. Joe Tikvart, of EPA's Office of Air Quality Planning and Standards (OAQPS), and Mr. Frank Schiermeier, of NOAA's Atmospheric Sciences Modeling Division. The authors are particularly grateful to Dr. Gary Briggs, and Mr. John Irwin, of NOAA's Atmospheric Sciences Modeling Division, for their thorough and constructive review of an earlier version of this document. Finally, we would like to thank the many scientists who participated in peer reviews and beta testing.

TABLE OF CONTENTS

ACKNOWLEDGMENTS 2

1 **Introduction** 6
1.1 *Background* 6
1.2 The AERMIC Focus: A Replacement for the ISC Model 7
1.3 *Model Development Process* 8
1.4 *Purpose of Document* 9

2 **Model Overview** 10

3 **Meteorological Preprocessor (AERMET)** 12
3.1 *Derived Parameters in the CBL* 13
3.1.1 SENSIBLE HEAT FLUX (H) IN THE CBL 13
3.1.2 FRICTION VELOCITY (u_*) & MONIN OBUKHOV LENGTH (L) IN THE CBL 15
3.1.3 CONVECTIVE MIXING HEIGHT (z_{ic}) 17
3.1.4 CONVECTIVE VELOCITY SCALE (w_*) 17
3.1.5 MECHANICAL MIXING HEIGHT (z_{im}) IN THE CBL 18
3.2 *Derived Parameters in the SBL* 20
3.2.1 FRICTION VELOCITY (u_*) IN THE SBL 20
3.2.2 SENSIBLE HEAT FLUX (H) IN THE SBL 22
3.2.3 MONIN OBUKHOV LENGTH (L) IN THE SBL 23
3.2.4 MECHANICAL MIXING HEIGHT (z_{im}) IN THE SBL 23

4 **AERMOD's Meteorological Interface** 24
4.1 *General Profiling Equations* 25
4.1.1 WIND SPEED PROFILING IN THE INTERFACE 25
4.1.2 WIND DIRECTION PROFILES IN INTERFACE 27
4.1.3 PROFILES OF THE POTENTIAL TEMPERATURE GRADIENT IN THE INTERFACE 27
4.1.4 POTENTIAL TEMPERATURE PROFILING IN THE INTERFACE 31
4.1.5 VERTICAL TURBULENCE CALCULATED BY THE INTERFACE 31
4.1.6 LATERAL TURBULENCE CALCULATED BY THE INTERFACE 36
4.2 *Vertical Inhomogeneity in the Boundary Layer* as Treated by the INTERFACE . . . 40

5 **The Terrain Preprocessor (AERMAP)** 45

6 **The AMS/EPA Regulatory Model AERMOD** 50
6.1 *General Structure of AERMOD Including Terrain* 50
6.2 *AERMOD Concentration Predictions in the CBL* 55
6.2.1 DIRECT SOURCE CONTRIBUTION TO CONCENTRATION

CALCULATIONS IN THE CBL 61
6.2.2 INDIRECT SOURCE CONTRIBUTION TO CONCENTRATION CALCULATIONS IN THE CBL 64
6.2.3 PENETRATED SOURCE CONTRIBUTION TO CONCENTRATION CALCULATIONS IN THE CBL 65
6.3 *Concentrations in the SBL Calculated by AERMOD* 66
6.4 *Estimation of Dispersion Coefficients* 69
6.4.1 AMBIENT TURBULENCE FOR USE IN CALCULATING DISPERSION . . . 71
6.4.2 BUOYANCY INDUCED DISPERSION (BID) COMPONENT OF σ_y AND σ_z 76
6.4.3 COMPONENT OF DISPERSION COEFFICIENTS DUE TO DOWNWASH 78
6.5 *Plume Rise* Calculations in AERMOD 81
6.5.1 PLUME RISE IN THE CBL 82
6.5.2 PLUME RISE IN THE SBL 83
6.6 *Source Characterization* 86
6.7 *Adjustments for the Urban Boundary Layer* 87

7 **List of Symbols** 91

8 **APPENDIX: Input / Output Needs and Data Usage** 97
8.1 *AERMET Input Data Needs* 97
8.1.1 METEOROLOGY 97
8.1.2 DIRECTIONALLY AND/OR MONTHLY VARYING SURFACE CHARACTERISTICS 97
8.1.3 OTHER 97
8.1.4 OPTIONAL 98
8.2 *Estimation of solar insolation for small solar elevation angles* 98
8.3 *Selection and Use of Measured Winds, Temperature and Turbulence in AERMET* 98
8.3.1 THRESHOLD WIND SPEED 98
8.3.2 REFERENCE TEMPERATURE AND HEIGHT 98
8.3.3 REFERENCE WIND SPEED AND HEIGHT 98
8.3.4 CALCULATING *THE POTENTIAL TEMPERATURE GRADIENT* ABOVE THE MIXING HEIGHT FROM SOUNDING DATA 99
8.3.5 MEASURED TURBULENCE 99
8.3.6 DATA SUBSTITUTION FOR MISSING ON-SITE DATA 99
8.4 *Information Passed by AERMET to AERMOD* 100
8.5 *Restrictions on the Growth of PBL Height* 100
8.6 *Initializing the Mechanical Mixing Height Smoothing Procedure* 100
8.7 *Determining The Mixing Height When the Sounding Is Too Shallow* 100
8.8 *Input Data Needs for AERMAP* 101
8.9 *Information Passed by AERMAP to AERMOD* 101

8.10 *Wind Speed & Turbulence Limits Used in Model Calculations* 101
8.11 *Using Profiles for Interpolating Between Observations* 102
8.12 *Using Measured Mixing Heights* 104

9 **References** 105

1 **Introduction**

1.1 *Background*

In 1991, the **A**merican **M**eteorological **S**ociety (AMS) and the U.S. **E**nvironmental **P**rotection **A**gency (EPA) initiated a formal collaboration with the designed goal of introducing current planetary boundary layer (PBL) concepts into regulatory dispersion models. A working group (**A**MS/**E**PA **R**egulatory **M**odel **I**mprovement **C**ommittee, **AERMIC**) comprised of AMS and EPA scientists was formed for this collaborative effort. The authors of this document are all members of AERMIC.

In most air quality applications, one is concerned with dispersion in the PBL, the turbulent air layer next to the earth's surface that is controlled by the surface heating and friction and the overlying stratification. The PBL typically ranges from a few hundred meters in depth at night to 1 - 2 km during the day. Major developments in understanding the PBL began in the 1970's through numerical modeling, field observations, and laboratory simulations; see Wyngaard (1988) for a summary. For the convective boundary layer (CBL), a milestone was Deardorff's (1972) numerical simulations which revealed the CBL's vertical structure and important turbulence scales. Major insights into dispersion followed from laboratory experiments, numerical simulations, and field observations (e.g., see Briggs, 1988; Lamb, 1982; Weil, 1988a for reviews). For the stable boundary layer (SBL), advancements occurred more slowly. However, a sound theoretical/experimental framework for surface layer dispersion and approaches for elevated sources existed by the mid 1980's (e.g., see Briggs, 1988; Venkatram, 1988).

During the mid 1980's, researchers began to apply this information to simple dispersion models for applications. This consisted of eddy-diffusion techniques for surface releases, statistical theory and PBL scaling for dispersion parameter estimation, a new probability density function (PDF) approach for the CBL, simple techniques for obtaining meteorological variables (e.g., surface heat flux) needed for turbulence parameterizations, etc. Much of this work was reviewed and promoted in workshops (Weil, 1985), revised texts (Pasquill and Smith, 1983), and in short courses and monographs (Nieuwstadt and van Dop, 1982; Venkatram and Wyngaard, 1988). By the mid 1980's, new applied dispersion models based on this technology had been developed including PPSP (Weil and Brower, 1984), OML (Berkowicz et al., 1986), HPDM (Hanna and Paine, 1989), TUPOS (Turner et al., 1986), CTDMPLUS (Perry et al., 1989); later, ADMS developed in the United Kingdom (see Carruthers et al., 1992) was added as well as SCIPUFF (Sykes et al., 1996). AERMIC members were involved in the development of three of these models - PPSP, CTDMPLUS and HPDM.

By the mid-to-late 1980's, a substantial scientific base on the PBL and new dispersion approaches existed for revamping regulatory dispersion models, but this did not occur. In a review of existing or proposed regulatory models developed prior to 1984, Smith (1984) reported that the techniques were many years behind the state-of-the-art and yielded predictions that did not agree

well with observations. Similar findings were reported by Hayes and Moore (1986), who summarized 15 model evaluation studies. The need for a comprehensive overhaul of EPA's basic regulatory models was clearly recognized. This need including a summary of background information and recommendations was the focus of an AMS/EPA Workshop on Updating Applied Diffusion Models held 24-27 January 1984 in Clearwater, Florida (see Weil (1985) and other review papers in the November 1985 issue of the Journal of Climate and Applied Meteorology).

In February 1991, the U.S. EPA in conjunction with the AMS held a workshop for state and EPA regional meteorologists on the parameterization of PBL turbulence and state-of-the-art dispersion modeling. One of the outcomes of the workshop was the formation of AERMIC. As noted above, the expressed purpose of the AERMIC activity was to build upon the earlier model developments and to provide a state-of-the-art dispersion model for regulatory applications. The early efforts of the AERMIC group are described by Weil (1992). In going through the design process and in considering the nature of present regulatory models, AERMIC's goal expanded from its early form. In addition to improved parameterization of PBL turbulence, other problems such as plume interaction with terrain, surface releases, and urban dispersion were recognized as needing attention.

The new model developed by AERMIC is aimed at short-range dispersion from stationary industrial sources, the same scenario currently handled by the EPA Industrial Source Complex (ISC) Model, ISC3 (U.S. EPA, 1995). This work clearly has benefitted from the model development activities of the1980's especially in the parameterization of mean winds and PBL turbulence, dispersion in the CBL, and the treatment of plume/terrain interactions. Techniques used in the new model for PBL parameterizations and CBL dispersion are similar to those used in earlier models. Turbulence characterization in the CBL adopts "convective scaling" as suggested by Deardorff (1972) and included in most of the models mentioned above - PPSP, OML, HPDM, etc. Algorithms used in these earlier models were considered along with variants and improvements to them. In addition, the developers of OML met with AERMIC to discuss their experiences. Thus, much credit for the AERMIC model development is to be given to the pioneering efforts of the 1980s.

1.2 The AERMIC Focus: A Replacement for the ISC Model

AERMIC's initial focus has been on the regulatory models that are designed for estimating near-field impacts from a variety of industrial source types. EPA's present regulatory platform for near-field modeling has, with few exceptions, remained fundamentally unchanged since the beginning of the air programs, some 25 years ago. ISC3 is the workhorse of current regulatory tools with code structure that is conducive to change. Therefore, AERMIC selected the EPA's ISC3 Model for a major overhaul. AERMIC's objective is to develop a complete replacement for ISC3 by: 1) adopting ISC3's input/output computer architecture; 2) updating, where practical, antiquated ISC3 model algorithms with newly developed or current state-of-the-art modeling

techniques; and 3) insuring that the source and atmospheric processes presently modeled by ISC3 will continue to be handled by the AERMIC Model (AERMOD), albeit in an improved manner. Although the current model described here does not fully satisfy this third objective (the wet and dry deposition algorithms in AERMOD are not complete), it is AERMIC's intent to continue the development of AERMOD, beyond this work, until all objectives are satisfied..

The AERMOD modeling system consists of two pre-processors and the dispersion model. The AERMIC meteorological preprocessor (AERMET) provides AERMOD with the meteorological information it needs to characterize the PBL. The AERMIC terrain pre-processor (AERMAP) both characterizes the terrain and generates receptor grids and elevations for the dispersion model (referred to simply as AERMOD).

AERMET uses meteorological data and surface characteristics to calculate boundary layer parameters (e.g. mixing height, friction velocity, etc.) needed by AERMOD. This data, whether measured off-site or on-site, must be representative of the meteorology in the modeling domain. AERMAP uses gridded terrain data for the modeling area to calculate a representative terrain-influence height associated with each receptor location. At the present time, the gridded data must be supplied to AERMAP in the format of the Digital Elevation Mapping (DEM) data (USGS, 1994). The terrain preprocessor can also be used to compute elevations for both discrete receptors and receptor grids.

In developing AERMOD, AERMIC adopted design criteria to yield a model with desirable regulatory attributes. We felt that the model should: 1) provide reasonable concentration estimates under a wide variety of conditions with minimal discontinuities; 2) be user friendly and require reasonable input data and computer resources as is the current ISC3 model; 3) capture the essential physical processes while remaining fundamentally simple; and, 4) accommodate modifications with ease as the science evolves.

Relative to ISC3, AERMOD currently contains new or improved algorithms for: 1) dispersion in both the convective and stable boundary layers; 2) plume rise and buoyancy; 3) plume penetration into elevated inversions; 4) computation of vertical profiles of wind, turbulence, and temperature; 5) the urban boundary layer; and 6) the treatment of receptors on all types of terrain from the surface up to and above the plume height. AERMET contains an improved approach to characterizing the fundamental boundary layer parameters. High priority items for future efforts include new or improved algorithms dealing with building downwash and both wet and dry deposition.

1.3 *Model Development Process*

AERMOD was developed in the following stages:
1) initial model formulation; 2) developmental evaluation; 3) internal peer review and beta testing; 4) revised model formulation; 5) performance evaluation and sensitivity testing; 6)

external peer review; and 7) submission to EPA's **O**ffice of **A**ir **Q**uality **P**lanning and **S**tandards (OAQPS) for consideration as a regulatory model. We are currently at stage 7.

The initial formulations of AERMOD are summarized in Perry, et al. (1994) and Cimorelli, et al. (1996). Once formulated, the model was tested (developmental evaluation) against a variety of field measurements in order to identify areas needing improvement. The developmental evaluation provided a basis for selecting formulation options.

This developmental evaluation was conducted using five data bases. Three consisted of event-based tracer releases, while the other two each contain up to a full year of continuous SO_2 measurements. These data bases cover elevated and surface releases, complex and simple terrain, and rural and urban boundary layers. A description of the early developmental evaluation is presented in Lee, et al., (1995) and in a later report by Lee et al. (1998a). Many revisions to the original early formulation have resulted from this evaluation as well as comments received during peer review, beta testing, and the public forum at the EPA's Sixth Modeling conference (in 1995). Lee et al. (1998a, 1998b) describe the developmental evaluation repeated with the current model.

In addition, AERMOD has undergone a comprehensive performance evaluation (PES, 1998), designed to assess how well AERMOD's concentration estimates compare against a variety of independent data bases and to assess the adequacy of the model for use in regulatory decision making. That is, to assess how well the model predicts concentrations at the high end of the concentration distribution. AERMOD was evaluated against five independent data bases (two in simple terrain and three in complex terrain), each containing one full year of continuous SO_2 measurements. Additionally, AERMOD's performance was compared against the performance of four other applied, regulatory models: they are: ISC3, CTDMPLUS (Perry, 1992), RTDM (Paine and Egan,1987) and HPDM (Hanna and Paine, 1989: Hanna and Chang, 1993). The performance of these models against AERMOD has been compared using the procedures in EPA's "Protocol for Determining the Best Performing Model" (EPA, 1992). Finally, upon completion of the peer review and presentation of the model at EPA's Seventh Modeling Conference in early 1999, AERMOD will be submitted to EPA's Office of Air Quality Planning and Standards (OAQPS) for inclusion in the Guideline on Air Quality Models (Code of Federal Regulations, 1997).

1.4 *Purpose of Document*

The purpose of this document is to describe the technical formulation of AERMOD and its preprocessors. Our intent is to provide model developers, peer reviewers and model users with a comprehensive listing of all significant algorithms contained in the model. Performance and evaluation of the current model are described in other reports (Lee et al., 1998b; PES, 1998).

2 Model Overview

This section provides a general overview of the most important features of AERMOD. With the exception of applications involving wet and dry deposition, AERMOD serves as a replacement for ISC3. Thus, it is applicable to rural and urban areas, flat and complex terrain, surface and elevated releases, and multiple sources (including, point, area and volume sources). Every effort has been made to avoid model formulation discontinuities wherein large changes in calculated concentrations result from small changes in input parameters.

AERMOD is a steady-state plume model. In the stable boundary layer (SBL), the concentration distribution is assumed to be Gaussian in both the vertical and horizontal. In the convective boundary layer (CBL), the horizontal distribution is assumed to be Gaussian, but the vertical distribution is described with a bi-Gaussian probability density function (p.d.f.). This behavior of the concentration distributions in the CBL was demonstrated by (Willis, and Deardorff, 1981) and (Briggs, 1993). Additionally, in the CBL, AERMOD treats "plume lofting," whereby a portion of plume mass, released from a buoyant source, rises to and remains near the top of the boundary layer before becoming mixed into the CBL. AERMOD also tracks any plume mass that penetrates into elevated stable layer, and then allows it to re-enter the boundary layer when and if appropriate.

AERMOD incorporates, with a new simple approach, current concepts about flow and dispersion in complex terrain. Where appropriate the plume is modeled as either impacting and/or following the terrain. This approach has been designed to be physically realistic and simple to implement while avoiding the need to distinguish among simple, intermediate and complex terrain, as is required by present regulatory models. As a result, AERMOD removes the need for defining complex terrain regimes; all terrain is handled in a consistent, and continuous manner that is simple while still considering the dividing streamline concept (Snyder, et al., 1985) in stably-stratified conditions.

One of the major improvements that AERMOD brings to applied dispersion modeling is its ability to characterize the PBL through both surface and mixed layer scaling. AERMOD constructs vertical profiles of required meteorological variables based on measurements and extrapolations of those measurements using similarity (scaling) relationships. Vertical profiles of wind speed, wind direction, turbulence, temperature, and temperature gradient are estimated using all available meteorological observations. AERMOD was designed to run with a minimum of observed meteorological parameters. As a replacement for the ISC3 model AERMOD can operate using data of a type that is readily available from an NWS station. AERMOD requires only a single surface (generally, 10m) measurement of wind speed (reference wind speed (between 7 z_o and 100m)), direction and ambient temperature (reference temperature). Like ISC3, AERMOD also needs observed cloud cover. However, AERMOD also requires the full morning upper air sounding (RAWINSONDE). ISC3 required only the morning and afternoon mixing heights derived form that sounding. In addition, AERMOD needs surface characteristics (surface roughness, Bowen ratio, and albedo) in order to construct its PBL profiles.

Recommended minimum meteorological data requirements for AERMOD will be published in a future revision to the Guideline on Air Quality Models.

Unlike existing regulatory models, AERMOD accounts for the vertical inhomogeneity of the PBL. This is accomplished by "averaging" the parameters of the actual PBL into "effective" parameters of an equivalent homogeneous PBL.

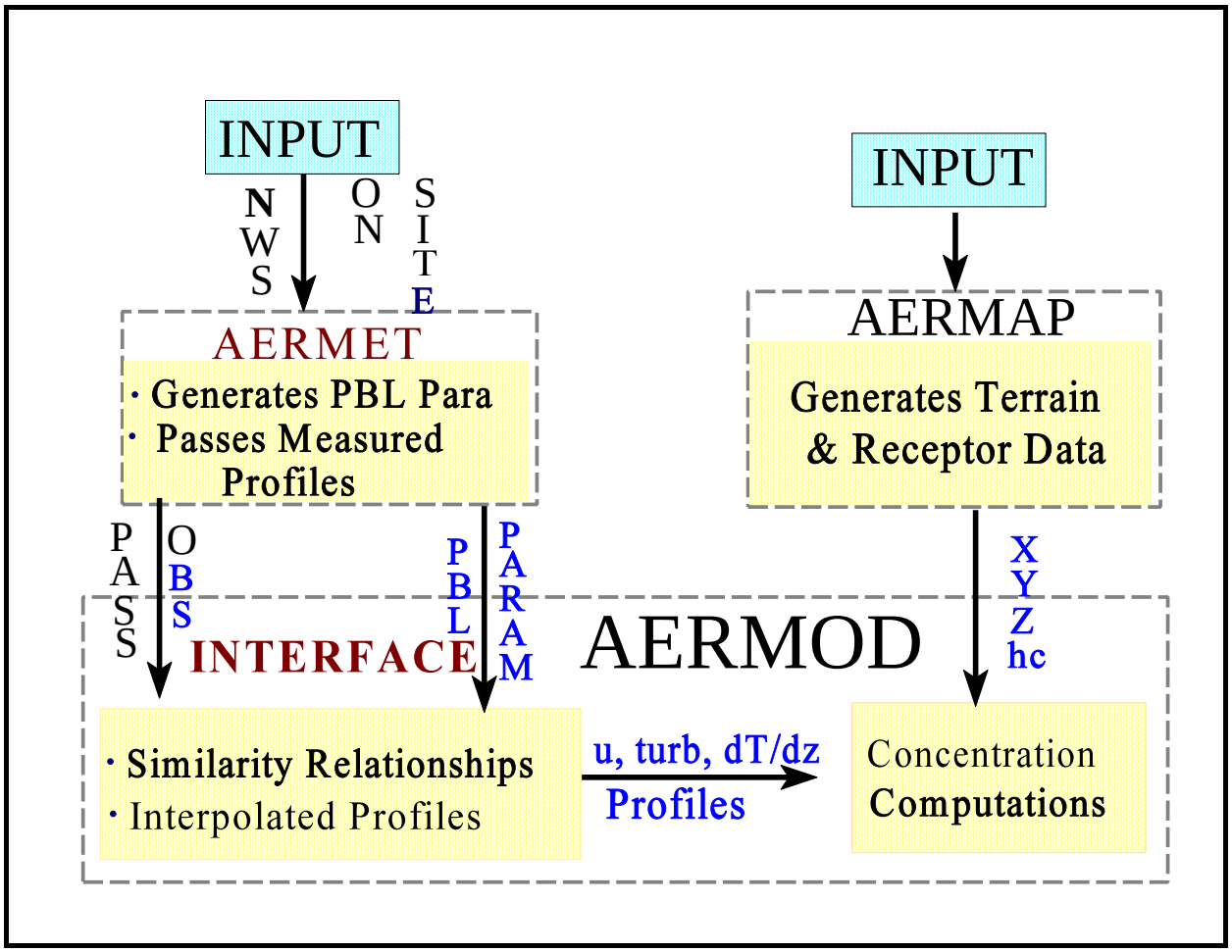

Figure 1: Data Flow in the AERMOD Modeling System

Figure 1 shows the flow and processing of information in AERMOD. The modeling system consists of one main program (AERMOD) and two pre-processors (AERMET and AERMAP). The major purpose of AERMET is to calculate boundary layer parameters for use by AERMOD. The meteorological INTERFACE, internal to AERMOD, uses these parameters to generate profiles of the needed meteorological variables. In addition, AERMET passes all meteorological observations to AERMOD.

Surface characteristics in the form of albedo, surface roughness and Bowen ratio, plus standard meteorological observations (wind speed, wind direction, temperature, and cloud cover), are input to AERMET. AERMET then calculates the PBL parameters: friction velocity (u_*), Monin-Obukhov length (L), convective velocity scale (w_*), temperature scale (θ_*), mixing height (z_i), and surface heat flux (H). These parameters are then passed to the INTERFACE (which is within AERMOD) where similarity expressions (in conjunction with measurements) are used to calculate vertical profiles of wind speed (u), lateral and vertical turbulent fluctuations (σ_v, σ_w), potential temperature gradient ($d\theta/dz$), potential temperature (θ), and the horizontal Lagrangian time scale (T_{Ly}).

The AERMIC terrain pre-processor AERMAP uses gridded terrain data to calculate a representative terrain-influence height (h_c), also referred to as the terrain height scale. The terrain height scale h_c, which is uniquely defined for each receptor location, is used to calculate the dividing streamline height. The gridded data needed by AERMAP is selected from Digital Elevation Mapping (DEM) data. AERMAP is also used to create receptor grids. The elevation for each specified receptor is automatically assigned through AERMAP. For each receptor, AERMAP passes the following information to AERMOD: the receptor's location (x_r, y_r), its height above mean sea level (z_r), and the receptor specific terrain height scale (h_c).

A comprehensive description of the basic formulation of the AERMOD dispersion model including the INTERFACE, AERMET, and AERMAP is presented in this document. Included are: 1) a complete description of the AERMET algorithms that provide quantitative hourly PBL parameters; 2) the general form of the concentration equation with adjustments for terrain; 3) plume rise and dispersion algorithms appropriate for both the convective and stable boundary layers; 4) handling of boundary layer inhomogeneity; 5) algorithms for developing vertical profiles of the necessary meteorological parameters; and 6) a treatment of the nighttime urban boundary layer. The model described here represents the version of AERMOD that has been submitted to OAQPS for regulatory considerations. In addition, all of the symbols used for the many parameters and variables that are referred to in this document are defined, with their appropriate units, in the section titled "List of Symbols."

3 Meteorological Preprocessor (AERMET)

The basic purpose of AERMET is to use meteorological measurements, representative of the modeling domain, to compute certain boundary layer parameters used to estimate profiles of wind, turbulence and temperature. These profiles are estimated by the AERMOD interface (described in section 4).

The structure of AERMET is based upon an existing regulatory model preprocessor, the Meteorological Processor for Regulatory Models (MPRM) (Irwin, et al., 1988). However, AERMET's processing of meteorological data is similar to that done for the CTDMPLUS (Perry, 1992) and HPDM (Hanna and Paine, 1989: Hanna and Chang, 1993) models. The surface

parameters provided by AERMET are the Monin-Obukhov Length, L, surface friction velocity, u_*, surface roughness length, z_o, surface heat flux, H, and the convective scaling velocity, w_*. AERMET also provides estimates of the convective and mechanical mixed layer heights, z_{ic} and z_{im}, respectively. Although AERMOD is capable of estimating meteorological profiles with data from as little as one measurement height, it will use as much data as the user can provide for defining the vertical structure of the boundary layer. In addition to PBL parameters, AERMET passes all measurements of wind, temperature, and turbulence in a form AERMOD needs.

The growth and structure of the atmospheric boundary layer is driven by the fluxes of heat and momentum which in turn depend upon surface effects. The depth of this layer and the dispersion of pollutants within it are influenced on a local scale by surface characteristics such as the roughness of the underlying surface, the reflectivity (albedo), and the availability of surface moisture. Unlike ISC3, which is based on an assumed open-country vegetation cover for all sites, the state of the PBL computed by AERMET is a function of the underlying surface characteristics. Therefore, meteorological profiles and ambient concentrations may change from site to site (all other things being equal) or as the up-wind fetch changes with wind direction.

3.1 *Derived Parameters in the CBL*

In this section we discuss how AERMET calculates the PBL parameters in the convective boundary layer. AERMET first estimates the sensible heat flux (H), then calculates the friction velocity (u_*) and the Monin Obukhov Length (L). With H, u_*, L, AERMET can then estimate the height of the mixed layer and the convective velocity scale (w_*).

3.1.1 SENSIBLE HEAT FLUX (H) IN THE CBL

The fluxes of heat and momentum drive the growth and structure of the PBL. To properly characterize the PBL one first needs a good estimate of the surface sensible heat flux (H) which depends on the net radiation (R_n). When the net radiation is positive for a given hour AERMET

defines the PBL as convective (net radiation is either measured or estimated as a function of cloud cover, solar angle, albedo, and surface temperature). In the CBL, a simple energy balance approach (as in Oke, 1978) is used to derive the following expression for H:

$$H = \frac{0.9\, R_n}{(1 + 1/B_o)}, \qquad \textbf{(1)}$$

where: $B_o \equiv$ *Bowen Ratio*
$H \equiv$ *Sensible Heat Flux*
$R_n \equiv$ *Net Radiation.*

The underlying assumption in eq.**(1)** is that the soil heat flux is 10% of the net radiation. If measured values for R_n are not available, R_n can be estimated from the insolation and the thermal radiation balance at the ground following the method of Holtslag and Van ulden (1983) where the insolation for clear skies, R_o, is calculated from Collier and Lockwood (1975).

$$R_n = \frac{[1 - r\{\phi\}]\, R + c_1\, T_{ref}^6 - \sigma_{SB}\, T_{ref}^4 + c_2\, n}{1 + c_3}, \qquad \textbf{(2)}$$

where:

$$c_1 \equiv 5.31\, x\, 10^{-13}\, Wm^{-2} K^{-6}$$
$$c_2 \equiv 60\, Wm^{-2}$$
$$c_3 \equiv 0.12$$
$$\sigma_{SB} \equiv \textit{Stefan Boltzman Constant}\ (5.67\, x\, 10^{-8}\, Wm^{-2} K^{-4})$$
$$T_{ref} \equiv \textit{Ambient Air Temperature at reference height for temperature}$$
$$R_n \equiv \textit{Net Radiation}$$

and:

$$r\{\phi\} \equiv \textit{Albedo} = r' + (1 - r')\, exp[a\phi + b]$$

where:

$$a = -0.1$$
$$b = -0.5(1 - r')^2$$
$$r' \equiv r\{\phi = 90^o\}. \qquad \textbf{(3)}$$

Solar radiation, R, corrected for cloud cover is taken from (Kasten and Czeplak, 1980):

$$R = R_o\,(1 - 0.75\, n^{3.4}), \qquad \textbf{(4)}$$

where:

$$R \equiv \textit{Solar radiation}$$
$$n \equiv \textit{Cloud Cover}\ \{0.0 - 1.0\}.$$

and

$$R_o = 990 \sin\phi - 30 , \qquad \textbf{(5)}$$

where:

$$\phi = \frac{\phi\{t_p\} + \phi\{t\}}{2}; \qquad t_p \equiv \textit{previous hour}$$

and: $t \equiv$ *present hour*

$R_o \equiv$ *Clear Sky Insolation* (Wm^{-2})

$\phi \equiv$ *Solar Elevation Angle.*

3.1.2 FRICTION VELOCITY (u_*) & MONIN OBUKHOV LENGTH (L) IN THE CBL

In the CBL, AERMET computes the surface friction velocity, u_*, and the Monin-Obukhov length, L, using the value of H estimated from eq. **(1)**. Since the friction velocity and the Monin Obukhov length depend on each other, an iterative method, similar to that used in CTDMPLUS (Perry, 1992) is used. AERMOD initializes u_* assuming neutral conditions, calculates L, then proceeds with subsequent estimates of u_* and L until convergence is reached (i.e., there is less than a 1% change between successive iterations). The expression for u_* (e.g., Panofsky and Dutton, 1984) is

$$u_* = \frac{k\, u_{ref}}{\ln(z_{ref}/z_o) - \psi_m\{z_{ref}/L\} + \psi_m\{z_o/L\}}, \qquad \textbf{(6)}$$

where:

$$\psi_m\left\{\frac{z_{ref}}{L}\right\} = 2\ln\left(\frac{1+\mu}{2}\right) + \ln\left(\frac{1+\mu^2}{2}\right) - 2\tan^{-1}\mu + \pi/2$$

$$\mu = \left(1 - 16\frac{z_{ref}}{L}\right)^{1/4}$$

and:

$$\psi_m\left\{\frac{z_o}{L}\right\} = 2\ln\left(\frac{1+\mu_o}{2}\right) + \ln\left(\frac{1+\mu_o^2}{2}\right) - 2\tan^{-1}\mu_o + \pi/2 \qquad \textbf{(7)}$$

$$\mu_o = \left(1 - 16\frac{z_o}{L}\right)^{1/4},$$

and: $k \equiv$ *von Karman constant* $= 0.4$
$u_{ref} \equiv$ *wind speed at reference height*
$u_* \equiv$ *friction velocity*
$z_{ref} \equiv$ *reference height for wind*
$z_o \equiv$ *roughness height*
$L \equiv$ *Monin Obukhov length*.

The initial step in the iteration solves eq.**(6)** for u_* assuming that $\psi_m = 0$ (neutral limit) and setting $u = u_{ref}$. Having an initial estimate of u_*, L is calculated from the following definition for L (eg. see Wyngaard, 1988):

$$L = -\frac{\rho\, c_p\, T_{ref}\, u_*^3}{k\, g\, H}, \qquad \textbf{(8)}$$

where: $g \equiv$ *acceleration due to gravity*
$c_p \equiv$ *specific heat of air at constant pressure*
$\rho \equiv$ *density of air*
$k = 0.4$; *von Karman's constant*.

u_* is recalculated with eqs. **(6)** and **(7)** and with L for eq. **(8)**. This procedure is continued until the values of u_* and L changes by less than 1%.

The reference heights for wind speed and temperature to be used in the determination of friction velocity and Monin-Obukhov length are optimally chosen to be representative of the surface layer in which the similarity theory has been formulated and tested with experimental data. Typically, a 10-m height for winds and a temperature within the range of 2 to 10 meters is chosen. However, for excessively rough sites (such as urban areas with z_o in excess of 1 meter), AERMET has a safeguard to accept wind speed reference data in the vertical height range between 7 z_o and 100 meters. Below 7 z_o (roughly, the height of obstacles or vegetation), measurements are unlikely to be representative of the general area. A similar restriction for temperature measurements is imposed, except that temperature measurements as low as z_o are permitted. Above 100 meters, the wind and temperature measurements are likely to be above the surface layer, especially during stable conditions. Therefore, AERMET imposes an upper limit of 100 meters for reference wind speed and temperature measurements for the purpose of computing the similarity theory friction velocity and Monin-Obukhov length each hour. Of course, other US EPA guidance for acceptable meteorological siting should be consulted in addition to keeping the AERMET restrictions in mind.

3.1.3 CONVECTIVE MIXING HEIGHT (z_{ic})

If measurements of the convective boundary layer height (z_{ic}) are available they are selected and used by the model. If measurements are not available, z_{ic} is calculated with a simple one-dimensional energy balance model (Carson, 1973) as modified by Weil and Brower (1983). This model uses the early morning potential temperature sounding (prior to sunrise), and the time varying surface heat flux to calculate the time evolution of the convective boundary layer as

$$z_{ic}\,\theta\{z_{ic}\} - \int_0^{z_{ic}} \theta\{z\}\,dz = (1+2A)\int_0^{t} \frac{H\{t'\}}{\rho\, c_p}\,dt', \qquad \textbf{(9)}$$

where:

$\theta \equiv$ *potential temperature*
$A \equiv 0.2$ (*Deardorff*, 1980)
$z_{ic} \equiv$ *convective mixing height*
$t \equiv$ *hour after sunrise*.

Weil and Brower found good agreement between predictions and observations of z_{ic}, using this approach.

3.1.4 CONVECTIVE VELOCITY SCALE (w_*)

Field observations, laboratory experiments, and numerical modeling studies show that the large turbulent eddies in the CBL have velocities proportional to the convective velocity scale (w_*) (Wyngaard, 1988). Thus in order to estimate turbulence in the CBL, an estimate of, w_* is needed. AERMET calculates the convective velocity scale from its definition (see Wyngaard, 1988) as:

$$w_* = \left(\frac{g\,H\,z_{ic}}{\rho\, c_p\, T_{ref}}\right)^{1/3}, \qquad \textbf{(10)}$$

where: $w_* \equiv$ *convective velocity scale*.

3.1.5 MECHANICAL MIXING HEIGHT (z_{im}) IN THE CBL

In the early morning when the convective mixed layer is small, the full depth of the PBL may be controlled by mechanical turbulence. AERMET estimates the height of the PBL during convective conditions as the maximum of the estimated (or measured if available) convective boundary layer height (z_{ic}) and the estimated (or measured if available) mechanical mixing height (z_{im}). AERMET uses this procedure to insure that in the early morning, when z_{ic} is very small but considerable mechanical mixing may exist, the height of the PBL is not underestimated. When measurements of the mechanical mixed layer are not available, the mechanical boundary layer height is calculated by assuming that it approaches its equilibrium height given by Zilitinkevich (1972):

$$z_{ie} = 0.4\left(\frac{u_* L}{f}\right), \qquad \textbf{(11)}$$

where: $z_{ie} \equiv$ *equilibrium mechanical mixing height*
$f \equiv$ *Coriolis parameter*.

Although eq. **(11)** was designed for application in the SBL, it is used in the CBL only for the short transitional period at the beginning of the day when mechanical turbulence dominates. The procedure, used by AERMET, guarantees the use of the convective mixing height once adequate convection has been established even though the mechanical mixing height is calculated during all convective conditions. Since AERMET used eq. **(11)** to estimate the height of the mixed layer in the SBL, discontinuities in z_i from night to day are avoided.

Venkatram (1980) has shown that, in mid-latitudes, eq. **(11)** can be empirically represented as

$$z_{ie} = 2300\, u_*^{3/2}, \qquad \textbf{(12)}$$

where z_{ie} is in (*m*) and u_* is in (*m/s*). z_{ie} (calculated from Eq. **(12)**) is the unsmoothed mechanical mixed layer height. When measurements of the mechanical mixed layer height are available they are used in lieu of z_{ie}.

We smooth the equilibrium height, whether measured or calculated from eq. **(12)**, in order to avoid sudden and unrealistic drops in z_{im} during hours that experience a large decrease in wind speed. This smoothing is accomplished by controlling the time evolution of z_{ie}.

The time evolution of the mechanical mixed layer height, z_{im}, is taken to be

$$\frac{dz_{im}}{dt} = \frac{\left(z_{ie} - z_{im}\right)}{\tau}, \qquad \textbf{(13)}$$

where τ is the time scale at which the mechanical mixed layer height approaches its equilibrium value given by eq. **(12)**. Notice that when $z_{im} < z_{ie}$, the mechanical mixed layer height increases to catch up with its current equilibrium value; conversely, when $z_{im} > z_{ie}$, the mechanical mixed layer height decreases towards its equilibrium value.

It is reasonable to assume that the time scale, τ, that governs the evolution of the stable boundary layer is governed by the boundary layer height and the surface friction velocity, so that

$$\tau = \frac{z_{im}}{\beta_\tau u_*}, \qquad \textbf{(14)}$$

where β_τ is an empirical constant, which, we have tentatively assigned the value of 2. As an example, with u_* of order 0.2ms^{-1}, and z_{im} of order 500 m, the time scale is of the order of *1250* seconds.

Because the friction velocity, u_*, changes with time, we integrate eq. **(13)** numerically as follows:

$$z_{im}\{t+\Delta t\} = z_{im}\{t\}\, e^{(-\Delta t/\bar{\tau})} + z_{ie}\{t+\Delta t\}\left[1 - e^{(-\Delta t/\bar{\tau})}\right], \qquad \textbf{(15)}$$

where the average time scale, $\bar{\tau}$, is given by:

$$\bar{\tau} = \frac{z_{im}\{t\}}{\beta_\tau u_*(t+\Delta t)} \qquad \textbf{(16)}$$

where: $t + \Delta t \equiv$ *current hour*
$t \equiv$ *previous hour*.

In eq. **(15)** $z_{im}\{t\}$ is the smoothed value at time t (previous hour) and $z_{ie}\{t + \Delta t\}$ is the current hour's unsmoothed value. Therefore eq. **(15)** produces a smoothed value for use in AERMOD

for the current hour.

3.2 *Derived Parameters in the SBL*

During stable conditions the energy budget term associated with the ground heating component is highly site-specific. During the day, this component is only about 10% of the total net radiation, while at night, its value is comparable to that of the net radiation (Oke, 1978). Therefore, errors in the ground heating term can generally be tolerated during the daytime, but not at night. To avoid using a nocturnal energy balance approach that relies upon detailed knowledge of the ground heating characteristics, AERMIC has adopted a much simpler semi-empirical approach for computing u_* and L in stable conditions.

3.2.1 FRICTION VELOCITY (u_*) IN THE SBL

The computation of u_* depends on the empirical observation that the temperature scale, θ_*, defined as

$$\theta_* = -H / \rho c_p u_* \qquad \textbf{(17)}$$

varies little during the night. Following the logic of Venkatram (1980) we combine the definition of L eq. **(8)** with eq. **(17)** to express the Monin-Obukhov length in the SBL as

$$L = \frac{T_{ref}}{k g \theta_*} u_*^2 , \qquad \textbf{(18)}$$

or

$$L = A u_*^2 ; \qquad where \quad A = \frac{T_{ref}}{k g \theta_*} .$$

From Panofsky and Dutton (1984) the wind speed profile in stable conditions takes the form

$$u = \frac{u_*}{k}\left[\ln\left(\frac{z}{z_o}\right) + \frac{\beta_m z_{ref}}{L}\right], \tag{19}$$

where $\beta_m = 5$
and z_{ref} = *wind speed reference measurement height*.

Substituting eq. **(18)** into eq. **(19)** and defining the drag coefficient, C_D, as $k / \ln(z_{ref} / z_o)$ (Garratt, 1992), results in

$$\frac{u}{u_*} = \frac{1}{C_D} + \frac{\beta_m z_{ref}}{k A u_*^2}. \tag{20}$$

Multiplying eq. **(20)** by u_*^2 and rearranging yields a quadratic of the form

$$u_*^2 - C_D u u_* - C_D u_o^2 = 0, \tag{21}$$

where $u_o^2 = \dfrac{\beta_m z_{ref}}{kA}$.

This quadratic has a solution, as is used in HPDM (Hanna and Chang, 1993) and CTDMPLUS (Perry, 1992), of the form

$$u_* = \frac{C_D u_{ref}}{2} \cdot \left(1 + \left[1 - \left(\frac{2 u_o}{C_D^{1/2} u_{ref}}\right)^2\right]^{1/2}\right) \quad \textit{for} \quad u \geq u_{cr} \tag{22}$$

where

$$u_{cr} = \left[\frac{4 \beta_m z_{ref} g \theta_*}{T_{ref} C_D} \right]^{1/2} \qquad \textbf{(23)}$$

u_{cr} is the minimum wind speed for which eq. **(22)** produces real-valued solutions.

The temperature scale, θ_*, is taken from the empirical expression of van Ulden and Holtslag (1985) as:

$$\theta_* = 0.09(1 - 0.5 n^2). \qquad \textbf{(24)}$$

For the wind speed less than the critical value which results from eq. **(23)**, we assume that u_* and θ_* can be parameterized by the following linear expression:

$$u_* = u_* \{u = u_{cr}\} \cdot \left(\frac{u}{u_{cr}} \right) \qquad for \quad u < u_{cr}$$

$$\theta_* = \theta_* \{u = u_{cr}\} \cdot \left(\frac{u}{u_{cr}} \right) \qquad for \quad u < u_{cr},$$

These expressions approximate the u_* verses θ_* dependence found by van Ulden and Holtslag (1983).

3.2.2 SENSIBLE HEAT FLUX (*H*) IN THE SBL

Having computed u_* and θ_*, AERMET calculates the surface heat flux from the definition for θ_* found in eq. **(17)**

$$H = -\rho c_p u_* \theta_*. \qquad \textbf{(25)}$$

AERMET limits the amount of heat that can be lost by the underlying surface to approximately 60Wm^{-2}. This value is based on a restriction that Hanna et al., (1986) placed on the product of θ_* and u_*. That is, for typical conditions

$$[\theta_* u_*]_{\max} = 0.05\ m\,s^{-1}K. \qquad \textbf{(26)}$$

When the heat flux, calculated from eq. **(25)**, is such that $\theta_*\ u_{*}. > 0.05\text{ms}^{-1}$ K, AERMET recalculates u_{*}. by substituting $0.05/u_*$ into eq. **(22)** for θ_* (u_o in eq. **(22)** is a function of θ_*) and solving for u_{*}.. Using the recalculated value for u_{*}., θ_* is then calculated from eq. **(26)**.

3.2.3 MONIN OBUKHOV LENGTH (L) IN THE SBL

The Monin Obukhov Length (L) is calculated from eq. **(8)** using the sensible heat flux of eq.**(25)** and u_* from eq. **(22)**.

3.2.4 MECHANICAL MIXING HEIGHT (z_{im}) IN THE SBL

The mixing height in the SBL results exclusively from mechanical (or shear induced) turbulence. The value of z_{im} is calculated from eq. **(12)**, which is the same expression as is used in the CBL. The SBL height is smoothed in time using eq. **(15)** in the same manner as in the CBL.

4 AERMOD's Meteorological Interface

The AERMOD interface, a set of routines within AERMOD, uses similarity relationships with the boundary layer parameters, the measured meteorological data, and other site-specific information provided by AERMET to compute vertical profiles of: 1) wind direction, 2) wind speed, 3) temperature, 4) vertical potential temperature gradient, 5) vertical turbulence (σ_w) and 6) horizontal turbulence (σ_v).

For any one of these six variables (or parameters), the interface (in constructing the profile) compares each height at which a meteorological variable must be calculated with the heights at which observations were made and if it is below the lowest measurement or above the highest measurement (or in some cases there is no data at all), the interface computes an appropriate value from selected PBL similarity profiling relationships. If data are available both above and below a given height, an interpolation is performed which is based on both the measured data and the shape of the computed profile (see the Appendix for a complete description of this procedure). This overall profiling approach simultaneously takes advantage of the information contained in both the measurements and parameterizations from similarity formulas. As will be discussed, at least one level of measured wind speed, wind direction, and temperature is required. However, turbulence can be parameterized without any direct turbulence measurements.

In AERMOD, the mixing height z_i, has an expanded role in comparison to how it is used in ISC3. In AERMOD the mixing height is used as an elevated reflecting/penetrating surface, an important scaling height, and enters in the w_* determination eq. **(10)** . z_i is defined as follows:

$$\begin{aligned} z_i &= MAX\,[z_{ic};\ z_{im}] \qquad && For \quad L < 0 \quad (CBL) \\ z_i &= z_{im} && For \quad L > 0 \quad (SBL). \end{aligned} \qquad \textbf{(27)}$$

Since algorithms used for profiling differ in the SBL and CBL, the INTERFACE must determine the stability of the PBL; this is accomplished by examining the sign of L. If $L < 0$ then the PBL is considered to be convective (CBL) by AERMOD. If $L > 0$ then the PBL is stable (SBL).

The following sections provide a comprehensive description of the algorithms used to generate profiles of the boundary layer meteorology and how AERMOD uses the profiles to extract pertinent layer-averaged meteorology for the transport and dispersion calculations.

4.1 *General Profiling Equations*

4.1.1 WIND SPEED PROFILING IN THE INTERFACE

At least one wind speed measurement is required for each simulation with AERMOD. The AERMOD profile equation for wind speed is:

$$
\begin{aligned}
u &= u\{7z_o\}\left[\frac{z}{7z_o}\right] && for \quad z < 7z_o \\
u &= \frac{u_*}{k}\cdot\left[ln\left(\frac{z}{z_o}\right) - \psi_m\left\{\frac{z}{L}\right\} + \psi_m\left\{\frac{z_o}{L}\right\}\right] && for \quad 7z_o \le z \le z_i \\
u &= u\{z_i\} && for \quad z > z_i
\end{aligned}
\qquad \textbf{(28)}
$$

For the CBL, the ψ_m's are evaluated using eq. **(7)** with z_{ref} replaced by z, and during stable conditions they are calculated as follows (Van Ulden and Holtslag, 1985):

$$
\begin{aligned}
\psi_m\left\{\frac{z}{L}\right\} &= -17\left[1 - exp\left(-0.29\frac{z}{L}\right)\right] \\
\psi_m\left\{\frac{z_o}{L}\right\} &= -17\left[1 - exp\left(-0.29\frac{z_o}{L}\right)\right].
\end{aligned}
\qquad \textbf{(29)}
$$

For small z/L ($<<1$), eq. **(29)** reduces to the well-known ψ_m form given in eq. **(19)**, $\psi_m = -\beta_m\, z/L$ with $\beta_m = 5$; in eq. **(29)** the effective constant β_m in the small z/L limit is 4.93. However, for large z/L (>1) and heights as great as 200 meters in the SBL, the ψ_m given by eq. **(29)** is found to fit wind observations much better than the ψ_m given by eq.**(19)** (see van Ulden and Holtslog, 1985).

Figure 2 and **Figure 3** show the form of the wind profiles used by AERMOD. In order to produce these figures, and others which follow, we constructed two typical cases, one each for the CBL and the SBL. For the CBL we assumed that $z_i=1000m$, $L=-10m$ and $z_o=0.1m$ ($\therefore z_o=.0001z_i$ and $L=-.01z_i$). For the SBL we assumed that $z_i=100m$, $L=10m$ and $z_o=0.1m$ ($\therefore z_o=.001z_i$ and $L=.1z_i$).

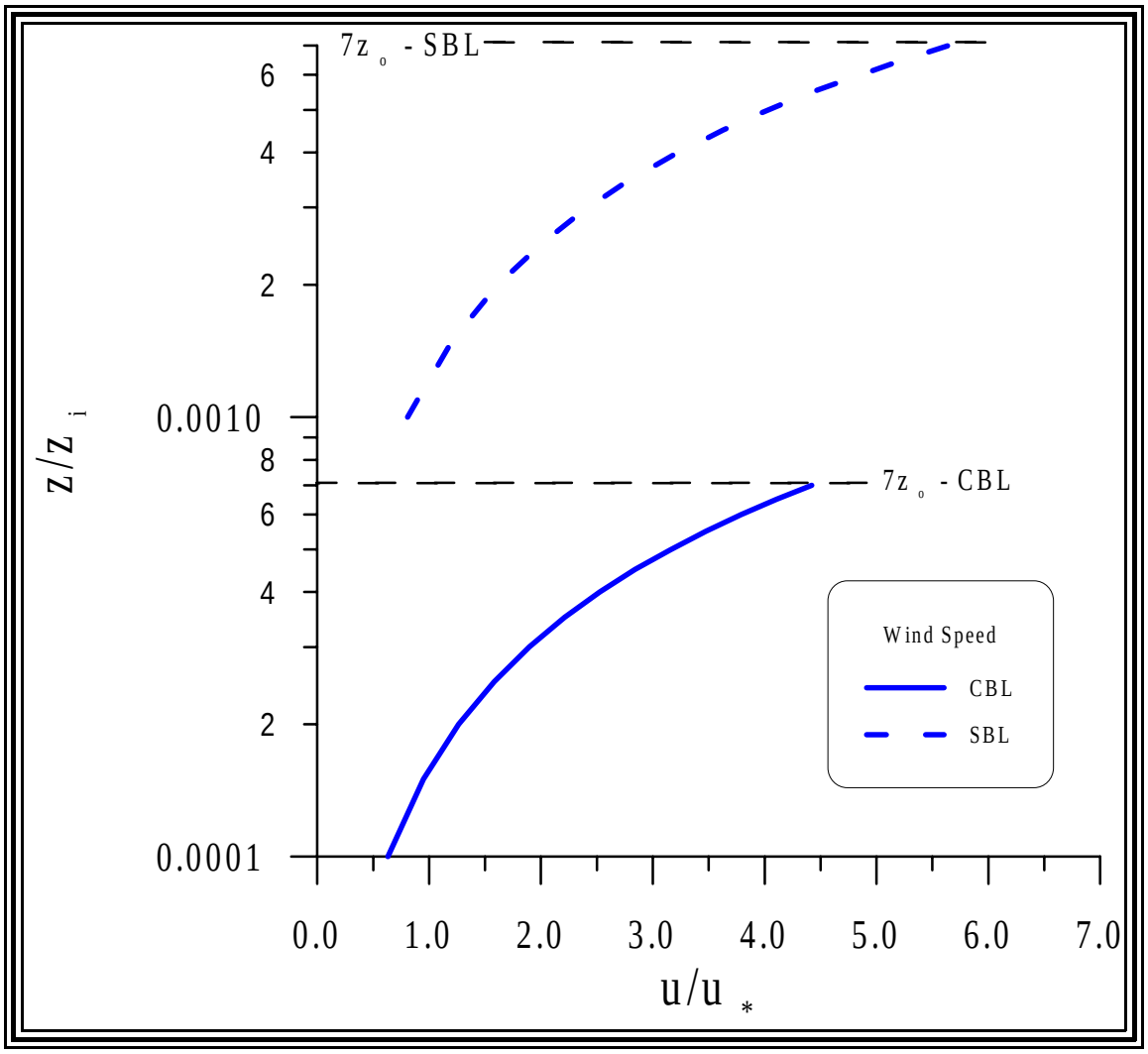

Figure 2: Wind speed profile, for both the CBL and SBL, in the region below $7Z_o$.

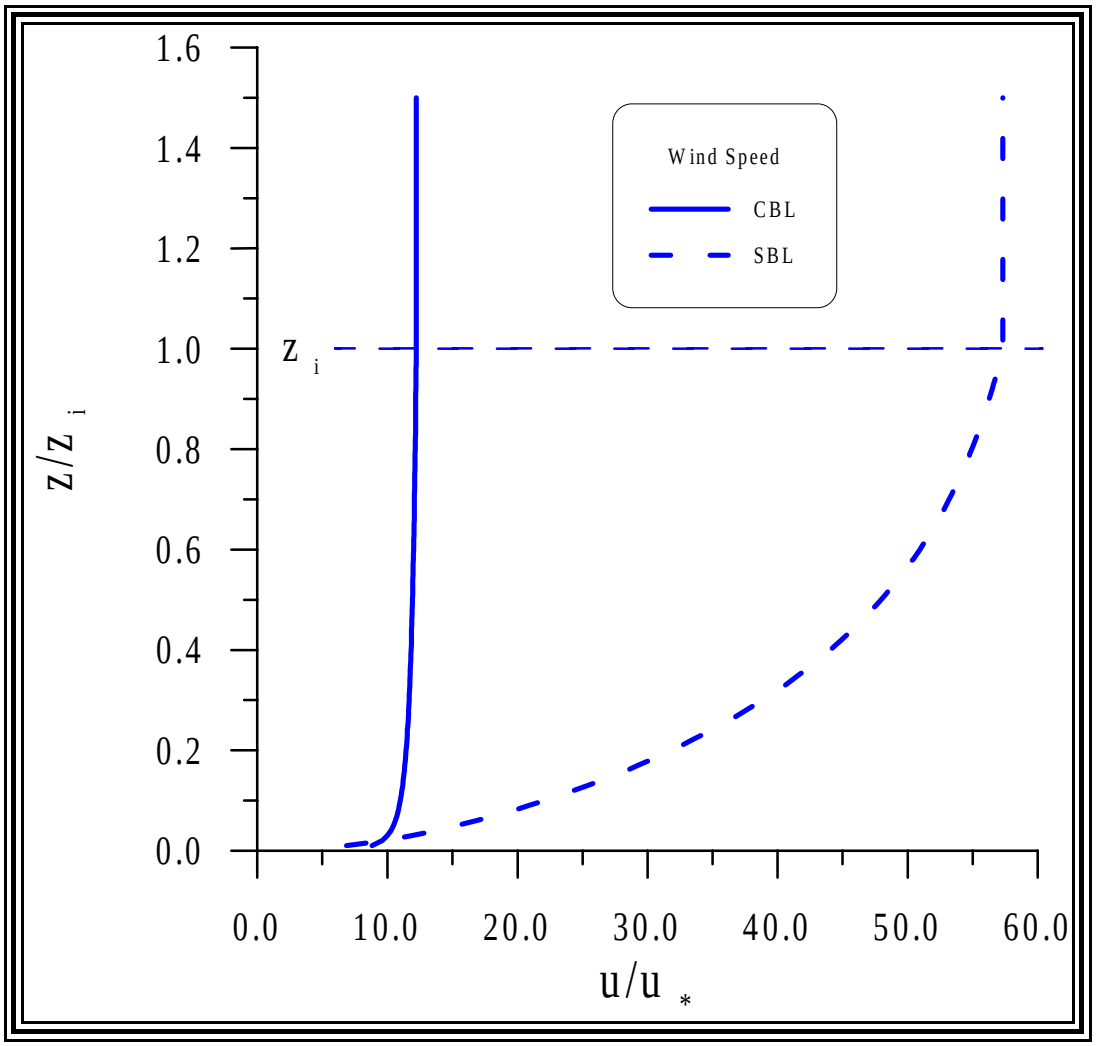

Figure 3 Wind speed profile, for both the CBL and SBL, in the region above $7Z_o$.

4.1.2 WIND DIRECTION PROFILES IN INTERFACE

For both the CBL & SBL wind direction is assumed to be constant with height both above the highest and below the lowest measurements. For intermediate heights, AERMOD linearly interpolate between measurements.

4.1.3 PROFILES OF THE POTENTIAL TEMPERATURE GRADIENT IN THE INTERFACE

Ignoring the shallow superadiabatic surface layer, the potential temperature gradient in the well mixed CBL is taken to be zero. The gradient in the stable interfacial layer just above the mixed layer is taken from the morning temperature sounding. This gradient is an important factor in

determining the potential for buoyant plume penetration into and above that layer. Above the interfacial layer, the gradient is typically constant and slightly stable. These three layers (well mixed, interfacial, and stable layer aloft) in the CBL have $d\theta/dz$ computed in AERMOD as

$$\begin{aligned}
\frac{d\theta}{dz} &= 0.0 && \textit{for} \quad z \le z_i \\
\frac{d\theta}{dz} &= \textit{from AERMET (based on the morning sounding)} && \textit{for} \quad z_i < z \le z_i + 500m \\
\frac{d\theta}{dz} &= 0.005 && \textit{for} \quad z > z_i + 500m,
\end{aligned} \qquad \textbf{(30)}$$

where z_i is taken from eq. **(27)**.

Although the interfacial layer depth varies with time, we fixed it at 500 m for these calculations to insure that a sufficient layer of the morning sounding is sampled. This avoids unrealistic kinks often present in these data. The constant value of 0.005 above the interfacial layer is suggested by Hanna and Chang (1991). Using the morning sounding to compute the interfacial temperature gradient assumes that as the mixed layer grows throughout the day, the temperature profile in the layer above z_i changes little from that of the morning sounding. Of course, this assumes that there is neither significant subsidence nor cold or warm air advection occurring in that layer. Field measurements (e.g., Clark et al., 1971) of observed profiles throughout the day lend support to this approach. These data point out the relative invariance of upper level temperature profiles even during periods of intense surface heating.

For the SBL and in the absence of measurements, the potential temperature gradient is calculated as

$$\begin{aligned}
\frac{d\theta}{dz} &= \frac{\theta_{*p}}{k(2m)} \cdot \left[1 + 5\frac{(2m)}{L} \right] && \textit{for} \quad z \le 2m \\
\frac{d\theta}{dz} &= \frac{\theta_{*p}}{kz} \cdot \left[1 + 5\frac{z}{L} \right] && \textit{for} \quad 2m < z \le 100m
\end{aligned} \qquad \textbf{(31)}$$

where $\theta_{*p} \equiv \theta_*$ determined from the local measured temperature gradient

$$\frac{d\theta}{dz} = \frac{d\theta\{100m\}}{dz} \exp\left[-\frac{(z-100m)}{0.44\, z_{i\theta}}\right] \qquad for\ z > 100m \qquad \textbf{(32)}$$

$$where, \quad z_{i\theta} = MAX\left[z_{im}; 100m\right].$$

In the SBL if $d\theta/dz$ measurements are available below100m and above z_o, then θ_{*p} is calculated from eq. **(31)** using the value of $d\theta/dz$ at the lowest measurement level and z_{Tref} replaced by the height of the $d\theta/dz$ measurements. The upper limit of 100 meters for the vertical temperature gradient measurements is consistent with that imposed by AERMET for wind speed and temperature reference data used to determine similarity theory parameters such as the friction velocity and the Monin-Obukhov length. Similarly, the lower limit of z_o for the vertical temperature gradient measurements is consistent with that imposed for reference temperature data. If no measurements of $d\theta/dz$ are available, in that height range, then θ_{*p} is assumed to be equal to θ_* (the cloud cover parameterized temperature scale eq. **(24)** used in AERMET to estimate nighttime heat flux) and is calculated by combining Eqs. **(8)** and **(25)**. θ_* is not used in the CBL.

Figure 4 shows the inverse height dependency of $d\theta/dz$ in the SBL. To create this curve we assumed that: $Z_{im}=100m$; and therefore, $Z_{i\,\theta}=100m$; $L=10m$; $u_*=.124$, which is consistent with a mixing height of $100m$; $T_{ref}=293^oK$; and therefore based on eq. **(18)** $\theta_*=0.115^ok/m$. These parameter values were chosen to represent a strongly stable boundary layer. Below 2m $d\theta/dz$ is persisted downward from its value of 0.228 ^{o}K/m at 2m. Above 100m $d\theta/dz$ is allow to decay exponentially with height.

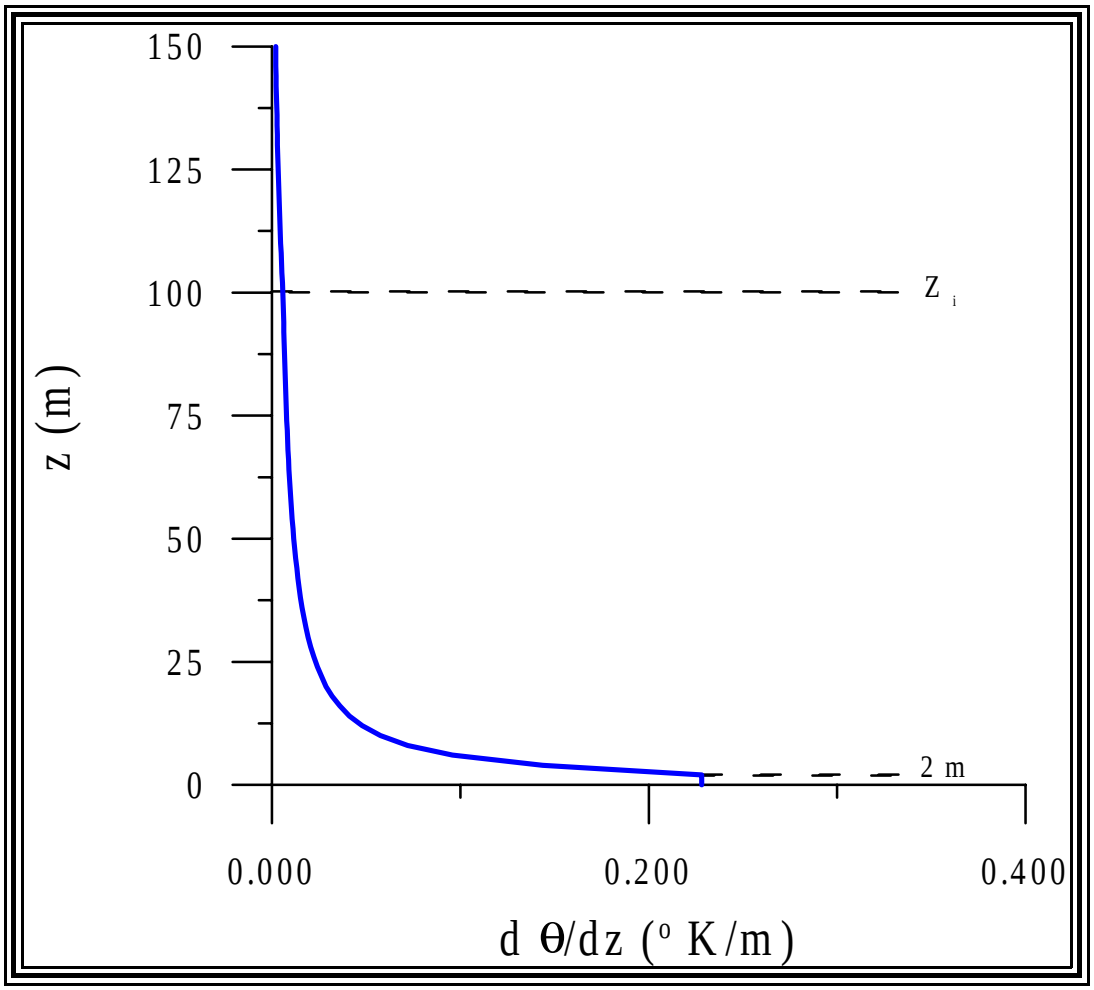

Figure 4: Profile of potential temperature gradient for the SBL.

For all *z*, $d\theta/dz$ is limited to a minimum of *0.002 K/m* (Paine and Kendall, 1993). Eq. **(31)** is taken from Businger et al. (1971). Eq. **(32)** is from Stull (1988) and Van Ulden and Holtslag (1985). The constant of *0.44* within the exponential term of eq. **(32)** is inferred from typical profiles within the Wangara experiment (Andre and Mahrt, 1982).

When measurements of $d\theta/dz$ are available, eqs. **(31)** and **(32)** are applied in a slightly different way. Between measurements we interpolate. Above the highest measurement level the $d\theta/dz$ profile is extrapolated from the value at that height while maintaining the shape as defined by eq. **(31)** and eq. **(32)**. When extrapolating below the lowest measurement height eq. **(31)** is first solved for θ_* (using the $d\theta/dz$ measurement at that lowest height). The $d\theta/dz$ profile is extrapolated down from the lowest measurement height while maintaining the shape as defined by eq. **(31)**.

4.1.4 POTENTIAL TEMPERATURE PROFILING IN THE INTERFACE

Primarily for use in plume rise calculations, AERMOD develops the vertical profile of potential temperature from its estimate of the temperature gradient. First the model computes the potential temperature at the reference height for temperature (i.e., z_{Tref}) and from the reference temperature corrected to sea level pressure such that

$$\theta\left\{z_{Tref}\right\} = T_{ref} + \frac{g z_{MSL}}{c_P}. \qquad \textbf{(33)}$$

$$where: \quad z_{MSL} = z_{Tref} + \overline{z_{SB}}$$

and $\overline{z_{SB}}$ is the stack base height above mean sea level averaged over all sources.

Then for both the CBL and SBL the potential temperature is calculated as follows:

$$\theta\{z+\Delta z\} = \theta\{z_{Tref}\} + \left.\frac{d\theta}{dz}\right|_{\bar{z}} \Delta z \qquad for \quad z \le z_{Tref} \qquad \textbf{(34)}$$

$$\theta\{z+\Delta z\} = \theta\{z\} + \left.\frac{d\theta}{dz}\right|_{\bar{z}} \Delta z \qquad for \quad z > z_{Tref}$$

where:

$$\bar{z} = z + \frac{\Delta z}{2}.$$

Note that for $z < z_{Tref}$, $\Delta z < 0$.

4.1.5 VERTICAL TURBULENCE CALCULATED BY THE INTERFACE

In the CBL, the vertical velocity variance or turbulence (σ^2_{wT}) is profiled using an expression that contains a mechanical and convective portion and is similar to one introduced earlier by Panofsky et al. (1977) and included in other dispersion models (e.g., Berkowicz at al., 1986, Hanna and Paine, 1989, Weil, 1988). It is

$$\sigma_{wT}^2 = \sigma_{wc}^2 + \sigma_{wm}^2 , \qquad \textbf{(35)}$$

where:

$\sigma_{wT} \equiv$ *Total vertical turbulence*

$\sigma_{wc} \equiv$ *Convective portion of the vertical turbulence*

$\sigma_{wm} \equiv$ *Mechanical portion of the vertical turbulence*.

The above expression effectively interpolates between a mechanical or neutral stability limit ($\sigma_{wT} \sim \sigma_{wm} \propto u_*$) and a strongly convective limit ($\sigma_{wT} \sim \sigma_{wc} \propto w_*$).

The convective portion (σ^2_{wc}) of the total variance is calculated as follows:

$$\sigma_{wc}^2 = 1.6 \left(\frac{z}{z_{ic}} \right)^{2/3} \cdot w_*^2 \qquad \textit{for} \quad z \le 0.1\, z_{ic}$$

$$\sigma_{wc}^2 = 0.35\, w_*^2 \qquad \textit{for} \quad 0.1 z_{ic} < z \le z_{ic} \qquad \textbf{(36)}$$

$$\sigma_{wc}^2 = 0.35\, w_*^2\, exp\left[-\frac{6(z - z_{ic})}{z_{ic}} \right] \qquad \textit{for} \quad z > z_{ic} ,$$

where the expression for $z \le 0.1\, z_{ic}$ is the free convection limit (Panofsky et al, 1977), for $0.1 z_i < z \le z_{ic}$ is the mixed-layer value (Hicks,1985) and for $z > z_{ic}$ is a parameterization to connect the mixed layer σ^2_{wc} to the assumed near-zero value well above the CBL. The profile of convective vertical turbulence described in eq. **(36)** is also presented pictorially in **Figure 5**.

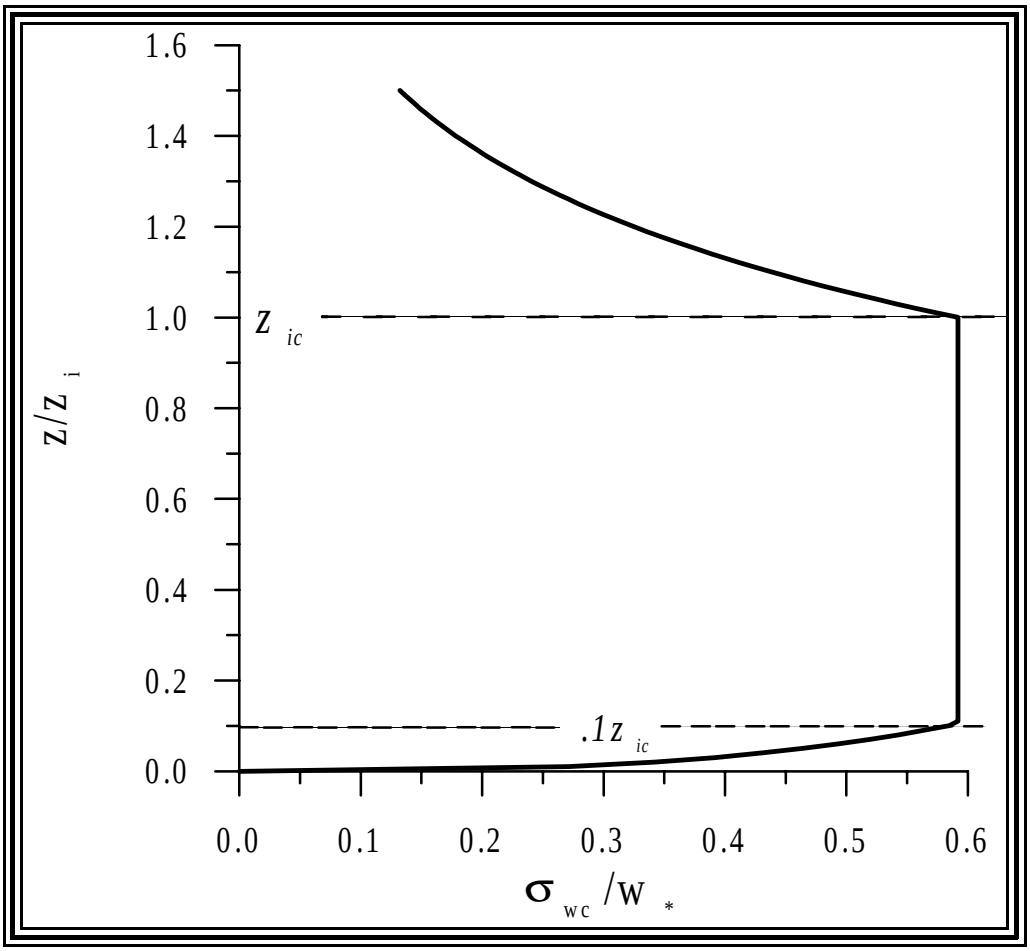

Figure 5: Convective portion of the vertical turbulence in the CBL.

In an earlier AERMOD formulation for mechanical (or shear induced) turbulence, values at the top of the mechanically mixed layer, i.e., $\sigma_v\{z_{im}\}$ and $\sigma_w\{z_{im}\}$, were based on their values at the surface. Peer review comments suggested that since the surface is generally decoupled from higher layers, a formulation based either on measurements above z_{im} or an assumed parameterized turbulent intensity at z_{im} coupled with wind speed estimates would be more appropriate.

Therefore, the mechanical turbulence portion of σ^2_{wT} is assumed to consist of a contribution from the boundary layer and from a "residual layer" above the boundary layer ($z>z_i$). This is done to: 1) satisfy the assumed decoupling between the turbulence aloft ($z>z_i$) and at the surface in the CBL shear layer, and 2) maintain a continuous variation of σ^2_{wm} with z near $z=z_i$. The mechanical turbulence is parameterized by:

$$\sigma_{wm}^2 = \sigma_{wml}^2 + \sigma_{wmr}^2 , \qquad \textbf{(37)}$$

where: $\sigma_{wml} \equiv$ *mechanical portion of the vertical turbulence within the boundary layer*

$\sigma_{wmr} \equiv$ *mechanical portion of the vertical turbulence above the boundary layer* (*residual*).

The expression used to calculate σ_{wml} is

$$\begin{aligned} \sigma_{wml} &= 1.3\, u_* \left(1 - \frac{z}{z_i} \right)^{1/2} && \textit{for} \quad z < z_i \\ \sigma_{wml} &= 0.0 && \textit{for} \quad z \geq z_i \end{aligned} \qquad \textbf{(38)}$$

where the $\sigma_{wml} = 1.3u_*$ at $z=0$ is consistent with Panofsky et al. (1977).

For $z > z_i$ σ_{wmr} is set equal to σ_{wmx}, the maximum value of the mechanical turbulence in the residual layer. σ_{wmx} is calculated as the average of all measured values above z_i. If measurements are not available, then σ_{wmx} is taken as the default value of $0.02u\{z_i\}$. The *0.02* is an assumed turbulence intensity i_z ($= \sigma_w / u$) for the very stable conditions presumed to exist above z_i. This value of turbulence intensity is similar to that assumed in Gifford (1975).

Within the mixed layer, i.e. $z<z_i$, the residual turbulence is reduced from its value at z_i to zero at the surface. Therefore, for all z the residual turbulence takes the form

$$\sigma_{wmr} = \sigma_{wmx}\, MIN\left[z/z_i ;1.0 \right] \qquad \textbf{(39)}$$

Figure 6 presents the profile of the mechanical portion of the vertical turbulence in the CBL. The effect of combining the residual and boundary layer mechanical turbulence (eq. **(37)**) can be seen in this figure. For the purposes of computing σ_{wmr} in **Figure 6** we set $L=.1z_i$ and $z_o=.0001Z_i$

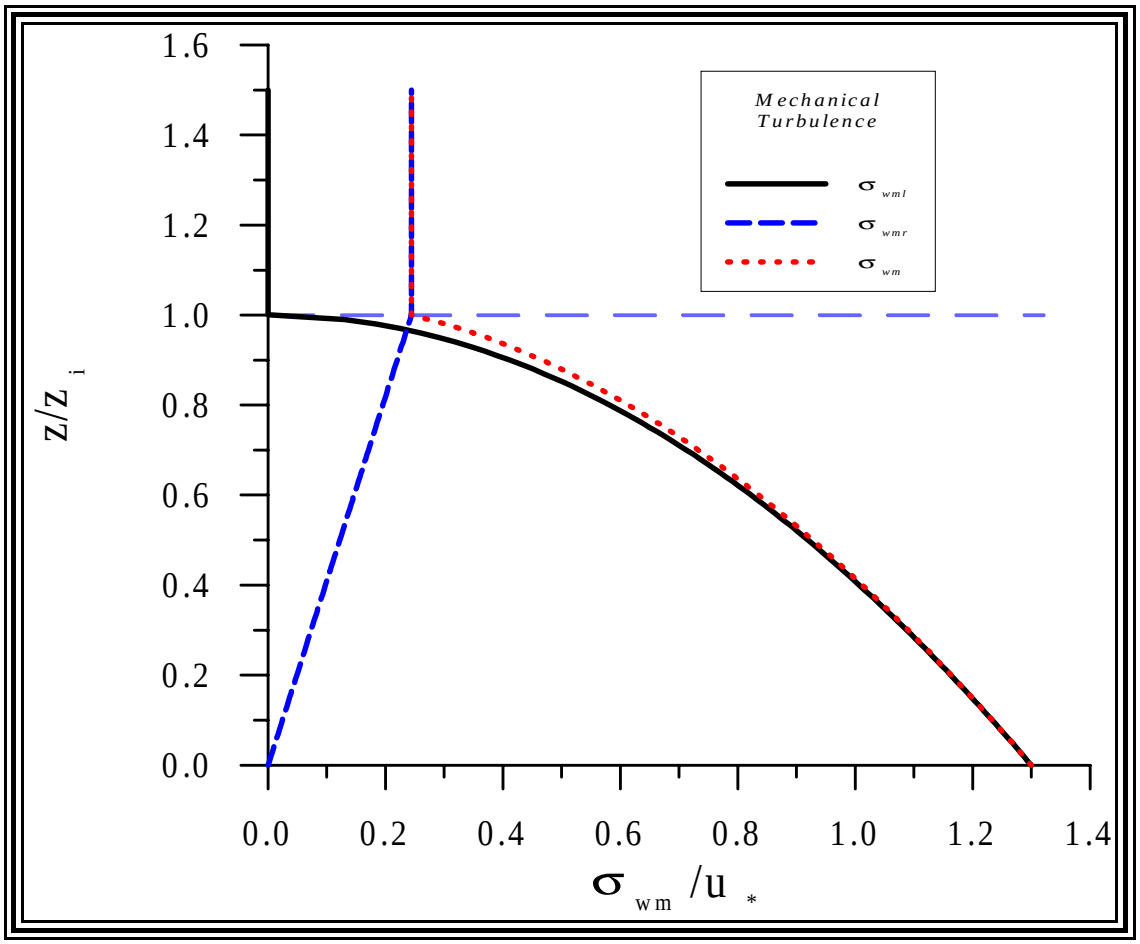

Figure 6: Mechanical portion of the vertical turbulence in the CBL

In the SBL the vertical turbulence contains only a mechanical portion and it is given by eq. **(37)** and eq. **(38)**. The use of the same σ^2_{wm} expressions for the SBL and CBL is done to ensure continuity of turbulence in the limit of neutral stability, i.e., as $z \rightarrow 0$ or $|L| \rightarrow \infty$. That is, the turbulence should be the same as neutral stability is approached either from unstable or stable conditions. **Figure 7** is similar to **Figure 6** except for a notably increase in the value of σ_{wmr}. Values for σ_{wmr} are based on the magnitude of the wind speed at z_i. Therefore the differences in the two figures stem from setting $z_o = .0001 Z_i$ in the CBL and $z_o = .001 Z_i$ in the SBL.

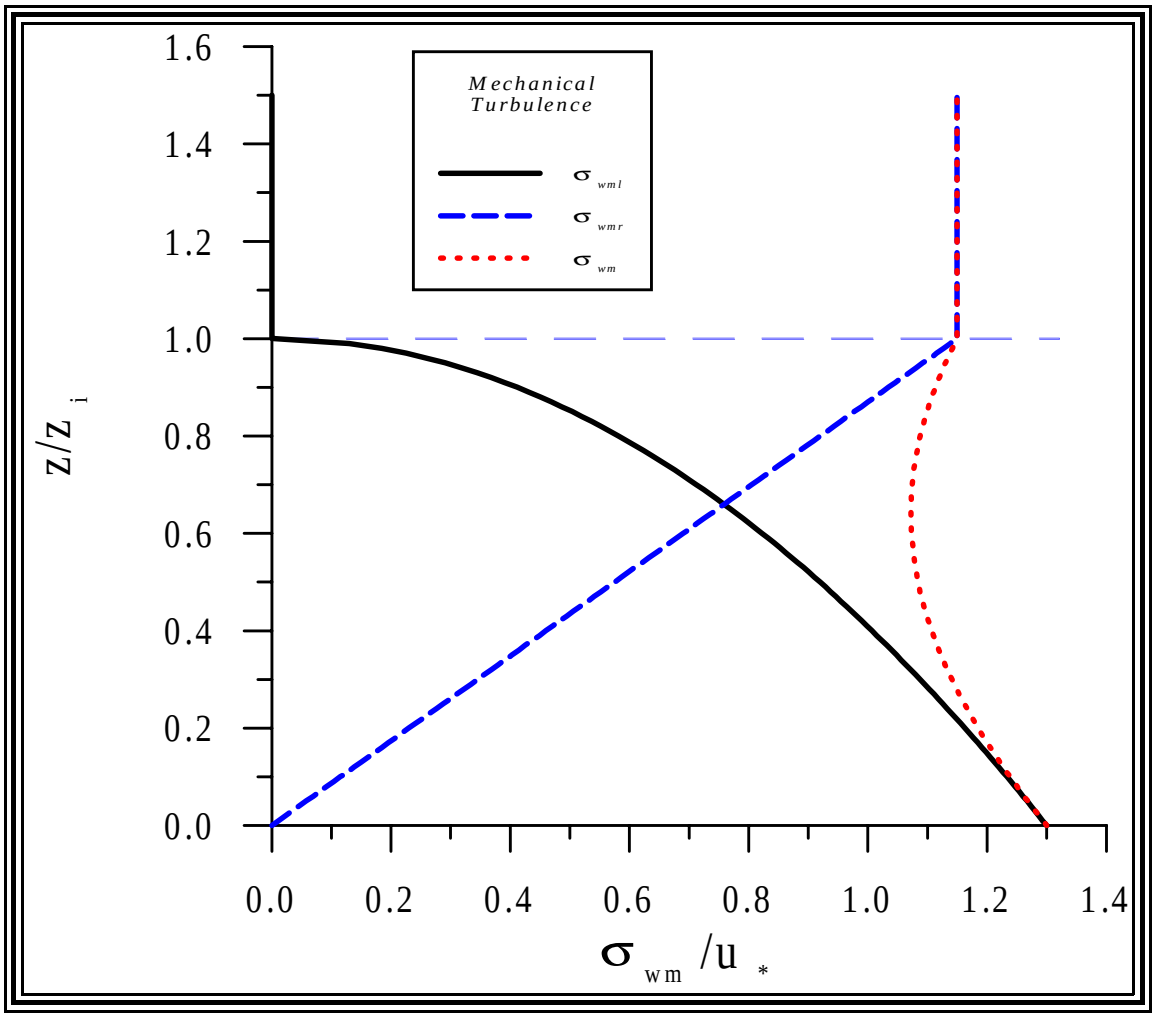

Figure 7: Profile of vertical turbulence in the SBL

4.1.6 LATERAL TURBULENCE CALCULATED BY THE INTERFACE

In the CBL the total lateral turbulence , σ^2_{vT}, is computed as a combination of a mechanical and convective portion (as was adopted for σ^2_{wT}) such that

$$\sigma^2_{vT} = \sigma^2_{vc} + \sigma^2_{vm}, \qquad \textbf{(40)}$$

where:

$\sigma_{vT} \equiv$ *Total lateral turbulence*

$\sigma_{vc} \equiv$ *Convective portion of the lateral turbulence*

$\sigma_{vm} \equiv$ *Mechanical portion of the lateral turbulence*.

In the SBL the total lateral turbulence contains only a mechanical portion.

4.1.6.1 *Mechanical Portion of the Lateral Turbulence*

The variation with height of the mechanical portion of the lateral turbulence is bounded by its value at the surface and an assumed residual value at the top of the mechanical mixed layer. The variation between these two limits is assumed to be linear. Based on observations from numerous field studies, Panofsky and Dutton (1984) report that, in purely mechanical turbulence, the lateral variance near the surface has the form

$$\sigma_{v0}^{\ 2} = C u_*^{\ 2} \qquad \textbf{(41)}$$

where the constant, *C*, ranges between 3 and 5 with an average value of approximately 3.6. Hicks (1985) supports the form of eq. **(41)** and the value of 3.6 for *C*.

Above the mechanically mixed layer, we expect the lateral turbulence to maintain a modest residual level. Hanna (1983) has analyzed ambient measurements of lateral turbulence in stable conditions. He has found that even in the lightest wind conditions, the measurements of σ_v were typically 0.5 m/sec, but were observed to be as low as 0.2 m/sec. AERMOD adopts the lower limit of 0.2 m/sec for σ_v for near-surface conditions (eq. **(44)**), but uses the more typical value of 0.5 m/sec for the residual σ_v above the mixed layer. Furthermore, we found that a value of the order $\sigma_v^{\ 2} = 0.25 m^2 s^{-2}$ provided consistently good model performance (for plumes commonly above z_{im}) during the developmental evaluation thus supporting the presence of residual lateral turbulence in this layer.

Between the near-surface and the top of the mechanically mixed layer, we assume the σ_v^2 varies linearly as

$$\begin{aligned} \sigma_{vm}^2 &= \left[\frac{\sigma_{vm}^2\{z_{im}\} - \sigma_{vo}^2}{z_{im}} \right] z + \sigma_{vo}^2 \qquad && for \quad z \le z_{im} \\ \sigma_{vm}^2 &= \sigma_{vm}^2\{z_{im}\} && for \quad z > z_{im}, \end{aligned} \qquad \textbf{(42)}$$

where:

$$\sigma_{vm}^2\{z_{im}\} = MIN\left[\sigma_{vo}^2;\ 0.25\,m^2/s^2\right]$$

$$\sigma_{vo}^2 = 3.6 \cdot u_*^2 \qquad \textbf{(43)}$$

$$\equiv \textit{Surface value of the lateral turbulence}.$$

The linear variation of σ^2_{vm} with z is consistent with field observations (e.g., Brost et al 1982).

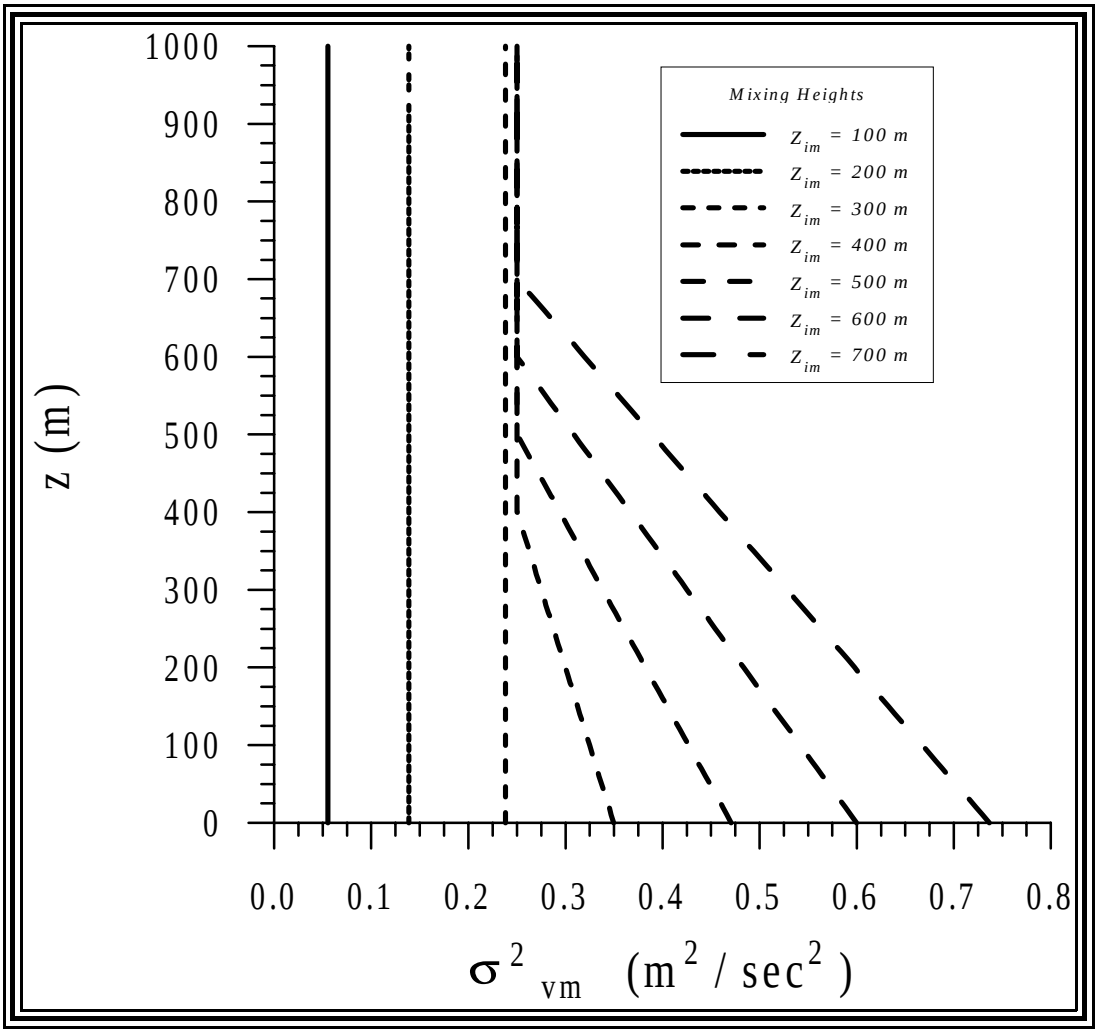

Figure 8: Family of lateral mechanical turbulence profiles over a range of mechanical mixing heights

Figure 8 shows how the vertical profile of lateral turbulence changes over a range of mechanical

mixing heights. The values of u_* used to produce these curves are consistent with the relationship between z_{im} and u_* which is found in eq. **(12)**. In the SBL **Figure 8** represents the total lateral turbulence. In the CBL these curves depict only the mechanical portion of the total lateral variance. This in conjunction with the convective portion eq. **(45)** constitute the turbulence as expressed in eq. **(40)**

In very light wind conditions, u_* may also be quite small and σ_{vo} from eq. **(43)** may be unrealistically small. Based in part on model performance comparisons with data during the developmental evaluation, σ_{vm} is bounded (when used in calculations of σ_y and thus concentration) as follows

$$\sigma_{vm} = MAX\left[\sigma_{vm};\ 0.2\,m/s;\ 0.05\,u\right] \qquad \textbf{(44)}$$

The wind speed u, in eq. **(44)** is evaluated at the same height as σ_{vm}.

4.1.6.2 *Convective Portion of the Lateral Turbulence*

The convective portion of the lateral turbulence is calculated in AERMOD from:

$$\sigma_{vc}^2 = 0.35 \cdot w_*^2 \qquad \textit{for} \quad z \le z_{ic}\,. \qquad \textbf{(45)}$$

This constant value of $\sigma_{vc}^2 / w_*^2 = 0.35$ in the convective mixed layer is supported by the Minnesota data (Reading et al., 1974 and Kaimal et al., 1976) and by data collected at Ashchunch England (Canghey and Palmer, 1979).

For $z > z_{ic}$, the model linearly decreases σ_{vc}^2 from $\sigma_{vc}^2\{z_{ic}\}$ to *0.25* at *1.2* z_{ic} and holds σ_{vc}^2 constant above *1.2* z_{ic}. However, if $\sigma_{vc}^2\{z_{ic}\} < .25\ m^2s^{-2}$, then $\sigma_{vc}^2\{z_{ic}\}$ is persisted upward from z_{ic}.

If observations of σ_v are available below z_{ic}, then the value at the lowest level is assumed to persist down to the surface and at the highest level up to z_{ic}. If the highest observed σ_v is above 1.2 z_{ic} then that value is persisted up. For observations which extend to a level between z_{ic} and 1.2 z_{ic} we linearly extrapolate the highest observed value to 1.2 z_{ic}, based on the slope of the reference profile. Above 1.2 z_{ic} we persist the value σ_v at 1.2 z_{ic}.

In the SBL the total lateral turbulence contains only a mechanical portion and it is given by eqs.**(42)** thru **(44)**. Use, by AERMOD, of the same σ_{vm} expression in the CBL and SBL is done to maintain continuity of σ_{vm} in the limit of neutral stability.

4.2 *Vertical Inhomogeneity in the Boundary Layer* as Treated by the INTERFACE

AERMOD, unlike existing regulatory models, is designed to treat the effects on dispersion from vertical variations in wind and turbulence. This treatment is needed to properly handle releases that are near the ground (the gradient of the variables is strongest here) and to provide a mechanism by which sources that exit the top of the mixed layer and penetrate into an elevated stable layer can re-enter the CBL further downwind. Since AERMOD uses a single value of the meteorological parameters to represent a layer through which these parameters are varying, AERMOD "converts" the inhomogeneous values (as measured or estimated) into equivalent (effective) homogeneous value. The averaging procedure used to create effective boundary layer parameters is discussed here. This technique, in general, is applied to u, σ_{vT}, σ_{wT}, and T_{Ly}. Wind direction is treated separately.

Fundamental to this approach is the concept that the primary layer of importance, relative to receptor concentration, is the one through which plume material travels **directly** from source to receptor. Transport and diffusion of plume material located outside of this layer is assumed to be relatively unimportant until the reflected plume contributes significantly to the receptor concentration. Therefore, the effective parameters, which are denoted by an underscore throughout the document (e.g., effective wind speed is denoted by $\underline{u}$), are determined by averaging their values over that portion of the layer between the plume centroid height ($H_p\{x\}$) (a simplified surrogate for the height of the plume's center of mass) and the receptor height(z_r) that contains plume material. In other words, the averaging layer is determined by the vertical half-depth of the plume but is bounded by the $H_p\{x_{sr}\}$ and z_r. The values used in the averaging process are taken from the vertical profiles generated in the AERMOD interface (Section 4.a.).

Since $\sigma_z\{x_{sr}\}$ depends on the effective values of σ_{wT} and u, the plume size is estimated using the initial values of $\sigma_{wT}\{H_p\}$ and $u\{H_p\}$ to calculate $\sigma_z\{x_{sr}\}$. $\sigma_z\{x_{sr}\}$ is then used to determine the layer over which $\underline{\sigma}_{wT}\{x_{sr}\}$ and $\underline{u}\{x_{sr}\}$ are calculated. **Figure 9** illustrates this approach.

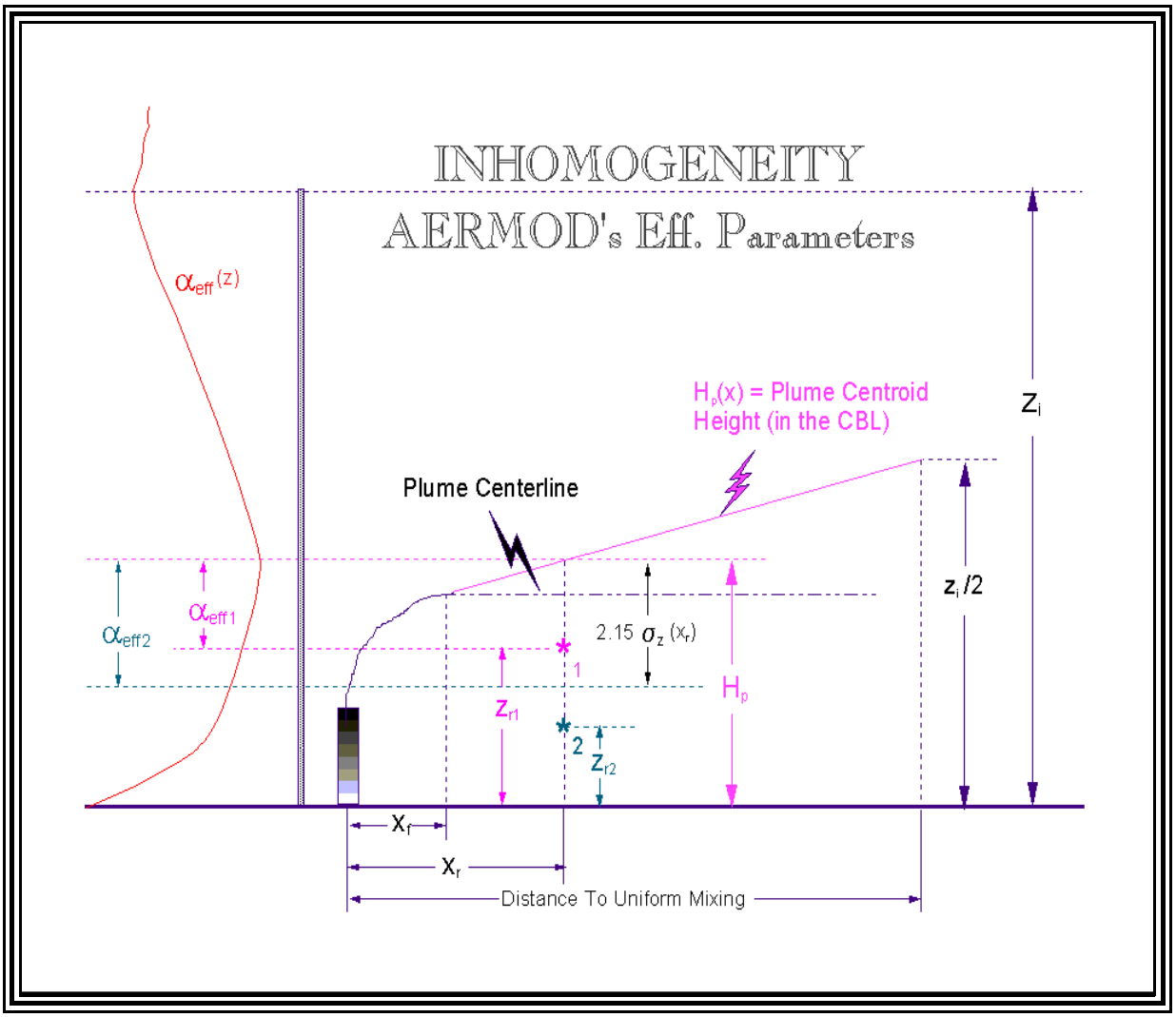

Figure 9:AERMOD's Treatment of the Inhomogeneous Boundary Layer

The specific procedure for calculating any effective parameter (denoted here generically as $\underline{\alpha}$) is as follows:

$$\underline{\alpha} = \frac{1}{(h_t - h_b)} \int_{h_b}^{h_t} \alpha\{z\}\, dz\,, \qquad \textbf{(46)}$$

where:

$$h_b = \begin{cases} H_p\{x_r,y_r\}, & \text{if } H_p\{x_r,y_r\} < z_r \\ MAX\{[H_p\{x_r,y_r\} - 2.15\,\sigma_z\{x_{sr}\}], z_r\}, & \text{if } H_p\{x_r,y_r\} > z_r \end{cases}$$

$$h_t = \begin{cases} \sigma\ MIN\{[H\{x_r,y_r\} + 2.15\,\sigma_z\{x_{sr}\}], z_r\}, & \text{if } H_p\{x_r,y_r\} < z_r \\ H_p\{x_r,y_r\}, & \text{if } H_p\{x_r,y_r\} > z_r \end{cases} \qquad \textbf{(47)}$$

and: $H_p \equiv$ *Plume centroid height*.

For all plumes, both limits are bounded by either the z_r or H_p.

In stable conditions, H_p is always set equal to the plume centerline height. That is,

$$H_p = \Delta h_s + h_s, \qquad \textbf{(48)}$$

where:

$\Delta h_s \equiv$ *Stable Source Plume Rise*

$h_s \equiv$ *Stack height corrected for stack tip downwash*.

The stable source plume rise Δh_s is calculated from eq.**(126)**.

In the CBL, the specification of H_p is somewhat more complicated. Because of limited mixing in the CBL the center of mass of the plume will be the plume height close to the source and the mid-point of the PBL at the distance where it becomes well mixed. Beyond final plume rise, H_p is varied linearly between these limits.

Prior to plume stabilization, i.e., $x < x_f$ (distance to plume stabilization)

$$H_p = h_s + \Delta h_{d,p} \qquad \text{for all } x, \qquad \textbf{(49)}$$

where:

$\Delta h_d \equiv$ *Plume rise for the direct source*

$\Delta h_p \equiv$ *Plume rise for the penetrated source*,

and $\Delta h_{d,}$ is estimated from eqs. **(116)** and Δh_p is h_{ep} - h_s where h_{ep} is calculated from eq. **(119)**.

The distance to plume stabilization, x_f , is determined as follows (Briggs, 1971, 1975) :

$$x_f = 49 F_b^{5/8} \qquad for \quad F_b < 55$$
$$and: \quad x_f = 119 F_b^{2/5} \qquad for \quad F_b \geq 55, \tag{50}$$

where the buoyancy flux (F_b) is calculated from eq.**(117)**.

However, for $F_b = 0$ the distance to final rise is calculated from the ISC3 (U.S.EPA, 1995) expression as:

$$x_f = \frac{8 r_s \left(w_s + 3 u_p \right)^2}{w_s u_p} \tag{51}$$

$$where: \quad u_p \equiv wind \;\; speed \;\; at \;\; source height,$$

and the stabilized rise due to momentum alone is:

$$\Delta h_m = \frac{6 r_s w_s}{u_p} \tag{52}$$

$$where: \quad \Delta h_m \equiv momemtum \; rise.$$

Beyond plume stabilization ($x>x_f$), H_p varies linearly between the stabilized plume height ($H\{x_f\}$) and the mid-point of the mixed layer ($z_i /2$). This interpolation is performed over the distance range x_f to x_m, where x_m is the distance at which pollutants first become uniformity mixed throughout the boundary layer.

The distance x_m is taken to be the product of the average mixed layer wind speed and the mixing time scale, $z_i / \overline{\sigma_{wT}}$. That is,

$$x_m = \frac{\bar{u} z_i}{\overline{\sigma_{wT}}}, \tag{53}$$

where the averaging of u and σ_{wT} are taken over the depth of the boundary layer.

For distances beyond x_f , H_p is assumed to vary linearly between the plume's stabilized height, $H\{x_f\}$, and $z_i/2$ such that:

$$H_p = H\{x_f\} + \left(\frac{z_i}{2} - H\{x_f\} \right) \cdot \frac{(x - x_f)}{(x_m - x_f)}. \qquad \textbf{(54)}$$

Furthermore, for all x, H_p is limited to a maximum value of z_i.

Note that in the CBL, both the direct and indirect source will have the same α (effective parameter) values. In eq. **(47)** σ_z is the average of the updraft σ_z and the downdraft σ_z , the maximum value of h_t is z_i , and when $h_b \geq z_i$, $\alpha = \alpha\{z_i\}$.

As discussed previously, when multiple vertical measurements of wind direction are available a profile is constructed by linearly interpolating between measurements and persisting the highest and lowest measurements up and down, respectively. The approach taken for selecting a transport wind direction from the profile is different from the above. The transport wind direction is selected as the mid point of the range between stack height and the stabilized plume height.

5 The Terrain Preprocessor (AERMAP)

CTDMPLUS (Perry, 1992), an EPA regulatory model for complex terrain, uses the dividing streamline concept with terrain characterized as individual idealized terrain features.
As such, the interaction of plume material with the idealized hill (i.e., plume mass partitioning above and below the dividing streamline height, H_c) is considered directly in the calculation of concentration at any receptor defined to be on the hill. Since it is particularly difficult to both represent actual complex terrain as a collection of idealized terrain features and associate each receptor with a unique hill, AERMAP (the terrain preprocessor for AERMOD), operating from a receptor's point of view, samples the landscape around each receptor to objectively specify a representative "hill" height associated with that receptor.

Like the CTDMPLUS terrain preprocessor, AERMAP is also designed to provide the terrain information necessary to calculate H_c (the dividing streamline height and its use in the model is described in section 6.a.). The AERMAP method defines a "height scale" (h_c) that represents the terrain that dominates the flow in the vicinity of the receptor (representative hill height). In other words, h_c can be thought of as the height of the terrain surrounding the receptor that will most influence the flow in stable conditions. This height, h_c , is not necessarily the highest elevation in the modeling domain nor is it necessarily the actual peak of any individual terrain feature. Use of the height scale (instead of an actual terrain feature height, selected by the user as in CTDMPLUS) to calculate H_c, provides a reasonable and more objective method for calculating the weighting factor, f, in eq **(59)**.

In defining h_c for a given receptor, all terrain elevations within the user defined modeling domain and the distances of those elevations from the receptor are considered. Therefore each receptor may have a unique height scale. Consider a domain of interest, and a receptor at (x_r,y_r,z_r) for which an associated terrain height scale is needed. The inherent assumption in this objective scheme is that 1) the effect of surrounding terrain on the flow near the receptor decreases with increasing distance and 2) the effect increases with increasing elevation of that terrain. In other words, the "effective elevation", h_{eff}, of surrounding terrain is a function of its actual elevation and its distance from the receptor.

The terrain height scale (h_c) is determined for each receptor location (x_r , y_r) by use of the following procedure: The weighted effective height surface (h_{eff}) is calculated for each terrain point (x_t , y_t) in the domain of interest as follows.

$$h_{eff}\{x_t, y_t\} = z_t \, f_t\{x_{rt}/r_o\} , \qquad \textbf{(55)}$$

where:

$$x_{rt} = \left[(x_r - x_t)^2 + (y_r - y_t)^2 \right]^{1/2} \qquad \textbf{(56)}$$

$$\begin{aligned}
f_t\{x_{rt}/r_o\} &\equiv \textit{Terrain weighting function} = \exp(-x_{rt}/r_o) \qquad \textbf{(57)} \\
r_o &= 10.0\,\Delta h_{\max} \\
x_{rt} &\equiv \textit{Horizontal Distance between receptor and terrain locations} \\
h_{eff}\{x_t, y_t\} &\equiv \textit{Weighted effective height surface} \\
\Delta h_{\max} &\equiv \textit{Difference between the maximum \& minimum terrain heights within the entire modeling domain} \\
r_o &\equiv \textit{Terrain weighting factor}.
\end{aligned}$$

For a given receptor, h_{eff} is calculated for all terrain points within the modeling domain, thereby creating an effective height surface. This is why it is very desirable to have the terrain information already digitized or in gridded form. The height scale for each receptor is then related to the maximum effective value. **Figure 10** gives an example of how this effective height surface is determined for a specific receptor.

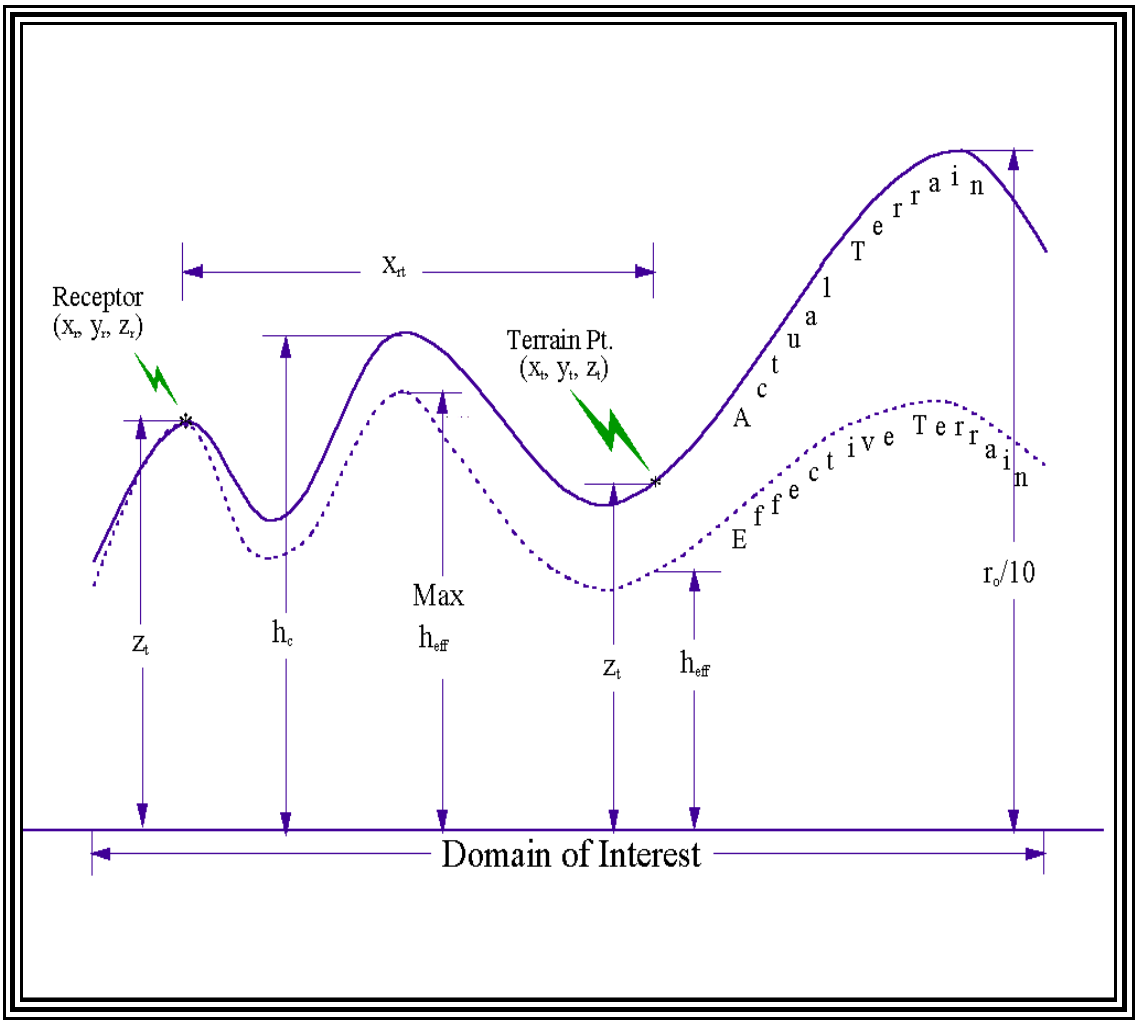

Figure 10: Finding h_c for a specific receptor (x_r, y_r, z_r). For simplicity this figure presents only one direction within the domain of interest. To calculate h_c for an actual domain this procedure would have to be performed in all directions about the receptor.

Once the effective height surface is defined through eq. **(55)**, the height scale for a given receptor is defined as the actual height of the terrain point having the largest effective height (terrain with the greatest effect on the receptor). That is, h_c is the actual terrain elevation at the location with the maximum h_{eff}.

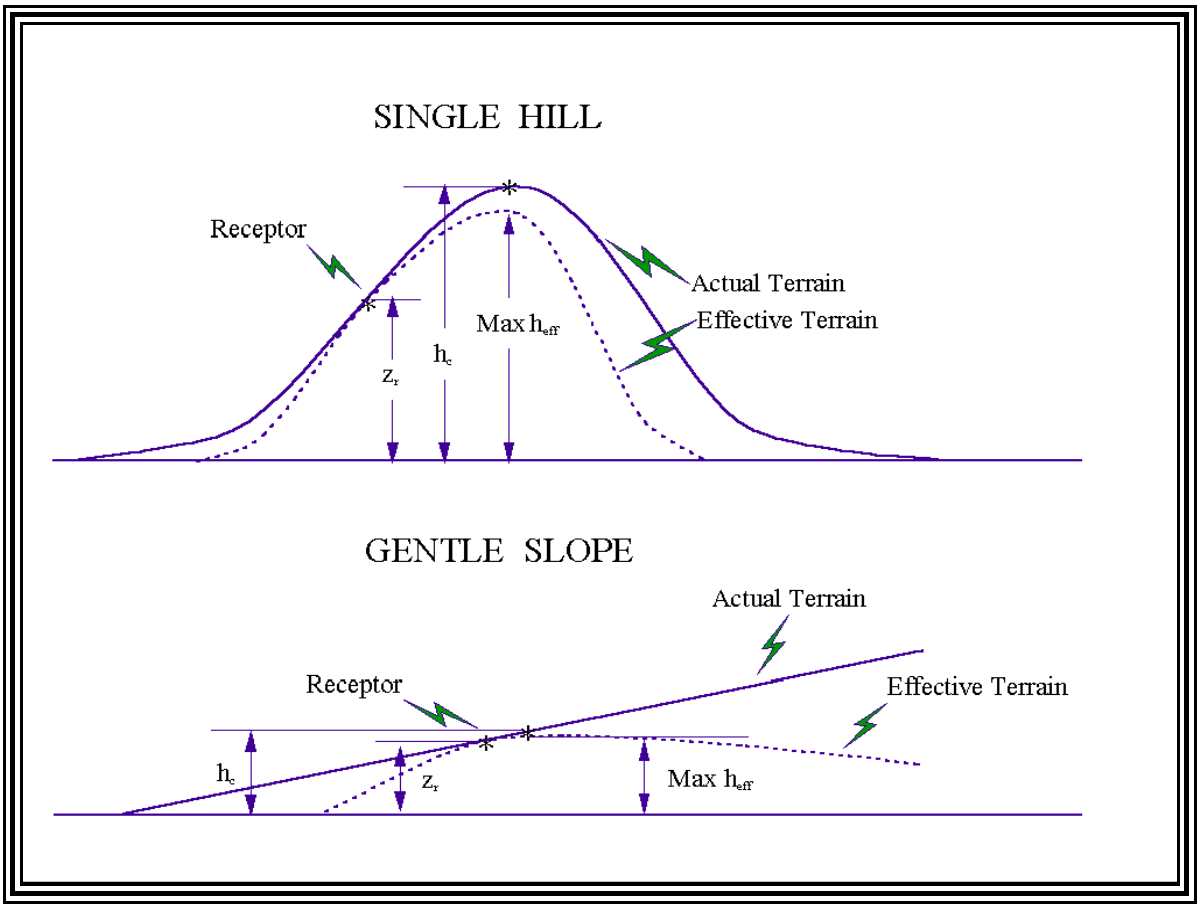

Figure 11: Determination of h_c for a single hill and gently sloping terrain

Figure 11 provides an example of how h_c is determined for two different cases: 1) a single hill, and 2) gently slopping terrain. These cases demonstrate that this procedure produces a height scale that is consistent with the critical dividing streamline height . **Figure 11** shows that for the single hill h_c is the hill height; what one would expect for the H_c in this case. For a gentle slope one would expect h_c to be close to the height of the receptor. **Figure 11** demonstrates that for the gentle slope the height scale is essentially equal to the receptor height.

The height scale is computed by solving eq. **(55)** at the terrain point associated with the maximum h_{eff} such that:

$$h_c\{x_r, y_r\} = \frac{h_{eff}\big|_{\max}}{f_t\{x_{rt}/r_o\}}, \tag{58}$$

where:

$h_{eff}\big|_{\max} \equiv$ *maximum* h_{eff} *within the modeling domain*

$h_c \equiv$ *receptor specific height scale*.

6 The AMS/EPA Regulatory Model AERMOD

AERMOD is a steady-state plume model. It is designed to apply to source releases and meteorological conditions that can be assumed to be steady over individual modeling periods (typically one hour or less). AERMOD has been designed to handle the computation of pollutant impacts in both flat and complex terrain within the same modeling framework. In fact, with the AERMOD structure, there is no need for the specification of terrain type (flat, simple, or complex) relative to stack height since receptors at all elevations are handled with the same general methodology. To define the form of the AERMOD concentration equations, it is necessary to simultaneously discuss the handling of terrain.

6.1 *General Structure of AERMOD Including Terrain*

AERMOD incorporates, with a simple approach, current concepts about flow and dispersion in complex terrain. Generally, in stable flows, a two-layer structure develops in which the lower layer remains horizontal while the upper layer tends to rise over the terrain. This two-layer concept was first suggested by theoretical arguments of Sheppard (1956) and demonstrated through laboratory experiments, particularly those of Snyder et al. (1985). These layers are distinguished, conceptually, by the dividing streamline, denoted by H_c. In neutral and unstable conditions, the lower layer disappears and the entire flow (with the plume) tends to rise up and over the terrain.

A plume embedded in the flow below H_c tends to remain horizontal; it might go around the hill or impact on it. A plume above H_c will ride over the hill. Associated with this is a tendency for the plume to be depressed toward the terrain surface, for the flow to speed up, and for vertical turbulent intensities to increase. These effects in the vertical structure of the flow are accounted for in models such as the Complex Terrain Dispersion Model (CTDMPLUS). However, because of the model complexity, input data demands for CTDMPLUS are considerable. EPA policy (Code of Federal Regulations, 1995) requires the collection of wind and turbulence data at plume height when applying CTDMPLUS in a regulatory application. As previously stated, the model development goals for AERMOD include having methods that capture the essential physics, provide plausible concentration estimates, and demand reasonable model inputs while remaining as simple as possible. Therefore, AERMIC arrived at a terrain formulation in AERMOD that considers vertical flow distortion effects in the plume, while avoiding much of the complexity of the CTDMPLUS modeling approach. Lateral flow channeling effects on the plume are not considered by AERMOD.

AERMOD deals with the two-layer concept in the following way. AERMOD assumes that the value of the concentration on a hill lies between the values associated with two possible extreme states of the plume. One of these states is the horizontal plume that occurs under very stable conditions when the flow is forced to go around the hill. The other extreme state is when the plume follows the terrain vertically (terrain following state) so that its centerline height above terrain is equal to the initial plume height. AERMOD calculates the concentration at a receptor,

located at a position (x_r,y_r,z_r), as the weighted sum of the two limiting estimates. **Figure 12** presents a schematic of the two state concept.

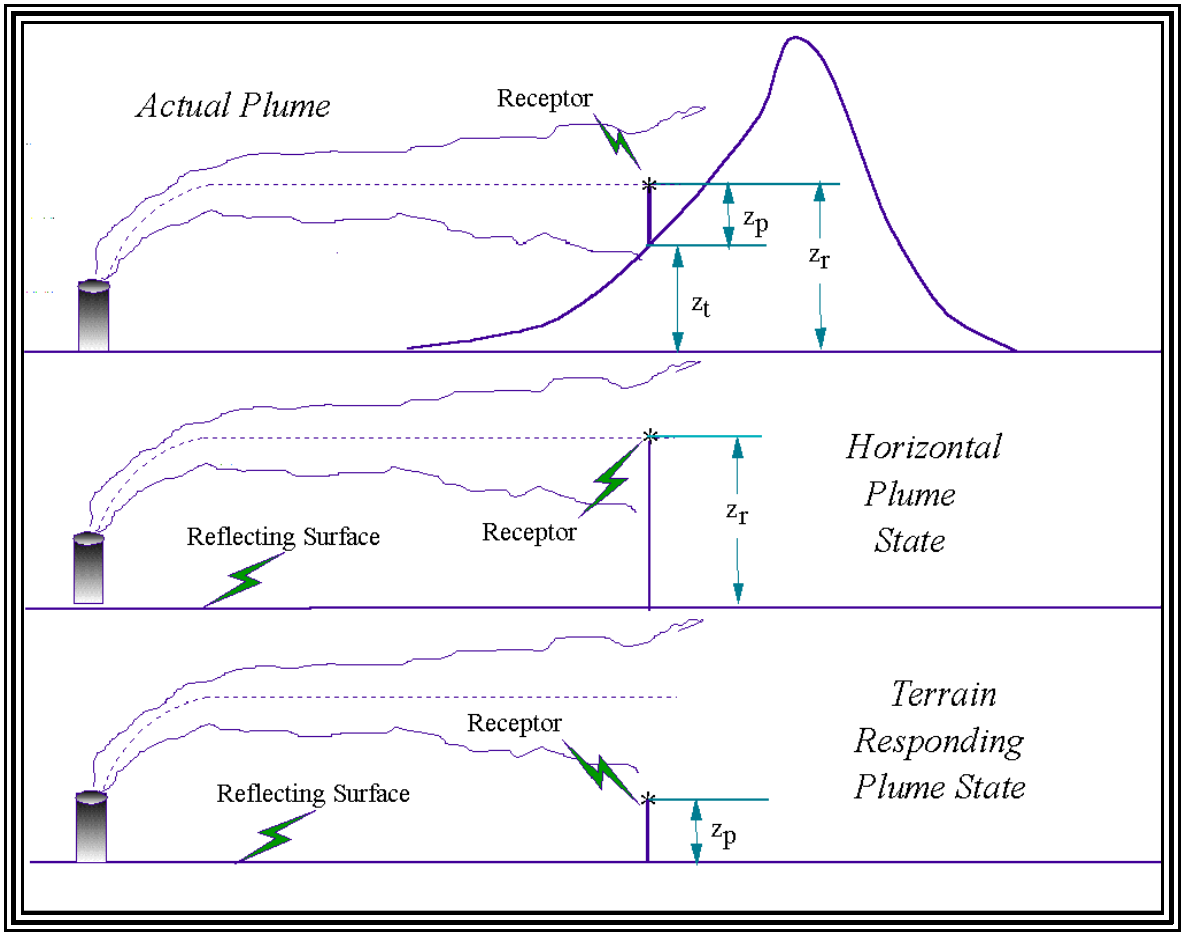

Figure 12: AERMOD Two State Approach. The total concentration predicted by AERMOD is the weighted sum of the two extreme possible plume states.

The relative weighting of the two states depends on: 1) the degree of atmospheric stability; 2) the wind speed; and 3) the plume height relative to terrain. In stable conditions, the horizontal plume "dominates" and is given greater weight while in neutral and unstable conditions, the plume traveling over the terrain is more heavily weighted. The specific approached used to calculate this weighting function is presented below and illustrated in **Figure 13**.

The concentration, estimated by AERMOD, in the presence of the hill is given by

$$C_T\{x_r, y_r, z_r\} = f \cdot C_{c,s}\{x_r, y_r, z_r\} + (1-f) \cdot C_{c,s}\{x_r, y_r, z_p\}, \qquad \textbf{(59)}$$

where:

$C_T\{x_r, y_r, z_r\} \equiv$ *Total concentration*

$C_{c,s}\{x_r, y_r, z_r\} \equiv$ *Concentration from the horizontal plume state*

$C_{c,s}\{x_r, y_r, z_p\} \equiv$ *Concentration from the terrain following plume state*

$f \equiv$ *Plume state weighting function*

$z_p \equiv$ *Height of receptor* (*flagpole height*).

The concentration subscripts (c, s) in eq. **(59)** relate to the total concentration during convective conditions "*c*" and stable conditions "*s*". It is important to note that for any concentration calculation all heights (*z*) are referenced to stack base elevation.

The formulation of the weighting factor draws on the concept of the dividing streamline height, H_c. Using the h_c from AERMAP as the receptor specific height scale ("hill height") H_c is calculated from the same algorithms found in CTDMPLUS (Perry, 1992). That is:

$$1/2 \cdot u^2\{H_c\} = \int_{H_c}^{h_c} N^2 (h_c - z)\, dz, \qquad \textbf{(60)}$$

where:

$$N = \left[\frac{g}{\theta}\frac{\partial\theta}{\partial z}\right]^{1/2}$$

$\equiv$ *Brunt–Vaisala frequency*.

We first define ϕ_p, the fraction of the plume mass below H_c, as

$$\phi_p = \frac{\int_0^{H_c} C_T\{x_r, y_r, z_r\}\, dz}{\int_0^{\infty} C_T\{x_r, y_r, z_r\}\, dz}, \qquad \textbf{(61)}$$

where $C_T\{x_r, y_r, z_r\}$ refers to the concentration in the absence of the hill. Then, the weighting factor, f, which relates to the fraction of plume material (ϕ_p) that is below the height of the dividing streamline (H_c), is given by

$$f = 0.5 \cdot (1 + \phi_p). \qquad \textbf{(62)}$$

Defined this way, when the plume is entirely below the critical dividing streamline, $\phi_p = 1.0$, and $f = 1$, and the terrain concentration is only affected by the flat plume. On the other hand, when the plume is entirely above the critical dividing streamline height, $\phi_p = 0$, and $f = 0.5$. This means that we never allow the plume to approach the terrain responding state completely. That is, even as the plume encounters the terrain and rises up, there is a tendency for some plume material to spread out around the sides. Thus, under purely neutral or unstable conditions, the plume state is half way between the horizontal state and the terrain responding state.

The first term on the right side in eq.**(59)** is the contribution from the horizontal plume state. The second term is the contribution from the terrain responding state, in which the concentration is calculated at the receptor flag pole height, z_p, as $z_p = z_r - z_t$, where z_r is the receptor height (above stack base elevation), and z_t is the terrain height (above mean sea level). Therefore, z_p is defined as the height above terrain. If $z_p = 0.0$, the terrain responding state sees the receptor on the hill as a ground-level receptor. Although a complete terrain responding state is not likely to occur in practice, even under very unstable conditions, its associated concentration value sets one of the possible limits. As seen in eq. **(62)**, we do not allow the actual plume to completely attain this state. Note that in flat terrain (i.e., $z_t = 0$), the concentration equation eq. **(59)** reduces to the form for a single horizontal plume.

Figure 13 illustrates how the weighting factor is constructed and its relationship to the estimate of concentration as a weighted sum of two limiting plume states.

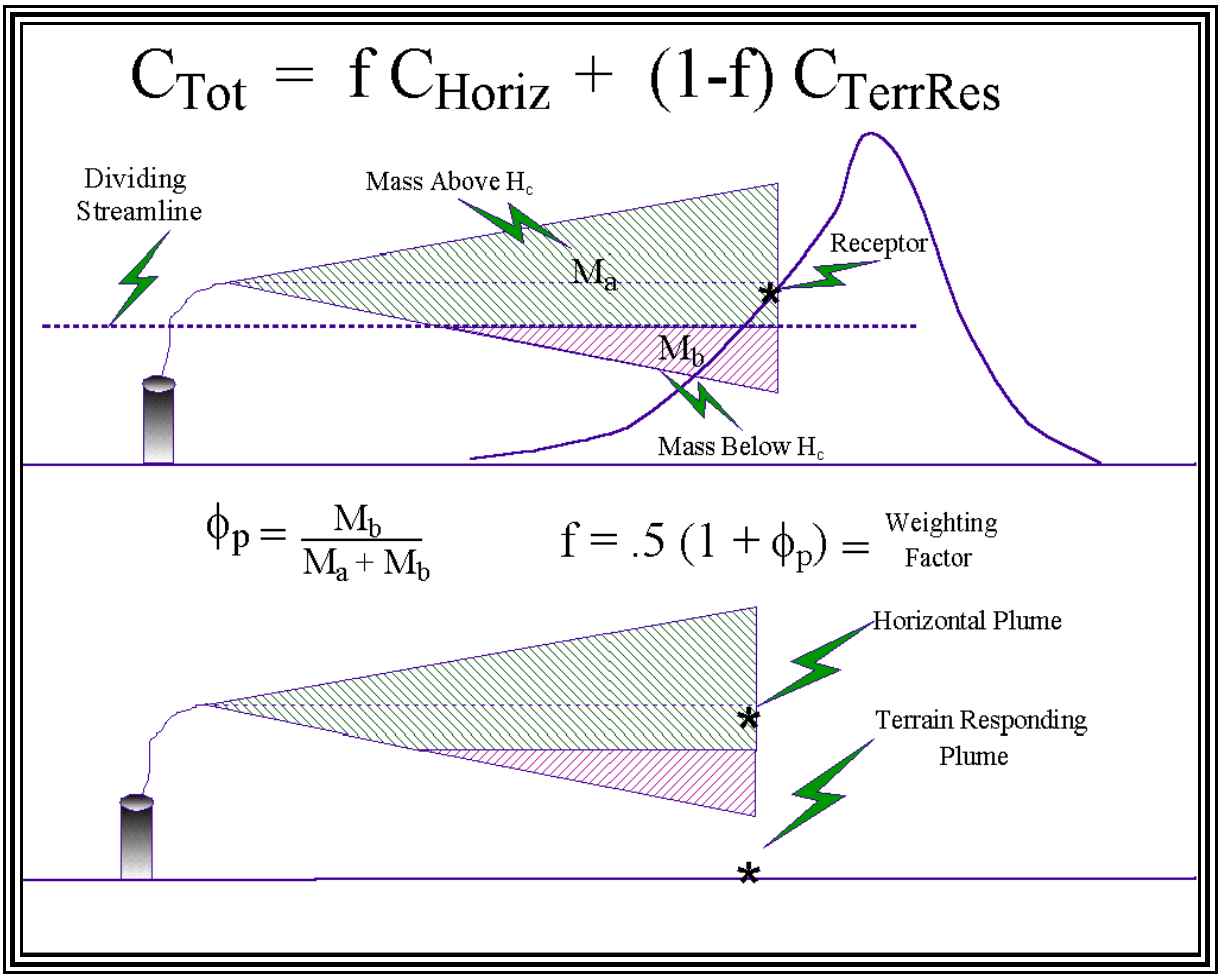

Figure 13: Treatment of Terrain in AERMOD. Construction of the weighting factor used in calculating total concentration.

The general form of the expressions for concentration in each term of eq. **(59)** for both the CBL and the SBL can be written as follows:

$$C\{x,y,z\} = \left(Q/\underline{u}\right) p_y\{y;x\}\, p_z\{z;x\}\,, \qquad \textbf{(63)}$$

where Q is the source emission rate, $\underline{u}$ is the effective wind speed, and p_y and p_z are probability density functions (p.d.f.) which describe the lateral and vertical concentration distributions, respectively. AERMOD assumes a traditional Gaussian p.d.f. for both the lateral and vertical distributions in the SBL and for the lateral distribution in the CBL. The CBL's vertical distribution of plume material reflects the distinctly non-Gaussian nature of the vertical velocity distribution in convectively mixed layers. The specific form for the concentration distribution in the CBL is found in eq. **(66)** which uses the notation $C_c\{x,y,z\}$. Similarly, in the SBL, the

concentration takes the form of eq. **(77)** and used the notation $C_s\{x.y.z\}$.

AERMOD simulates five different plume types depending on the atmospheric stability and on the location in and above the boundary layer: 1) direct, 2) indirect, 3) penetrated, 4) injected and 5) stable. All of these plumes will be discussed, in detail, throughout the remainder of this document. During stable conditions, plumes are modeled with the familiar horizontal and vertical Gaussian formulations. During convective conditions ($L<0$) the horizontal distribution is still Gaussian; the vertical concentration distribution results from a combination of three plume types: 1) the direct plume material within the mixed layer that initially does not interact with the mixed layer lid; 2) the indirect plume material within the mixed layer that rises up and tends to initially loft near the mixed layer top; and 3) the penetrated plume material that is released in the mixed layer but, due to its buoyancy, penetrates into the elevated stable layer.

During convective conditions, AERMOD also handles a special case referred to as an injected source where the stack top (or release height) is greater than the mixing height. Injected sources are modeled as plumes in stable conditions, however the influence of the turbulence and the winds within the mixed layer are considered in the inhomogeneity calculations as the plume material passes through the mixed layer to reach receptors.

6.2 *AERMOD Concentration Predictions in the CBL*

In its formulation of the vertical distribution for the CBL, AERMOD parts company with traditional Gaussian models such as ISC3. Since downdrafts are more prevalent in the CBL than updrafts, the observed vertical concentration distribution is not Gaussian. **Figure 14** presents a schematic representation of an instantaneous plume in a convective boundary layer and its corresponding ensemble average. The base concentration prediction in AERMOD is representative of a one hour average. Notice that since a larger percentage of the instantaneous plume is effected by downdrafts, the ensemble average has a general downward trend. Since downdrafts are more prevalent the average velocity of the downdrafts is correspondingly weaker than the average updraft velocity to insure that mass is conserved.

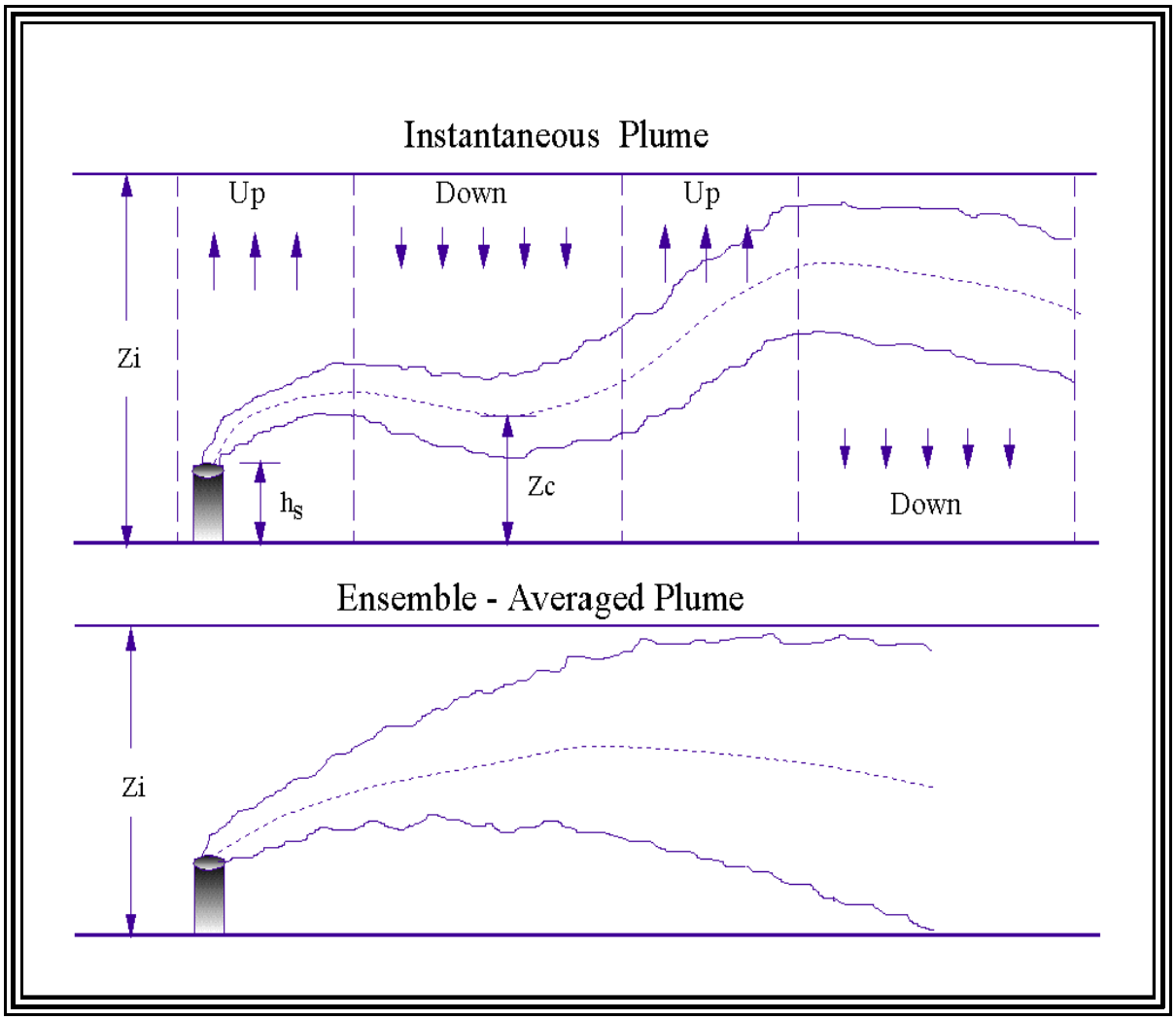

Figure 14: Instantaneous and corresponding ensemble-averaged plume in the CBL

The instantaneous plume is assumed to have a Gaussian concentration distribution about its randomly varying centerline. The mean or average concentration is found by summing the concentrations due to all of the random centerline displacements. This averaging process results in a skewed distribution which AERMOD represents as a bi-Gaussian p.d.f. (i.e., one for updrafts and the other for downdrafts). **Figure 15** shows the superposition of the updraft and downdraft plumes.

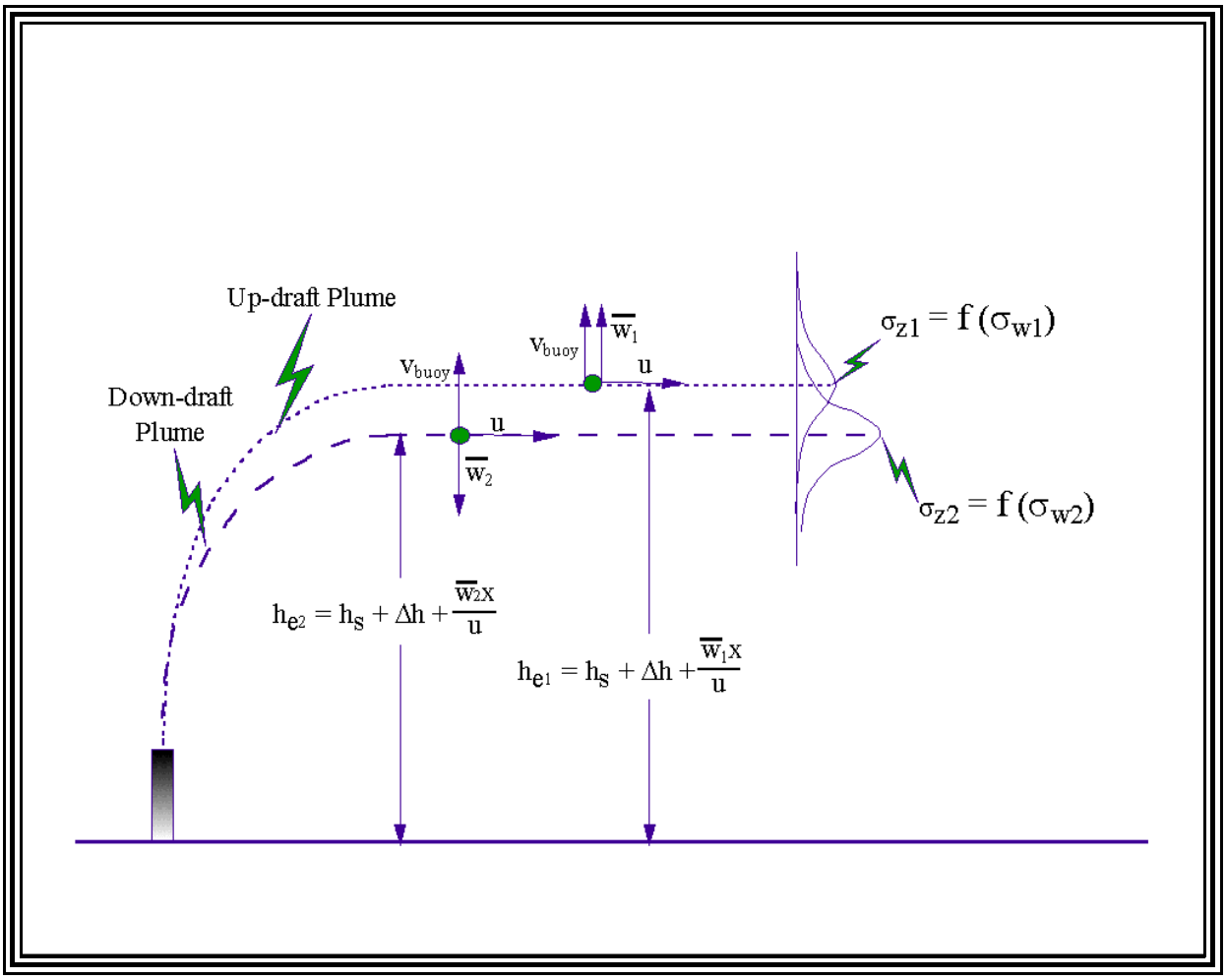

Figure 15: AERMOD's pdf approach for plume dispersion in the CBL. AERMOD approximates the skewed distribution by superimposing two Gaussian distributions, the updraft and downdraft distributions.

The dispersion algorithms for the convective boundary layer (CBL) are based on Gifford's (1959) meandering plume concept in which a small "instantaneous" plume wanders due to the large eddies in a turbulent flow. The specific model form is a probability density function (p.d.f.) approach in which the distribution of the centerline displacement is computed from p_w and p_v, the p.d.f. of the random vertical (w) and lateral (v) velocities in the CBL, respectively. This approach is discussed in Misra (1982), Venkatram (1983) and Weil, et al. (1988). The total vertical displacement z_c of the plume centerline is based on the superposition of the displacements due to the random w and the plume rise as described in Weil et al. (1986, 1997). Thus, the AERMOD approach extends Gifford's model to account for plume rise. In addition, it includes a skewed distribution of z_c because p_w in the CBL is known to be skewed; however, the lateral plume displacement is assumed to be Gaussian.

For material dispersing within a convective layer, the conceptual picture (see **Figure 14**) is a

plume embedded within a field of updrafts and downdrafts that are sufficiently large to displace the plume section within it. The p.d.f. of the plume centerline height z_c is found from the p.d.f. of w,(i.e., p_w), as discussed in Weil (1988), and z_c is obtained by superposing the plume rise (Δh) and the displacement due to the random convective velocity (w):

$$z_c = h_s + \Delta h + \frac{wx}{u}, \qquad \textbf{(64)}$$

where h_s is the stack height (corrected for stack tip downwash), u is the mean wind speed (a vertical average over the convective boundary layer) and x is the downwind distance. The Δh above includes source momentum and buoyancy effects as given by eq. **(116)** below (see Briggs, 1984).

A good approximation to the P_w in the CBL has been shown to be given by the superposition of two Gaussian distributions (e.g., Baerentsen and Berkowicz ,1984; Weil, 1988) such that

$$p_w = \frac{\lambda_1}{\sqrt{2\pi}\sigma_1} exp\left(- \frac{(w - \overline{w_1})^2}{2\sigma_1^2} \right) + \frac{\lambda_2}{\sqrt{2\pi}\sigma_2} exp\left(- \frac{(w - \overline{w_2})^2}{2\sigma_2^2} \right), \qquad \textbf{(65)}$$

where λ_1 and λ_2 are weighting coefficients for the two distributions (1=updrafts, 2=downdrafts) and $\lambda_1 + \lambda_2 = 1$. The $\overline{w_i}$ and σ_i $(I = 1,2)$ are the mean vertical velocity and standard deviation for each distribution and are assumed to be proportional to σ_w. A simple approach for finding $\overline{w_1}$, $\overline{w_2}$, σ_1 , σ_2 , λ_1 , λ_2 as a function of σ_w and the vertical velocity skewness $S = \overline{w^3} / \sigma_w^3$ is given by Weil (1990, 1997).

In the p.d.f. approach used here (Weil et al., 1997), there are three primary sources that contribute to the modeled concentration field: 1) the "direct" or real source at the stack, 2) an "indirect" source that the model locates above the CBL top to account for the slow downward dispersion of buoyant plumes that "loft" or remain near, but below, z_i , and 3) a "penetrated source" that contains the portion of plume material that has penetrated into the stable layer above z_i. The direct source describes the dispersion of plume material that reaches the ground directly from the source via downdrafts. The indirect source is included to treat the first interaction of the "updraft" plume with the elevated inversion - that is, for plume sections that initially rise to the CBL top in updrafts and return to the ground via downdrafts. Image sources are added to treat

the subsequent plume interactions with the ground and inversion and to satisfy the zero-flux conditions at $z = 0$ and at $z = z_i$. This source plays the same role as the first image source above z_i in the standard Gaussian model, but differs in the treatment of plume buoyancy. For the indirect source, a modified reflection approach is adopted in which the vertical velocity is reflected at $z = z_i$, but an "indirect" source plume rise Δh_i is added to delay the downward dispersion of plume material from the CBL top. This is intended to mimic the lofting behavior. The penetrated source is included to account for material that initially penetrates the elevated inversion but subsequently can reenter the CBL via turbulent mixing of the plume and eventual reentrainment into the CBL. **Figure 16** illustrates this three plume approach; a fundamental feature of AERMOD's convective model.

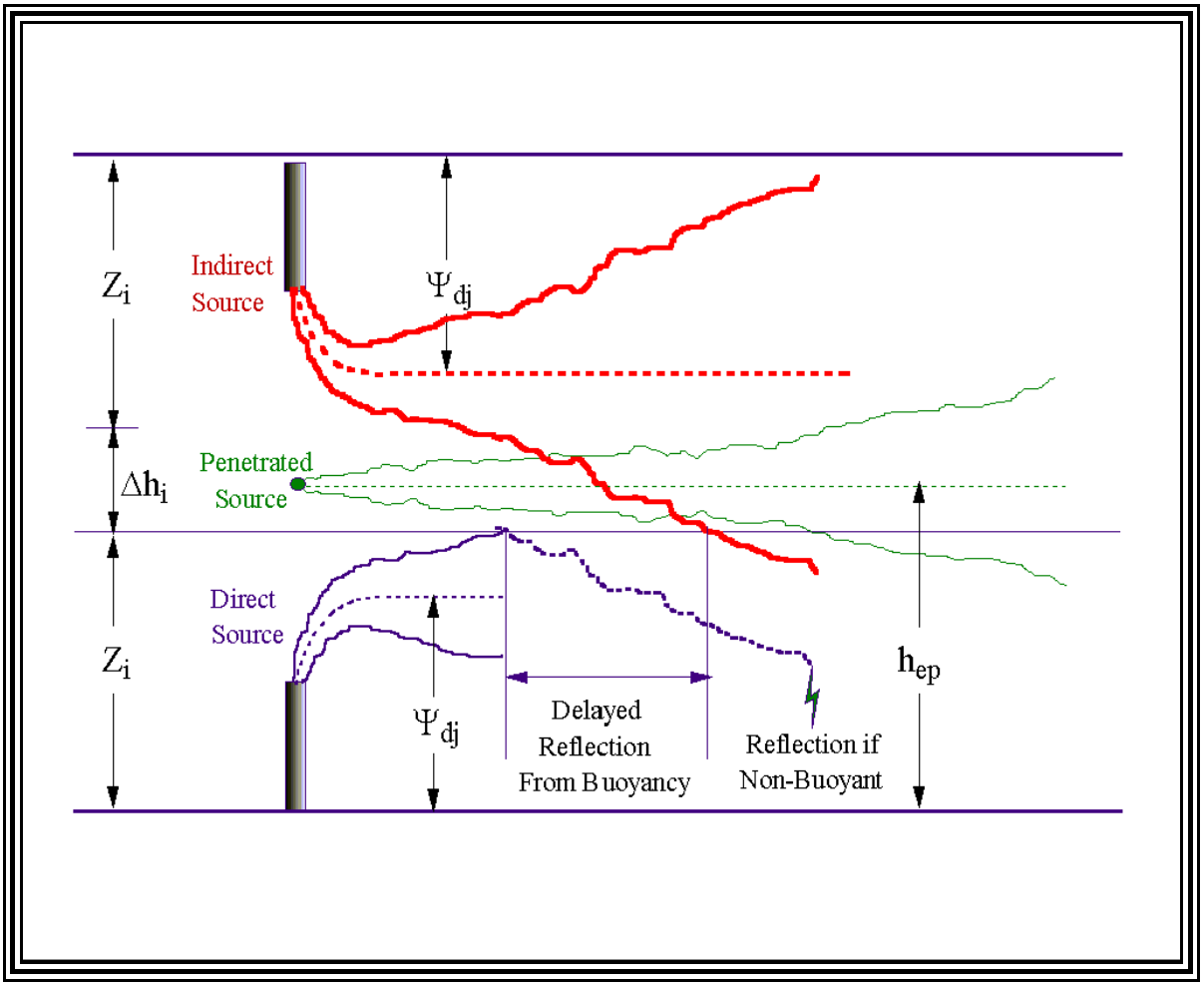

Figure 16: AERMOD's Three Plume Treatment of the CBL

The total concentration in the CBL for the horizontal plume state is

$$C_c\{x_r, y_r, z_r\} = C_d\{x_r, y_r, z_r\} + C_r\{x_r, y_r, z_r\} + C_p\{x_r, y_r, z_r\}, \qquad \textbf{(66)}$$

where:

$C_c\{x_r, y_r, z_r\} \equiv$ *Total concentration in CBL*

$C_d\{x_r, y_r, z_r\} \equiv$ *Direct Source concentration contribution*

$C_r\{x_r, y_r, z_r\} \equiv$ *Indirect Source concentration contribution*

$C_p\{x_r, y_r, z_r\} \equiv$ *Penetrated Source concentration contribution*.

The total concentration for the terrain responding state has the form of eq. **(66)** with z_r replaced by z_p.

In considering penetration, the fraction of the plume mass that remains in the CBL (f_P), is calculated as follows:

$$\begin{aligned} f_p &= 0 && \textit{if} \quad \Delta h_h < 0.5\Delta h_{eq} \\ f_p &= 1 && \textit{if} \quad \Delta h_h > 1.5\Delta h_{eq} \\ f_p &= \frac{\Delta h_h}{\Delta h_{eq}} - 0.5 && \textit{if} \quad 0.5\,\Delta h_{eq} < \Delta h_h < 1.5\,\Delta h_{eq}, \end{aligned} \qquad \textbf{(67)}$$

where $\Delta h_h = z_i - h_s$, and Δh_{eq} is the equilibrium plume rise in a stable environment (see Berkowicz et al., 1986) are calculated as follows:

$$\Delta h_{eq} = \left(2.6^3 P_s + (2/3)^3\right)^{1/3} \Delta h_h \qquad \textbf{(68)}$$

where:

$$P_s = \frac{F_b}{u_p N_h^2 \Delta h_h^3}$$

$$F_b = g w_s r_s^2 \frac{\Delta T_s}{T_s} \equiv \textit{Plume buoyancy flux}$$

$$w_s \equiv \textit{stack exit gas velocity}$$

$$r_s \equiv \textit{inside stack radius}$$

$$N_h = \left[\frac{g}{\theta\{z_i\}} \left.\frac{\partial\theta}{\partial z}\right|_{z > z_i}\right]^{1/2}$$

$$u_p = \textit{wind speed at plume rise}$$

$$(\textit{for the CBL } u_p = u\{h_s\}.$$

$$\left.\frac{\partial\theta}{\partial z}\right|_{z > z_i} \equiv \textit{potential temp grad above } z_i \textit{ in the layer}$$

$$\textit{from } z_i \textit{ to } z_i + 500m$$

6.2.1 DIRECT SOURCE CONTRIBUTION TO CONCENTRATION CALCULATIONS IN THE CBL

Following Weil et al. (1997), the concentration distribution for the horizontal state contribution to the direct plume is given by:

$$C_d\{x_r, y_r, z\} = \frac{Q f_P}{2\pi \underline{u} \sigma_y} \cdot exp\left(\frac{-y_r^2}{2\sigma_y^2}\right) \tag{69}$$

$$\cdot \sum_{j=1}^{2} \sum_{m=0}^{\infty} \frac{\lambda_j}{\sigma_{zj}} \left[exp\left(-\frac{\left(z - \Psi_{dj} - 2mz_i\right)^2}{2\sigma_{zj}^2} \right) + exp\left(-\frac{\left(z + \Psi_{dj} + 2mz_i\right)^2}{2\sigma_{zj}^2} \right) \right],$$

where:

$$\Psi_{dj} \equiv \textit{Height of the Direct Source}$$
$$Q \equiv \textit{Source emission rate}$$
$$z = \begin{Bmatrix} z_r \textit{ for the horizontal plume state} \\ z_p \textit{ for the terrain following state} \end{Bmatrix}$$

Here, Ψ_{dj} and σ_{zj} are the effective source height and vertical dispersion parameter corresponding to each of the two distributions in eq. **(65)**. The dispersion parameters (σ_y, σ_{z1} & σ_{z2}) resulting from the total turbulence are calculated using eqs. **(85)**, and **(98)** thru **(103)**. The subscripts 1 & 2 refer to the updraft & downdraft plumes respectively, and

$$\lambda_1 = \frac{\overline{w_2}}{\overline{w_2} - \overline{w_1}} = \frac{a_2}{a_2 - a_1}$$
$$\lambda_2 = -\frac{\overline{w_1}}{\overline{w_2} - \overline{w_1}} = -\frac{a_1}{a_2 - a_1} \tag{70}$$

with a_1 and a_2 given by eq. **(72)**.

In obtaining Eq.**(69)**, we use an "image" plume to satisfy the no-flux condition at the ground, i.e., an image plume from a source at $z_r = -h_s$, which results in the exponential terms containing $z_r + \Psi_{dj}$ on the right-hand side of Eq.**(69)**. The image source at $z_r = -h_s$ results in a positive flux of material at $z_r = z_i$. To satisfy the no-flux condition there, an image source is introduced at $z_r = 2 z_i + h_s$, which then leads to a series of image sources at $z_r = 2 z_i - h_s$, $4z_i + h_s$, $-4z_i - h_s$, etc.

The height of the direct plume is given by the following expression:

$$\Psi_{dj} = h_{ed} + \frac{\overline{w_j}\, x}{\underline{u}}\,; \qquad j = 1, 2\,, \tag{71}$$

where:

$$\overline{w_j} = a_j\, w_*$$

$$h_{ed} = h_s + \Delta h_d \equiv \textit{Plume height due to buoyancy}$$

with:

$$\Delta h_d \equiv \textit{Direct Source plume rise}\,.$$

The second term in eq. **(71)** is the plume rise due to convection.

Δh_d is calculated using eq. **(116)**, and

$$a_1 = \frac{\sigma_{wT}}{w_*}\left(\frac{\alpha S}{2} + \frac{1}{2}\left(\alpha^2 S^2 + \frac{4}{\beta}\right)^{1/2}\right)$$

$$a_2 = \frac{\sigma_{wT}}{w_*}\left(\frac{\alpha S}{2} - \frac{1}{2}\left(\alpha^2 S^2 + \frac{4}{\beta}\right)^{1/2}\right)\,. \tag{72}$$

Recall that $\underline{\sigma}_{wT}$ is an effective vertical turbulence component and is calculated from eq. **(35)**. The parameters appearing in eq. **(72)** are given by

$$\alpha = \frac{1 + R^2}{1 + 3R^2}$$

$$\beta = 1 + R^2\,;$$

$$S = \frac{\overline{w^3}/w_*^3}{(\sigma_{wT}/w_*)^3} \equiv \textit{Skewness factor}\,, \tag{73}$$

where:

$$\frac{\overline{w^3}}{w_*^3} = 0.125 \qquad \textit{for} \quad H_p\{x\} > 0.1 z_i$$

$$\frac{\overline{w^3}}{w_*^3} = 1.25\frac{H_p\{x\}}{z_i} \qquad \textit{for} \quad H_p\{x\} \le 0.1 z_i$$

and R is assumed to be 2.0 (Weil et al., 1997).

6.2.2 INDIRECT SOURCE CONTRIBUTION TO CONCENTRATION CALCULATIONS IN THE CBL

The concentration contribution from the horizontal state of the indirect source is calculated as follow:

$$C_r\{x_r, y_r, z_r\} = \frac{Q f_P}{2\pi \underline{u} \sigma_y} \cdot exp\left(\frac{-y^2}{2\sigma_y^2}\right) \cdot \sum_{j=1}^{2} \sum_{m=1}^{\infty} \frac{\lambda_j}{\sigma_{zj}} \left[exp\left(-\frac{\left(z_r + \Psi_{rj} - 2mz_i\right)^2}{2\sigma_{zj}^2} \right) + exp\left(-\frac{\left(z_r - \Psi_{rj} + 2mz_i\right)^2}{2\sigma_{zj}^2} \right) \right] \quad \textbf{(74)}$$

where:

$$\Psi_{rj} \equiv \textit{Total height of the Indirect Source plume}.$$

The height of the indirect source Ψ_{rj} is calculated from eq. **(75)**. The total concentration for the terrain responding state has the form of eq.**(74)** with z_r replaced by z_p.

The dispersion coefficients (σ_y, σ_{z1} & σ_{z2}) resulting from the total turbulence (ambient, buoyancy induced & building induced) are calculated using eqs. **(85)** and **(98)** thru **(103)**. The height of the indirect plume is given by the following expression:

$$\Psi_{rj} = h_s + \Delta h_r + \frac{\overline{w_j}\, x}{\underline{u}}; \qquad j = 1, 2, \quad \textbf{(75)}$$

where: $\overline{w_j} = a_j w_*$

and: $\Delta h_r = \Delta h_d - \Delta h_i$

$\Delta h_i \equiv \textit{Indirect Source plume rise}.$

Δh_i is calculated from eq. **(118)**. The a_j's in eq. **(75)** are calculated from eq. **(72)**.

6.2.3 PENETRATED SOURCE CONTRIBUTION TO CONCENTRATION CALCULATIONS IN THE CBL

The penetrated source concentration expression is a simple Gaussian form (for both vertical and horizontal plume distributions). The contribution from the horizontal plume state is given by the following:

$$C_p\{x_r, y_r, z_r\} = \frac{Q(1-f_p)}{2\pi \underline{u}\sigma_{yp}\sigma_{zp}} exp\left[-\frac{y_r^2}{2\sigma_{yp}^2}\right] \cdot \sum_{m=-\infty}^{\infty}\left[exp\left(-\frac{\left(z_r - h_{ep} - 2mz_{ieff}\right)^2}{2\sigma_{zp}^2}\right) + \exp\left(-\frac{\left(z_r + h_{ep} + 2mz_{ieff}\right)^2}{2\sigma_{zp}^2}\right)\right], \quad \textbf{(76)}$$

where:

$C_p\{x_r, y_r, z_r\}$ ≡ *Penetrated Source concentration contribution*

h_{ep} ≡ *Height of the Penetrated Source*

z_{ieff} ≡ *Height of the reflecting surface in a stable layer*.

The total concentration for the terrain responding state has the form of eq.**(76)** with z_r replaced by z_p.

The dispersion coefficients (σ_{yp} & σ_{zp}) resulting from the total turbulence (ambient, buoyancy induced & building induced) are calculated using eq.**(86)**.

6.3 *Concentrations in the SBL Calculated by AERMOD*

The form of the AERMOD concentration expression, for stable conditions ($L > 0$), is similar to that used in ISC3.

$$C_s\{x_r, y_r, z_r\} = \frac{Q}{\sqrt{2\pi}\,\underline{u}\,\sigma_{zs}} \cdot F_y \cdot \sum_{m=-\infty}^{\infty} \left[exp\left(- \frac{\left(z_r - h_{es} - 2mz_{ieff}\right)^2}{2\sigma_{zs}^2} \right) + \exp\left(- \frac{\left(z_r + h_{es} + 2mz_{ieff}\right)^2}{2\sigma_{zs}^2} \right) \right], \quad \textbf{(77)}$$

where:

$C_s\{x_r, y_r, z_r\}$ ≡ *Stable Source concentration contribution*

h_{es} ≡ *Height of the Stable Source*

F_y ≡ *Lateral distribution function* (*with meander*).

Although in stable conditions there is no analogous (to that in the CBL) lid to the mechanically mixed layer, AERMOD retards the plume material from unrealistically spreading into the region above the mixed layer height where the turbulence level is expected to be too small to support such plume mixing. When the final effective plume height is well below z_{im} (eq.**(13)**), we assume that the plume can not be vertically mixed above z_{im} and the plume is reflected back into the mixed layer. When the edge of the stabilized plume reaches the level of z_{im} , the height at which vertical mixing is assumed to cease is allowed to rise up with the spreading plume to remain at a level near the upper edge of the plume. In this way, plume reflection is allowed, consistent with the lack of vertical turbulence aloft, but there is no strong concentration doubling effect as occurs with reflections off of an assumed hard lid. With this quasi-lid approach, AERMOD allows the plume to disperse downwards, but where the turbulence above is low, vertical plume growth is limited by a reflecting surface that is defined by eq. **(78)**. The downward dispersion is determined by σ_w averaged from the receptor to the effective plume height. This means that if the effective plume height is above the mixed layer height, z_{im}, the calculation of the average σ_w will include regions in which σ_w is small. This will result in a decrease in both the average σ_w and downward plume spread as the effective height increases.

When the plume buoyancy carries the rising plume into the relatively non-turbulent layer above z_{im}, the reflecting surface is still placed at 2.15 σ_{zs} above the effective plume height because there will be plume spread due to plume buoyancy and downward mixing is still important. Therefore, in the SBL plume material is assumed to reflect off an elevated surface which is defined as

$$z_{ieff} = MAX\left[\left(h_{es} + 2.15\,\sigma_{zs}\{h_{es}\} \right);\ z_{im} \right], \quad \textbf{(78)}$$

where σ_{zs} in eq. **(78)** is determined from eq. **(87)** with σ_{wm} and u evaluated at h_{es}; not as an effective parameter. It is important to note that z_{ieff} depends on downwind distance since σ_{zs} is distance dependent. In fact, as eq. **(78)** suggests, this effective reflecting surface is only folding back the extreme tail of the upward distribution. Also, if $z_r \geq z_{ieff}$ then z_{ieff} is set equal to ∞. This approach is also implemented for the penetrated source. For the penetrated and injected sources z_{ieff} is calculated using eq. **(78)** with σ_{zs} and h_{es} replaced by σ_{zp} and h_{ep} respectively.

In AERMOD we include the effect that lower-frequency, non-diffusing eddies (i.e., meander) have on plume concentration. We include the effects of meander only in the SBL since it not expected to have a significant effect in the CBL.

Meander (or the slow lateral plume shift due to wind direction shifting during the modeling period) decreases the likelihood of seeing a coherent plume at long travel times from sources. This effect on plume concentration could best be modeled with a particle trajectory model, since these models estimate the concentration at a receptor by counting the number of times a particle is seen in the receptor volume. However, as a simple steady state model, AERMOD is not capable of producing such information. AERMOD accounts for meander by interpolating between two limits of the horizontal distribution function: the coherent plume limit and the random plume limit. For the coherent plume, the horizontal distribution function has the familiar Gaussian form:

$$F_{yC} = \frac{1}{\sqrt{2\pi}\sigma_y} \exp\left(\frac{-y}{2\sigma_y}\right)^2 \qquad \textbf{(79)}$$

$$\textit{where} \quad F_{yC} \equiv \textit{horizontal distribution function for a coherent plume}$$

When the plume's spread is assumed to be totally random, plume material will be uniformly distributed through an angle of 2π. Therefore, for the random plume limit, the horizontal distribution function can be written as follows:

$$F_{yR} = \frac{1}{2\pi x_r} \tag{80}$$

$$\text{where} \qquad F_{yR} \equiv \text{horizontal distribution function for a random plume}$$

To insure that as $x_r \to 0$ (a limit where the random or meander component should have minimum weight), F_{yR} does not approach ∞, we do not allow F_{yR} to grow larger than F_{yC}.. That is:

$$F_{yR} = MIN\left[\frac{1}{2\pi x_r}; F_{yC}\right] \tag{81}$$

Having defined the two limits (eq. **(79)** and eq. **(81)**), we can now interpolate between them by assuming that the total horizontal "energy" is distributed between the wind's mean and turbulent component. Noticing that close to the source, we can think of the horizontal wind as being composed of a mean component $\bar{u}$, and random components σ_u and σ_v. Then the total horizontal wind "energy" can be written as

$$\sigma_h = 2\sigma_v^{\ 2} + \bar{u}^2, \tag{82}$$

if we assume that $\sigma_u = \sigma_v$. The random energy component is initially $2\sigma_v^2$ and becomes equal to σ_h^2 at large travel times from the source when information on the mean wind at the source becomes irrelevant to the predictions of the plume's position. We can represent this evolution of the random component of the horizontal wind energy through the equation:

$$\sigma_r^{\,2} = 2\sigma_v^{\,2} + \bar{u}^2\left(1 - \exp\left(\frac{-x_r}{\underline{u}T_r}\right)\right) \qquad \textbf{(83)}$$

$$\begin{aligned} where \quad \sigma_r^{\,2} &\equiv random\ energy \\ \bar{u} &= \sqrt{\underline{u}^2 - 2\sigma_v^{\,2}} \\ &\equiv mean\ wind \\ T_r &\equiv time\ scale \\ &= 24hrs \end{aligned}$$

T_r is a time scale at which mean wind information at the source is no longer correlated with the location of plume material at a downwind receptor. Analyses involving autocorrelation of wind statistics, such as Brett and Tuller (1991), as well as physical intuition, suggest that after a period of one complete diurnal cycle ($T_r = 24$ hours), a "randomized" state of the plume transport would be realized. From eq. **(83)** we can see that at small travel times, $\sigma^2{}_r = 2\sigma_v^{\,2}$,while at large travel times (distances) $\sigma_r^{\,2} = 2\sigma_v^{\,2} + \overline{u^2}$, which is the total horizontal kinetic energy (i.e. σ_h^2) of the fluid. Based on the percentage of random energy contained in the system (i.e., $\sigma_r^{\,2}/\sigma_h^{\,2}$) we can effectively weight the relative contributions of the coherent and random horizontal distribution functions to obtain a composite distribution function as follows:

$$F_y = F_{yC}\left(1 - \sigma_r^{\,2}/\sigma_h^{\,2}\right) + F_{yR}\left(\sigma_r^{\,2}/\sigma_h^{\,2}\right) \qquad \textbf{(84)}$$

The total concentration for the terrain responding state has the form of eq. **(77)** with z_r replaced by z_p.

6.4 *Estimation of Dispersion Coefficients*

The standard deviations for both the lateral and vertical concentration distributions (σ_y and σ_z respectively) result from the combined effects of: ambient turbulence (σ_a); turbulence induced by plume buoyancy (σ_b); and, enhancements from building wake effects (σ_d).

Dispersion ($\sigma_{ya,za}$), induced by ambient turbulence, is known to vary significantly with height, having its strongest variation near the earth's surface. Unlike present regulatory models, AERMOD has been designed to account for this height variation.

In our earlier AERMOD formulations for σ_{ya} & σ_{za} we attempted to account for vertical variations in turbulence through treatment of vertical inhomogeneity. However, comparisons made using the Prairie Grass data showed this approach to be inadequate. Therefore, the current expression

for σ_{za} is a combination of a direct treatment of surface dispersion and the more traditional approach based on Taylor (1921) for elevated dispersion. With this, we obtained good results for all SBL comparisons. However, the results in the CBL indicated that our treatment of lateral dispersion near the surface was problematic. We corrected this with an empirical relationship for σ_{ya} near the surface using the full (CBL and SBL) Prairie Grass data set. In the remainder of this section we will describe those formulations for σ_{ya} & σ_{za} that resulted from this empirical analysis.

In the CBL, although the ambient induced dispersion for the Direct (D) and Indirect (I) sources is treated differently than for the Penetrated (P) source, the general approach of combining the effects from ambient turbulence, buoyancy and buildings, is the same. For the Direct and Indirect sources, the total dispersion coefficients (σ_y or σ_z) are calculated from the following general expression (Pasquill and Smith, 1983):

$$\sigma^2_{y,z} = \sigma^2_{ya,zaj} + \sigma^2_b + \sigma^2_{yd,zd}\,, \qquad \textbf{(85)}$$

where:

$\sigma_{y,z} \equiv$ *Total Dispersion – Direct & Indirect* (*D* & *I*)

$\sigma_{ya,zaj} \equiv$ *Ambient Turbulence Induced Dispersion – (D & I)*

$\sigma_b \equiv$ *Buoyancy Induced Dispersion – (D & I)*

$\sigma_{yd,zd} \equiv$ *Downwash Induced Dispersion – (Direct source only)*.

For the penetrated source, the total dispersion is calculated as follows:

$$\sigma^2_{yp,zp} = \sigma^2_{yap,zap} + \sigma^2_{bp}\,, \qquad \textbf{(86)}$$

where:

$\sigma_{yp,zp} \equiv$ *Total Dispersion – Penetrated Source* (*P*)

$\sigma_{yap,zap} \equiv$ *Ambient Induced Dispersion – (P)*

$\sigma_{bp} \equiv$ *Buoyancy Induced Dispersion – (P)*.

and building wakes are assumed to have little influence.

For the injected source, the total dispersion is calculated by eq. **(87)** as a source in stable

conditions.

In the SBL, the total dispersion is calculated as follows.

$$\sigma^2_{ys,\,zs} = \sigma^2_{yas,\,zas} + \sigma^2_{bs} + \sigma^2_{yd,\,zd}\,, \qquad \textbf{(87)}$$

where:

$\sigma_{ys,zs}$ ≡ *Total dispersion for the Stable source*

$\sigma_{yas,zas}$ ≡ *Ambient turbulence induced dispersion* (*SBL*)

σ_{bs} ≡ *Buoyancy induced dispersion – Stable source* (*S*)

$\sigma_{yd,zd}$ ≡ *Downwash induced dispersion* – (*S*).

6.4.1 AMBIENT TURBULENCE FOR USE IN CALCULATING DISPERSION

6.4.1.1 *Lateral Dispersion from Ambient Turbulence*

For the Direct and Indirect sources in the CBL the ambient component of the lateral dispersion is determined as follows:

$$\sigma_{ya} = \frac{\underline{\sigma_{vT}}\; x}{\underline{u}\,(1 + \alpha\,\mathrm{X})^p}\,, \qquad \textbf{(88)}$$

where:

$X = \dfrac{\underline{\sigma_{vT}}\; x}{\underline{u}\; z_i}$

x ≡ *Downwind distance, m*

$\alpha = z_i / h_{ed}$; *typically of order* 100

and: h_{ed} ≡ *Direct Source plume height less the effect from random convective velocities*.

The direct source plume height h_{ed} is calculated using eq. **(116)**.

The form of eq. **(88)**, with $\alpha = 78$ and $p = 0.3$, follows from an analysis of the lateral spread measured in the Prairie Grass experiment (Barad, 1958).

To account for the variations in release height from that at Prairie Grass we set

$$\alpha = MAX\left\{78\left(\frac{z_{PG}}{h_s}\right);\ 0.7\right\} \qquad \textbf{(89)}$$

The value of h_s, when applied in eq. **(89)** is limited to a minimum of z_{PG}.

For sources in the SBL, the ambient component of the lateral dispersion is determined from

$$\sigma_{yas} = \frac{\underline{\sigma_{yT}}\ x/\underline{u}}{\left(1 + \dfrac{x}{2\underline{u}\,\underline{T_{Lys}}\{h_{es}\}}\right)^{0.3}}, \qquad \textbf{(90)}$$

The Lagrangian time scale, in eq. **(90)** has been inferred from analysis of ground level concentrations in the Prairie Grass (Barad, 1958) experiments (see eqs. **(88)** and **(89)**) and extrapolated to more elevated sources and/or plume heights. This analysis resulted in a T_{Lys} given by

$$T_{Lys} = \frac{z_{im} \cdot z_{\max}}{z_{PG}\,(156\,\underline{\sigma_{vm}})}, \qquad \textbf{(91)}$$

where: $T_{Lys} \equiv Lateral\ Lagrangian\ Time\ Scale\ (SBL)$
$z_{PG} = 0.46m\ (PG\ release\ height)$
$z_{\max} = MAX\left[z; z_{PG}\right],$

and z, z_{PG} are the pollutant release heights. The appearance of z_{max} in the above accounts for plume heights greater than the Prairie Grass source height, z_{PG}, (note that T_{Lys} increases with release height). Furthermore, σ_{vm} in the above is limited by eq. **(44)**.

Substituting eq. **(91)** into eq. **(90)** yields a form for the lateral dispersion in the SBL that is similar to that for the CBL (eq. **(88)**).

The ambient component of the lateral dispersion for the penetrated source (σ_{yap}), i.e. a source

which has been released below z_i,, but penetrates above, is calculated using eqs.**(90)** with h_{es} set equal to h_{ep} (the height of the penetrated source). However, for the injected source, i.e. source released above z_i, no substitution is needed since these sources are modeled as a stable source.

6.4.1.2 *Vertical Dispersion from Ambient Turbulence*

For sources in the SBL, and for injected sources, the ambient portion of the vertical dispersion is composed of an elevated and surface portion. To produce a smooth transition between the expressions the following interpolation formula is used:

$$\sigma_{zas} = \left(1 - \frac{h_{es}}{z_i}\right)\sigma_{zss} + \left(\frac{h_{es}}{z_i}\right)\sigma_{zes}, \qquad \textbf{(92)}$$

where:

$h_{es} \equiv$ *Stable Source plume height above ground*

$h_{es} = h_s + \Delta h_s$

$\sigma_{zss} \equiv$ *Surface portion of* σ_{zas}

$\sigma_{zes} \equiv$ *Elevated portion of* σ_{zas}.

The expression for calculating h_{es} is found in eq.**(127)**.

The elevated portion of the vertical dispersion for the stable source in AERMOD follows the form of the familiar equation:

$$\sigma_{zes} = \frac{\underline{\sigma_{wT}}\, t}{\left(1 + \frac{t}{2T_{Lzs}}\right)^{1/2}}, \qquad where, \quad t \equiv x/\underline{u} \qquad \textbf{(93)}$$

The vertical Lagrangian time scale (T_{Lz}) used in eq. **(93)** is taken from Venkatram ,et al. (1982) as

$$T_{Lzs} = \frac{l}{\underline{\sigma_{wT}}} \qquad \textbf{(94)}$$

This form for T_{Lzs} is also used in CTDMPLUS. The length scale, l, interpolates between the

neutral length scale, l_n , and the stable length scale, l_s, as

$$\frac{1}{l} = \frac{1}{l_n} + \frac{1}{l_s}$$

$$where, \qquad \textbf{(95)}$$

$$l_n = 0.36 h_{es}$$

$$l_s = 0.27 \frac{\sigma_{wT}}{N}$$

Under very stable conditions or at large heights, the composite length scale, l, approaches the stable value, l_s. When conditions are near neutral, N is very small, and l approaches l_n.

Substituting eq. **(95)** into eq. **(94)** and eq. **(93)** results in the following expression that is used by AERMOD to compute the elevated portion of the vertical dispersion for the stable source:

Now, the surface portion of vertical dispersion for the stable source is given by (following from Venkatram, 1992)

SBL Surface:

$$\sigma_{zss} = \sqrt{\frac{2}{\pi}} \frac{u_* x}{\underline{u}} \left(1 + 0.7 \frac{x}{L}\right)^{-1/3}. \qquad \textbf{(97)}$$

In the CBL, the ambient portion of the vertical dispersion, for the Direct and Indirect sources, is also composed of an elevated and surface portion. The penetrated source is assumed unaffected by the underlying surface since this source is assumed to be decoupled from the ground surface by its location above z_i.. The total ambient components of the vertical dispersion for the Direct

$$\sigma_{zes} = \frac{\underline{\sigma_{wT} t}}{\left[1 + 2\underline{\sigma_{wT}}\left(\frac{1}{0.36 h_{es}} + \frac{N}{0.27 \underline{\sigma_{wT}}}\right)\right]^{1/2}} \qquad \textbf{(96)}$$

and Indirect sources is:

$$\sigma_{zaj}^2 = \sigma_{zej}^2 + \sigma_{zs}^2 , \qquad \textbf{(98)}$$

where:

σ_{zaj} ≡ *Ambient vertical dispersion for the updraft & downdraft plumes* ($j = 1,2$) *for both the Direct & Indirect sources*

σ_{zej} ≡ *Elevated portion of* σ_{zaj}

σ_{zs} ≡ *Surface portion of* σ_{zaj}.

The elevated portion of vertical dispersion for the Direct & Indirect Source is given by the following expression

$$\sigma_{zej} = \alpha_b \left[b_j \frac{w_* x}{\underline{u}} \right], \qquad \textbf{(99)}$$

where:

$$\alpha_b = 0.6 + 0.4 \left(\frac{H_p}{0.1\, z_i} \right) \qquad \textit{for} \quad H_p < 0.1 z_i$$

$$\alpha_b = 1.0 \qquad \textit{for} \quad H_p \geq 0.1 z_i .$$

The b_j's in eq. **(99)** result from the assumed bi-Gaussian p.d.f. (see Weil et al., 1997) and are given by

$$b_1 = R\, a_1 \qquad \textbf{(100)}$$
$$b_2 = -R\, a_2$$

with $R = 2$ and the a_j's given by eq. **(72)**.

The first constant (*0.6*) on the right-hand side of the α_b expression is included to maintain consistency in the neutral-limit forms of σ_z for a surface source in the CBL and the SBL. In this limit, σ_{zs} for the CBL (eq. **(103)**) is zero, and from eq. **(97)** for the SBL, we have $\sigma_{zs} \simeq 0.8\, u_* x / \underline{u}$. To avoid this near-surface, near-neutral discontinuity, the elevated form for σ_z (eq. **(99)**) remains non-zero even for $H_p = 0$. That is, the α_b (for $H_p = 0$) in combination

with eqs. **(98)** and **(99)** and the neutral limit for σ_w (= $1.3\ u_*$ from eq. **(38)**) yields a surface $\sigma_z = 0.8 u_* x / \underline{u}$ in the CBL (consistent with the neutral limit).

For the Direct & Indirect Sources (CBL), the surface portion of the vertical dispersion is calculated from

$$\sigma_{zs} = b_c \left[1 - 10 \cdot \left(\frac{H_p}{z_i} \right) \right] \cdot \left(\frac{u_*}{\underline{u}} \right)^2 \cdot \frac{x^2}{|L|} \qquad for \quad \frac{H_p\{x\}}{z_i} < 0.1$$

$$\sigma_{zs} = 0.0 \qquad for \quad \frac{H_p}{z_i} \geq 0.1, \qquad \textbf{(103)}$$

where: $b_c = 0.5$

The parameterization of eq. **(103)** is based on Venkatram's (1992) results for σ_z due to a surface source in the unstable surface layer; i.e., $\sigma_z \propto \frac{(u_*/\underline{u})^2 x^2}{|L|}$. The parameterization is designed to: 1) agree with Venkatram's result in the limit of a surface release (i.e., $H_p = 0$), 2) provide good agreement between the modeled and observed concentrations from the Prairie Grass experiment , and 3) decrease with source height in the surface layer ($H_p < 0.1\ z_i$) and ultimately vanish for $H_p > 0.1\ z_i$. The constant b_c was chosen to satisfy the second requirement above.

As indicated above the vertical dispersion for the penetrated source should be unaffected by the ground surface. Therefore, the vertical dispersion for the penetrated source is computed as the elevated portion of a stable source (eq. **(96)**) with $N = 0$ and with no contribution from the surface component. The Brunt-Vaisala frequency, H, assumes the neutral limit of zero because the penetrated plume passes through the well mixed layer prior to penetration and back through that layer in dispersing to receptors within the mixed layer.

As always, the injected source is modeled as any source in a stable layer.

6.4.2 BUOYANCY INDUCED DISPERSION (BID) COMPONENT OF σ_y AND σ_z

For the CBL's Direct & Indirect sources, Buoyancy Induced Dispersion (BID) is calculated following Weil (1988)

$$\sigma_b = \frac{0.4\,\Delta h_d}{\sqrt{2}}, \qquad \textbf{(104)}$$

$$\textit{where}: \quad \Delta h_d \equiv \textit{Direct Source plume rise}.$$

The direct source plume rise is calculated from eq. **(116)**.

For the Penetrated Source, BID is calculated as follows:

$$\sigma_{bp} = \frac{0.4(1 - f_p)\,\Delta h_p}{\sqrt{2}}, \qquad \textbf{(105)}$$

where:

$$\Delta h_p \equiv \textit{Penetrated Source plume rise}$$
$$= h_{ep} - h_s$$

and:

$$h_{ep} \equiv \textit{Height of the Penetrated Source above stack base}$$
$$h_s \equiv \textit{Stack height corrected for stack tip downwash}.$$

The height of the penetrated source *(h_{ep})* is calculated from eq. **(119)** in section 3.e.1).

For the Stable Source BID is calculated as follows:

$$\sigma_b = \frac{0.4\,\Delta h_s}{\sqrt{2}}, \qquad \textbf{(106)}$$

$$\textit{where}: \quad \Delta h_s \equiv \textit{Stable Source plume rise}.$$

The stable plume rise *(Δh_s)* is calculated from eq. **(120)**.

6.4.3 COMPONENT OF DISPERSION COEFFICIENTS DUE TO DOWNWASH

In ISC3, the primary effects of building downwash are on the plume growth (σ_y and σ_z) for both the Huber-Snyder (H-S) (Huber and Snyder, 1976 and 1982) and Schulman-Scire (S-S) (Schulman and Scire, 1980) algorithms and on the plume rise for the S-S algorithm. These effects are also present in AERMOD, with some changes due to the fundamental difference in the model formulation, as described below.

In AERMOD as in ISC3, the decision as to whether a plume is affected by downwash is determined by comparing the plume height due to momentum rise at *2* building heights downwind to the Good Engineering Practice (GEP) (Code of Federal Regulations, 1995) height of the building. Direction-specific building dimensions are used in the same manner in ISC3 and AERMOD. For stack heights at least $1.5\ L_b$ (where L_b is the lesser of the building height and width for the specific direction being considered), the H-S algorithm is invoked if downwash effects are to be considered. For stack heights less than $1.5\ L_b$, the S-S algorithm is used.

In both ISC3 and AERMOD, no concentration calculations are made for receptors less than $3\ L_b$ from the source. This is the cavity region that is currently accounted for in the model SCREEN3 (Environmental Protection Agency, 1995). For receptors between $3\ L_b$ and $10\ L_b$ downwind, both ISC3 and AERMOD compute the same building-induced σ_y and σ_z and compare these to the values of σ_y and σ_z due solely to ambient turbulence (which are <u>not</u> the same in the two models and will lead to differences in predictions). The larger of the values of the two sets of σ_y and σ_z are chosen for concentration calculations. One complication for AERMOD is that in convective conditions, only the direct plume is assumed to be affected by downwash conditions. The indirect and penetrated plumes are assumed to escape the effects of downwash. For the direct plume in AERMOD, the average value of σ_y and σ_z for the two components of the direct plume are used for comparison to the building downwash-induced σ_y and σ_z values.

For receptors beyond $10\ L_b$ downwind in AERMOD, the <u>added</u> enhancement in σ_y and σ_z due to the building effects (if positive) is "frozen" at the value attained at $10\ L_b$, and is added to the effects of turbulence, plume buoyancy, etc., in quadrature (the total variance is the sum of the squares of the components of ambient turbulence, buoyancy, and the excess due to downwash see eq. **(85)**). The ISC3 treatment is different in that the building-induced enhancement in σ_y and σ_z at $10\ L_b$ is used to determine a virtual source location as if ambient turbulence was the only factor in the plume growth up to the $10\ L_b$ distance. Due to the complicated nature of the ambient turbulence calculations in AERMOD, the virtual source treatment is not feasible.
For the S-S algorithm in both models, the buoyant plume rise is depressed due to increased entrainment from the building-induced turbulence of ambient air into the buoyant plume. In AERMOD for convective conditions, this condition only affects the direct plume. The following sections summarize the specific enhancements made to both the lateral and vertical dispersion coefficients by AERMOD to account for building downwash effects.

6.4.3.1 *Momentum Plume Rise Equations for Use in Determining Applicability of Downwash*

The application of enhanced dispersion due to building downwash is determined by comparing the plume's height after momentum rise (H_{em}) with the building height. The momentum plume rise equations used by AERMOD are as follows:

For convective conditions,

$$H_{em} = h_s + \left(\frac{3F_m x}{\beta^2{}_i u^2{}_p} \right)^{1/3} \qquad \textbf{(107)}$$

Where: h_s = stack height corrected for stack tip downwash
F_m = momentum flux (eq. **(117)**)
β_1 = entrainment parameter
u_p = wind speed used for plume rise
x = downwind distance

For stable conditions,

$$H_{em} = h_s + \left(3F_m \frac{\sin\left(xN/u_p\right)}{\beta^2{}_1 u_s N} \right) \qquad \textbf{(108)}$$

6.4.3.2 *Enhancement of the Lateral Dispersion Coefficient to Account for Downwash*

Enhancement of horizontal plume spread (σ_y) is assumed to occur when the convective direct plume height $h_{ed} = 1.2\ h_b$ or when the stable plume height $h_{es} = 1.2\ h_b$, where h_b is the building height.

6.4.3.2.1 *Downwind Distance Range Between 3 and 10 Building Heights*

For downwind distances, x, such that $3L_b \le x < 10L_b$,

$$\sigma_{yl} = 0.35\,MIN\left\{L_b, 5h_b\right\} + 0.67\left(x - 3L_b\right) \qquad \textbf{(109)}$$

where: σ_{yl} = lateral spread from combined effects of ambient turbulence and

building downwash

$$L_b = MIN\left\{h_b, h_w\right\}$$

h_b = the projected building height for the current wind direction

and, h_w = the projected building width for the current wind direction.

For convective cases, $\sigma_{ya} = \sigma_{yl}$ and σ_{yd} is not used (see eq. **(85)**). Note that only the direct plume is adjusted for building downwash in this manner. The indirect plume and penetrated plume are not changed. The injected plume is treated the same as the stable plume for building downwash calculations. Similarly, for stable cases, $\sigma_{ys} = \sigma_{yl}$, and σ_{yd} is not used (see eq. **(87)**).

6.4.3.2.2 *Downwind Distance Greater Than 10 Building Heights*

For downwind distances $x > 10L_b$, σ_{yl} is assumed to be a constant equal to its value at $x=10L_b$.

Then for convective conditions σ_{yd} in eq. **(85)** is calculated as

$$\sigma_{yd} = \sqrt{\sigma^2{}_{yl}\left\{10\,L_b\right\} - \sigma_{ya}}$$

where σ_{ya} is calculated from eq. **(88)**. For stable cases σ_{yd} in eq. **(87)** is calculated as

$$\sigma_{yd} = \sqrt{\sigma^2{}_{yl}\left\{10\,L_b\right\} - \sigma_{yas}}$$

where σ_{yas} is calculated from eq. **(90)**.

6.4.3.3 *Enhancement of the Vertical Dispersion Coefficient to Account for Downwash*

Enhancement of vertical plume spread (σ_z) is assumed to occur when the plume height, H_e, calculated as the sum of the physical stack height and the momentum plume rise, is less than or equal to h_b + 1.5 L_b.

6.4.3.3.1 *Downwind Distance Between Three and Ten Building Heights*

For downwind distances, x, such that $3L_b = x < 10L_b$ the vertical spread from the combined

effects of ambient turbulence and building downwash σ_{zl} is taken from ISC3 as

$$\sigma_{zl} = A\left(0.7\,L_b + 0.67\left(x - 3\,L_b\right)\right) \qquad \textbf{(112)}$$

For the domain in which the Huber-Snyder algorithms (Huber and Snyder, 1982) apply, i.e. for $\left(h_b + 0.5\,L_b\right) \le H_e \le \left(h_b + 1.5\,L_b\right)$ the coefficient A in eq. **(112)** is set equal to 1.0. For effective plume heights which are less than $h_b + 0.5L_b$ the Schulmann-Scrie (Schulmann and Scrie, 1980) algorithms apply and the coefficient A in eq. **(112)** is given as follows:

$$\begin{aligned} A &= 1.0 && \text{if} \quad H_e \le h_b \\ A &= \frac{h_b - H_e}{2\,L_b} + 1 && \text{if} \quad h_b < H_e \le h_b + 2\,L_b \\ A &= 0 && \text{if} \quad H_b > h_b + 2\,L_b \end{aligned} \qquad \textbf{(113)}$$

Then for convective conditions σ_{zaj} in eq.**(85)** is set equal to σ_{zl} from eq. **(112)**. Similarly, for stable conditions σ_{zas} in eq. **(87)** is set equal to σ_{zl}.

6.4.3.3.2 *Downwind Distances Greater than Ten Building Heights*

For all downwind distances greater than $10L_b$ σ_{zl} is first calculated for a downwind distance of $10L_b$. Then for convective conditions the building downwash component of the total vertical plume spread calculated after eq. **(85)** as

$$\sigma_{zd} = \sqrt{\sigma^2{}_{zl}\left\{10\,L_b\right\} - \sigma_{zaj}} \qquad \textbf{(114)}$$

And for stable conditions σ_{zd} is determined from eq. **(87)** as

$$\sigma_{zd} = \sqrt{\sigma^2{}_{zl}\left\{10\,L_b\right\} - \sigma_{zas}} \qquad \textbf{(115)}$$

6.5 *Plume Rise* Calculations in AERMOD

6.5.1 PLUME RISE IN THE CBL

For the direct source, Δh_d is taken from (Briggs, 1984) as:

$$\Delta h_d = \left(\frac{3F_m x}{\beta_1^2 u_p^2} + \frac{3}{2\beta_1^2} \frac{F_b x^2}{u_p^3} \right)^{1/3}, \qquad \textbf{(116)}$$

where: $u_p \equiv$ *wind speed used for plume rise*
$\beta_1 \equiv$ *entrainment parameter* ($\beta_1 = 0.6$)

and:

$$F_m = \frac{T}{T_s} w_s^2 r_s^2; \qquad F_b = g w_s r_s^2 \frac{\Delta T_s}{T_s}, \qquad \textbf{(117)}$$

where: $r_s \equiv$ *stack radius corrected for stack tip downwash*.
$\Delta T_s = \left(T_s - T\right)$

It should be noted that u_p is the wind speed used for calculating plume rise. In the CBL u_p is set equal to $u\{h_s\}$. While in the SBL u_p is initially set equal to $u\{h_s\}$ but its final value is determined by iterating.

The indirect source, which we include to treat the no flux condition at $z = z_i$, uses a modified reflection approach in which the reflected vertical velocity is adjusted by the addition of a plume rise term Δh_i, designed to keep the plume aloft (Weil et al., 1997), such that

$$\Delta h_i = \left(\frac{2F_b z_i}{\alpha u_p r_y r_z} \right)^{1/2} \frac{x}{u_p}, \qquad \textbf{(118)}$$

where:

$$r_y r_z = r_h^2 + \frac{a_e \lambda_y^{3/2}}{4} \cdot \frac{w_*^2 x^2}{u_p^2}$$

$\equiv$ *Lateral and vertical dimensions of an assumed elliptical plume cross section*

$$r_h = \beta_2 (z_i - h_s)$$

with: $\alpha = 1.4; \quad \beta_2 = 0.4; \quad \lambda_y = 2.3$

and $a_e = 0.1$ (*dimensionless entrainment parameter*).

The height that the penetrated source achieves above z_i is calculated as the equilibrium plume rise in a stratified environment and is determined by the source buoyancy flux, the stable stratification above z_i, and the mean wind speed. In line with Weil et al. (1997), we assume that the plume height h_{ep} is the centroid of the plume material above the inversion and take $h_{ep} = h_s + \Delta h_{eq}$ for $f_p = 0$ or complete penetration. However, for partial penetration ($f_p > 0$), h_{ep} is chosen as the average of the heights of the upper plume edge $h_s + 1.5\Delta h_{eq}$ and z_i, or

$$h_{ep} = \frac{h_s + z_i}{2} + 0.75 \Delta h_{eq}, \qquad \textbf{(119)}$$

where Δh_{eq} is defined in eq. **(68)**.

6.5.2 PLUME RISE IN THE SBL

Plume rise in the SBL is taken from Weil (1990), which is modified by using an iterative approach which is similar to that found in Perry, et al. (1989). When a plume rises in an atmosphere with a positive potential temperature gradient, plume buoyancy decreases because the ambient potential temperature increases as the plume rises; thus, plume buoyancy with respect to the surroundings decreases. The plume rise equations have to be modified to account for this. This modification (the reader should refer to Weil (1988b) for details) produces the following plume rise formula which is used by AERMOD.

$$\Delta h_s = 2.66\left(\frac{F_b}{N^2 u_p}\right)^{1/3}\left[\frac{N' F_m}{F_b}\sin\left(\frac{N' x}{u_p}\right) + 1 - \cos\left(\frac{N' x}{u_p}\right)\right]^{1/3}, \qquad \textbf{(120)}$$

$$\textit{where}: \qquad N' = 0.7N.$$

The velocity, u_p, and N are evaluated initially at stack height . Once plume rise has been computed from these stack top values, subsequent plume rise estimates are made, iteratively, by averaging the u_p and N values at stack top with these at $z = h_s + \frac{\Delta h_s}{2}$. Equation **(120)** applies only when the plume is still rising.

The distance at which the stable plume reaches its maximum rise is given by the following expression:

$$x_f = \frac{u_p}{N'}\arctan\left(\frac{F_m N'}{F_b}\right), \qquad \textbf{(121)}$$

$$\textit{where}: \qquad x_f \equiv \textit{The distance to final rise}.$$

Upon substituting eq. **(121)** for x in eq. **(120)** the maximum final rise of the stable plume $\Delta h_s\{x_f\}$ reduces to:

$$\Delta h_s\{x_f\} = 2.66\left(\frac{F_b}{u_p N^2}\right)^{1/3}. \qquad \textbf{(122)}$$

As with eq. **(120)**, the velocity, u_P, and N in eqs. **(122)** are evaluated initially at stack height and then iteratively.

When the atmosphere is close to neutral, the Brunt Vaisala frequency, N, is close to zero, and

eq.**(120)** can predict an unrealistically large plume rise. Under, these circumstances, we assume that plume rise is limited by atmospheric turbulence. This happens when the rate of plume rise under neutral conditions is comparable to σ_w. Under these conditions (neutral limit) the plume rise can be calculated from:

$$\Delta h_n = 1.2 L_n^{3/5} \left(h_s + 1.2 L_n \right)^{2/5} \qquad \textbf{(123)}$$

$$\text{where} \quad \Delta h_n \equiv \text{neutral plume rise}$$
$$L_n \equiv \text{neutral length scale}$$

L_n is calculated as:

$$L_n = \frac{F_b}{u_p u_*} \qquad \textbf{(124)}$$

Also, when the wind speed in near zero (calm conditions) unrealistically large plume rise estimates would result from applying eq. **(120)**. Under calm, stable atmospheric conditions we calculate plume rise from:

$$\Delta h_{sc} = \frac{4 F_b^{1/4}}{N^{3/4}} \qquad \textbf{(125)}$$

$$\text{where} \quad \Delta h_{sc} \equiv \text{plume rise for calm stable conditions}$$

By applying each of the above limits the final plume rise equation under stable conditions becomes:

$$\Delta h_s = MIN\left[\Delta h_s;\ \Delta h_s\{x_f\};\ \Delta h_n;\ \Delta h_{sc} \right]; \qquad \textbf{(126)}$$

i.e., the minimum value from eqs. **(120)**, **(122)**, **(123)** or **(125)**; see for example Hanna and Paine (1989) . In addition AERMOD prevents the stable plume rise from exceeding the rise expected during neutral or convective conditions (i.e. Δh_s eq. **(126)** is not to exceed the rise calculated from eq. **(116)**). Note, for situations when $F_b = 0$ no rise is calculated in stable conditions.

Therefore, the distance dependent height of the plume in the SBL is given by the following

expression:

$$h_{es} = h_s + \Delta h_s \qquad \textbf{(127)}$$

6.6 *Source Characterization*

AERMOD gives the user the ability to characterize a source as either a point, an area, or a volume. AERMOD additionally has the capability of characterizing irregularly shaped area sources.

Point sources are characterized exactly as in the ISC3 model (USEPA, 1995). The input to the model includes the location, elevation, emission rate, stack height, stack gas temperature, stack gas exit velocity, and stack inside diameter. The temperature, exit velocity, and diameter are required for plume rise calculations.

Similarly, volume sources require the same input as the ISC3 model. This includes the location, elevation height (optional), height of release, emission rate, the initial lateral plume size (σ_y) and initial vertical plume size (σ_z). AERMOD differs from ISC3 in the treatment of volume sources only in how the initial plume size is implemented. Where ISC3 uses the virtual source technique to account for initial plume size, AERMOD adds the square of the initial plume size to the square of the ambient plume size:

$$\sigma_y^2 = \sigma_{yl}^2 + \sigma_{yo}^2 , \qquad \textbf{(128)}$$

where $\sigma_{yo} \equiv$ *the initial horizonal plume size*
$\sigma_{yl} \equiv$ *the plume size before accounting for the initial size*
$\sigma_y \equiv$ *the resultant plume size, accounting for the initial size*.

The area source treatment is enhanced from that available in ISC3. In addition to being input as squares or rectangles, area sources may be input as circles or polygons. A polygon may be defined by up to 20 vertices. A circle is defined by inputting its center location and radius. The AERMOD code uses this information to create an equivalent nearly-circular polygon of 20 sides, with the same area as the circle.

As with ISC3, AERMOD allows for the calculation of a simple half-life decay.

6.7 *Adjustments for the Urban Boundary Layer*

AERMOD's urban formulation applies only to the nighttime boundary layer; there is no distinction made between urban and rural boundary layers during the day. The urban convective boundary layer forms in the night when stable rural air flows onto a warmer urban surface. The urban surface is warmer than the rural surface because the urban surface cools at a slower rate than the rural surface when the sun sets. Two reasons for the slower cooling are that buildings in the urban area trap the outgoing thermal radiation and the larger thermal capacity of the urban subsurface.

In order to account for the unique characteristics of the nighttime urban boundary layer, AERMOD enhances the turbulence of the rural stable boundary layer. This enhancement consists of a convective urban contribution to the total turbulence in the urban SBL. The convective contribution is a function of the convective velocity scale, which in turn, depends on the surface heat flux and the mixed layer height. The upward heat flux is a function of the urban-rural temperature difference.

The urban-rural temperature difference depends on a large number of factors that cannot easily be accounted for in applied models, such as AERMOD. For simplicity, we chose to use the data presented in Oke (1973, 1982) to construct an empirical model. Oke presents observed urban-rural temperature differences for a number of Canadian cities of size varying from a population of about 1000 up to 2,000,000. An empirical fit to the data yields the following relationship

$$\Delta T_{u-r} = \Delta T_{\max}\left[\ln\left(\frac{P}{P_o}\right) + 1.0\right], \qquad \textbf{(129)}$$

where: $\Delta T_{\max} = 12\ ^oC$

$P_o \equiv 2{,}000{,}000$ (*reference population*)

$P \equiv$ *population of the urban area*.

P_o is the city population associated with the maximum temperature difference.

Since the ambient nighttime temperature of an urban area is higher than its surrounding rural areas, an upward surface heat flux must exist in the urban area. We assume that this upward surface heat flux is related to this urban-rural temperature difference through the following relationship:

$$H_u = \alpha \rho c_p \Delta T_{u-r} u_* , \qquad \textbf{(130)}$$

where α is an empirical constant. We chose α to ensure that the upward heat flux is consistent with a maximum measured values of the order of 0.1 ms-1C . Because ΔT_{u-r} has a maximum value on the order of 10 °C, and u_* on the order of 0.1 m/s, α should have a maximum value on the order of 0.1. Although we assume that α has a maximum (city center) value of about 0.1, AERMOD uses an effective value of α that is averaged over the entire urban area. The variation of α from 0 at the edge of the urban area to about 0.1 at the center of the urban area is unknown, but a linear variation with distance from the edge of the urban area would result in an areal average equal to one-third of that at the center (since the volume of cone is one-third of that of a right circular cylinder of the same height). Therefore, AERMIC tested an area-averaged value of α equal to 0.03 against the Indianapolis data. This choice for α (i.e. α = 0.03) is consistent with measured values of the upward heat flux in certain Canadian cities reported by Oke (1973, 1982). The results of the developmental testing indicated that this choice for α resulted in an adequate fit between observations and AERMOD-predicted concentrations.

The mixing height in the nighttime urban boundary layer, z_{iu} is based on empirical evidence presented in Oke (1973, 1982), which suggests the following relationships:

$$z_{iu} \sim R^{1/2}, \quad \textit{and} \quad R \sim P^{1/2}, \qquad \textbf{(131)}$$

where R is a measure of the size of a city and P is the population of the city. The first relationship is based on observed growth of the internal convective boundary layer next to shorelines (See Venkatram, 1978 for example). The second relation implicitly assumes that population densities do not vary substantially from city to city. The assumptions that underlie the above equations are open for discussion. However, in the absence of better information, they represent our best estimate of the governing phenomena.

Eq. **(131)** leads to the following equation for z_{iuc},

$$z_{iuc} = z_{iuo} \left(\frac{P}{P_o} \right)^{1/4} \qquad \textbf{(132)}$$

where $z_{iuc} \equiv$ *height of the nightime urban boundary due to convective effects alone,*

where z_{iuo} is the boundary layer height corresponding to P_o.

Hanna and Chang (1991) report lidar measurements from the Indianapolis tracer study program for nocturnal conditions. While the mixing heights at night range from 100 to 500 meters, they approach 400 meters during clear, calm conditions. Using eq. **(132)** and an Indianapolis population of 700,000, the value of z_{iuo} is computed to be 500 meters. This is fairly consistent with the estimate for z_{iuo} on the order of 400 meters mentioned by Bornstein (1968).

In addition, since effects from urban heating should not cause z_{iu} to be less than the mechanical mixing height, z_{iu} is restricted from being less than z_{im}. Therefore, from eq. **(132)** the mixed layer height for the nighttime urban boundary layer is written as:

$$z_{iu} = MAX\left[z_{iuc};\, z_{im}\right], \qquad \textbf{(133)}$$

Once the urban mixing height has been estimated the enhancement to turbulence can be calculated. To calculate the enhanced turbulence in the nighttime urban boundary layer we first calculate a w_* (appropriate for the magnitude of convective turbulence present) by substituting z_{iu} and H_u into eq. **(10)**; i.e.,

$$w_{*u} = \left(\frac{g\, H_u\, z_{iuc}}{\rho\, C_p\, T}\right)^{1/3} \qquad \textbf{(134)}$$

$$\textit{where} \qquad w_{*u} \equiv \textit{urban nightime convective velocity scale}.$$

Then the total vertical and lateral turbulence used in the concentration calculations are calculated from σ_{wc} (eq.**(36)** is the convective portion of σ_{wT}) and σ_{vc} (eq. **(45)** is the convective portion of σ_{vT}) with the convective portion of the turbulence computed by setting z_{ic} equal to z_{iu} and by using w_* as calculated from eq. **(134)**. This in essence enhances turbulence at night in the urban boundary layer. Vertical dispersion due to ambient turbulence (σ_{za}), in the urban boundary layer, is calculated from eq. **(96)** (the SBL formulation for σ_{za}) with the urban PBL assumed to be neutral (i.e., $N = 0$). Similarly, for the lateral dispersion in the urban boundary layer, σ_{ya} is calculated using the SBL formulation given by eq. **(90)**.

The potential temperature gradient in the night-time urban boundary layer is set equal to the upwind rural profile (i.e., as measured or calculated from eq. **(31)**) for all heights above z_{iu}, and is assumed to be equal to a small positive value below z_{iu}; i.e.,

$$\begin{aligned} \partial\theta/\partial z &= 0.002 && \textit{for} \quad z \le z_{iu} \\ \partial\theta/\partial z &= \textit{rural value} && \textit{for} \quad z > z_{iu}. \end{aligned} \qquad \textbf{(135)}$$

For plumes below z_{iu} , the effective reflection surface is set equal to the height of the urban boundary layer (i.e., $z_{ieff} = z_{iu}$; this effective reflection surface in analogous to that calculated in eq. **(78)** for rural stable sources). Plumes that "penetrate" above z_{iu} are modeled in a manner similar to penetrated sources in the CBL. Plume rise in the urban stable boundary layer is calculated from eq. **(126)** with an assumed near-neutral potential temperature gradient (i.e., $\partial\theta/\partial z = 0.00001$). Use of this value for $\partial\theta/\partial z$ provides an appropriate near-neutral plume rise formulation that is expected within the nocturnal urban boundary layer. However, plume height in these conditions is not allowed to exceed $1.25\ z_{iu}$

Finally, in the nighttime urban boundary layer, plume meander is not modeled since this modified stable layer has many of the turbulent characteristics of a weak convective layer. Use of this urban boundary layer formulation has yielded satisfactory performance of AERMOD for the Indianapolis data. For daytime conditions ($L < 0$) in urban areas, AERMOD uses the same formulations as in rural areas (i.e., no adjustments to boundary layer characteristics).

7 List of Symbols

$\mathbf{B_o}$	Bowen ratio - ratio of the sensible to latent heat fluxes (dimensionless)
$\mathbf{C_{c,s}\{x_r,y_r,z_r\}}$	concentration contribution from the horizontal plume state - convective and stable (g/m^3)
$\mathbf{C_{c,s}\{x_r,y_r,z_p\}}$	concentration contribution from the terrain following plume state - convective and stable (g/m^3)
$\mathbf{C_c\{x_r,y_r,z_r\}}$	total concentration (CBL) (g/m^3)
$\mathbf{C_d\{x_r,y_r,z_r\}}$	concentration contribution from the direct source (CBL) (g/m^3)
$\mathbf{C_p\{x_r,y_r,z_r\}}$	concentration contribution from the penetrated source (CBL) (g/m^3)
$\mathbf{C_r\{x_r,y_r,z_r\}}$	concentration contribution from the indirect source (CBL) (g/m^3)
$\mathbf{C_s\{x_r,y_r,z_r\}}$	total concentration (SBL) (g/m^3)
$\mathbf{C_T\{x_r,y_r,z_r\}}$	total concentration (CBL) (g/m^3)
$\mathbf{C_D}$	neutral drag coefficient (cal/g-^{o}C)
$\mathbf{c_p}$	specific heat at constant pressure (= 1004 Joules-gm^{-1}-^{o}K^{-1})
$\mathbf{F_b}$	plume buoyancy flux (m^{4}s^3)
$\mathbf{F_y}$	total horizontal distribution function - with meander (m^{-1})
$\mathbf{F_{yC}}$	horizontal distribution function for a coherent plume (m^{-1})
$\mathbf{F_{yR}}$	horizontal distribution function for a random plume (m^{-1})
$\mathbf{F_G}$	flux of heat into the ground (W m^{-2})
$\mathbf{F_m}$	plume momentum flux (m^{4}s^2)
$\mathbf{f}$	plume state weighting function (dimensionless)
$\mathbf{f_p}$	fraction of plume mass contained in CBL = (1 - penetration factor) dimensionless)
$\mathbf{f_t}$	terrain weighting function (dimensionless)
$\mathbf{g}$	acceleration due to gravity (9.8 m/s^2)
$\mathbf{H}$	sensible heat flux (W m^{-2})
$\mathbf{H_c}$	critical dividing streamline (m)
$\mathbf{H_e}$	generic plume height (m)
$\mathbf{H_{em}}$	plume height after momentum rise (m)
$\mathbf{H_p}$	plume centroid height (m)
$\mathbf{H_u}$	heat flux in the nighttime boundary layer (W m^{-2})
$\mathbf{h_c}$	receptor specific height scale (m)
$\mathbf{h_{ed}}$	direct source plume height above stack base less the effect from the

	random convective velocities (m)
$\mathbf{h_{eff}}$	weighted effective height surface (m)
$\mathbf{h_{ep}}$	penetrated source plume height above stack base (m)
$\mathbf{h_{es}}$	stable source plume height above stack base (m)
$\mathbf{h_s}$	stack height corrected for stack tip downwash (m)
$\mathbf{\Delta h}$	general symbol for distance dependent plume rise (m)
$\mathbf{\Delta h_d}$	plume rise for the direct source (m)
$\mathbf{\Delta h_m}$	stabilized rise due to momentum alone (m)
$\mathbf{\Delta h_{eq}}$	equilibrium plume rise in a stable environment (m)
$\mathbf{\Delta h_h}$	depth of the layer between z_i and the stack top (m)
$\mathbf{\Delta h_{max}}$	difference between the maximum terrain height and the minimum terrain height within the modeling domain (m)
$\mathbf{\Delta h_n}$	plume rise limited for near neutral conditions (m)
$\mathbf{\Delta h_p}$	plume rise for the penetrated source (m)
$\mathbf{\Delta h_i}$	plume rise for the indirect source (m)
$\mathbf{\Delta h_s}$	plume rise for the stable source (m)
$\mathbf{\Delta h_{sc}}$	plume rise limited for calm conditions (m)
$\mathbf{\Delta h_r}$	Δh_d - Δh_i
$\mathbf{i_y}$	vertical turbulence intensity
$\mathbf{I_n}$	net long wave radiation (W m^{-2})
k	von Karman constant k = 0.4 (dimensionless)
l	length scale used in determining the vertical Lagrangian time scale for the SBL (m)
$\mathbf{l_n}$	neutral length scale - a component of **l** (m)
$\mathbf{l_s}$	stable length scale - a component of **l** (m)
L	Monin -Obukhov length (m)
$\mathbf{L_b}$	the lesser of a building's height and the projected width for a specific wind direction (m)
N	Brunt-Vaisala frequency (s^{-1})
$\mathbf{N_h}$	Brunt-Vaisala frequency above z_i (s^{-1})
n	cloud cover (fractional)
P	population of urban area
$\mathbf{p_y}$	lateral probability density function
$\mathbf{p_z}$	vertical probability density function

$\mathbf{p_w}$	probability density function of the instantaneous vertical velocities
Q	source emission rate (g/s)
R	solar insolation (W m^{-2})
$\mathbf{R_d}$	universal gas constant for dry air
$\mathbf{R_n}$	net radiation (W m^{-2})
$\mathbf{R_o}$	clear sky solar insolation (W m^{-2})
$\mathbf{r(\phi)}$	Albedo {solar elevation} (dimensionless)
$\mathbf{r'}$	noontime albedo (dimensionless)
$\mathbf{r_o}$	terrain weighting factor (m)
$\mathbf{r_s}$	stack radius - corrected for stack tip downwash (m)
$\mathbf{r_y}$	lateral dimension of an elliptical plume
$\mathbf{r_z}$	vertical dimension of an elliptical plume
S	skewness factor (dimensionless)
T	ambient temperature (^{o}K)
$\mathbf{T_{Lyc}}$	lateral lagrangian time scale for the CBL (sec)
$\mathbf{T_{Lys}}$	lateral lagrangian time scale for the SBL (sec)
$\mathbf{T_{Lzc}}$	vertical lagrangian time scale for the CBL (sec)
$\mathbf{T_{Lzs}}$	vertical lagrangian time scale for the SBL (sec)
$\mathbf{T_r}$	Time scale used in the meander algorithm (sec)
$\mathbf{T_{ref}}$	ambient temperature - at reference temperature height (^{o}K)
$\mathbf{T_s}$	stack gas temperature (^{o}K)
$\mathbf{T_u}$	urban surface temperature (^{o}K)
$\mathbf{T_v}$	virtual temperature (^{o}K)
t	time (sec)
$\mathbf{\Delta t_s}$	difference between stack gas and ambient temperature (^{o}K)
$\mathbf{\Delta T_{u\text{-}r}}$	urban-rural temperature difference (^{o}K)
u	wind speed (m-s^{-1})
$\mathbf{u_{cr}}$	minimum speed for which the expression for u_*, in the SBL, has a real valued solution (m-s^{-1})
$\mathbf{u_o}$	defined in eq. **(21)** and used in eq. **(22)**.
$\mathbf{u_p}$	wind speed that is used for plume rise (m-s^{-1})
$\mathbf{u_{ref}}$	wind speed at reference height (m-s^{-1})
$\mathbf{u_{Th}}$	wind speed instrument threshold - separate value for each data set (offsite & onsite) (m-s^{-1})

$\mathbf{u_*}$	surface friction velocity (m s^{-1})
v	random lateral velocity in the CBL (m-s^{-1})
w	random vertical velocity in the CBL (m-s^{-1})
$\overline{w_j}$	mean vertical velocity for the updraft (j = 1) and the downdraft (j = 2) distributions (m-s^{-1})
$\mathbf{w_s}$	stack exit gas velocity (m-s^{-1})
$\mathbf{w_*}$	convective velocity scale (m-s^{-1})
$\mathbf{w_{*c}}$	urban nighttime convective velocity scale (m-s^{-1})
X	non-dimensional downwind distance (dimensionless)
x	downwind distance (m)
$\mathbf{x_f}$	distance to final plume rise (m) - eq. **(50)** for the CBL and eq. **(121)** for the SBL
$\mathbf{x_m}$	downwind distance at which plume material uniformly mixed throughout the boundary layer (m)
$\mathbf{x_{rt}}$	distance between receptor and terrain point (m)
$\mathbf{x_{sr}}$	distance between source and receptor (m)
$\mathbf{(x_r,y_r,z_r)}$	receptor location
$\mathbf{(x_t,y_t,z_t)}$	terrain point location
$\mathbf{z_c}$	total height of the plume in the CBL considering both plume rise and effects from convective turbulence (m)
$\mathbf{z_i}$	mixing height (m): z_i = MAX [z_{ic}; z_{im}] in the CBL and $z_i = z_{im}$ in the SBL
$\mathbf{z_{ic}}$	convective mixing height (m)
$\mathbf{z_{ie}}$	equilibrium height of stable boundary layer
$\mathbf{z_{ieff}}$	height of the reflecting surface in the SBL or in the stable layer above the above the CBL (m)
$\mathbf{z_{im}}$	mechanical mixing height (m)
$\mathbf{z_{iu}}$	urban nighttime boundary layer mixing height (m)
$\mathbf{z_{iuc}}$	urban nighttime boundary layer mixing height due to convective effects alone (m)
$\mathbf{z_{i\theta}}$	The maximum of the mechanical mixing height and 100 meters
$\mathbf{z_{msl}}$	height of stack base above mean sea level (m)
$\overline{Z_{SB}}$	average stack base height, above mean sea level, among all sources being modeled (m)

$\mathbf{z_o}$	surface roughness length (m)
$\mathbf{z_{PG}}$	release height used in the Prairie Grass experiment (m)
$\mathbf{z_p}$	receptor "flagpole" height - the height of a receptor above local terrain (m)
$\mathbf{z_r}$	height of the receptor above local source base (m)
$\mathbf{z_{ref}}$	reference height for wind (m)
$\mathbf{z_{Tref}}$	reference height for temperature (m)
$\mathbf{z_t}$	height of the terrain above mean sea level (m)
$\underline{\alpha}$	General symbol used to represent the effective parameters in the treatment of the inhomogeneous boundary layer. In the text the effective values of the parameters u, σ_w, σ_v and T_L are denoted by underscoring the character.
θ	potential temperature (^{o}K)
θ_h	potential temperature above z_i (^{o}K)
θ_m	mixed layer temperature in the urban boundary layer (^{o}K)
θ_*	temperature scale (^{O}K)
θ_{*p}	temperature scale adjusted by local measured temperature gradient (^{O}K)
λ_E	latent heat of evaporation
λ_j	weighting coefficient for the updraft (j = 1) and downdraft (j = 2) distributions of eqs. **(65)**, **(69)** and **(74)**
ρ	density of air (Kgm-m^{-3})
σ_b	buoyancy induced dispersion for the direct & indirect sources (m)
σ_{bp}	buoyancy induced dispersion for the penetrated source (m)
σ_{bs}	buoyancy induced dispersion for the stable source (m)
σ_h^2	total horizontal wind "energy" used in the meander algorithm (m^2)
σ_i	standard deviation of the vertical velocities for the updraft (I = 1) and the downdraft (I = 2) distributions
σ_r^2	random "energy" component of the total horizontal wind "energy" used in the meander algorithm (m^2)
σ_{SB}	Stephen Boltzman constant (5.67x10^{-8} Wm^{-2}K^{-4})
σ_v	lateral turbulence (m-s^{-1})
σ_{vc}	convective portion of the lateral turbulence (m-s^{-1})
σ_{vo}	surface value of the lateral turbulence (m-s^{-1})
σ_{vm}	mechanical portion of the lateral turbulence (m-s^{-1})
σ_{vT}	total lateral turbulence (m-s^{-1})
σ_w	vertical turbulence (m-s^{-1})
σ_{wc}	convective portion of the vertical turbulence (m-s^{-1})

σ_{wm}	mechanical portion of the vertical turbulence (m-s^{-1})
σ_{wml}	mechanical portion of the vertical turbulence generated in the PBL (m-s^{-1})
σ_{wmr}	mechanical portion of the vertical turbulence above the PBL (residual) (m-s^{-1})
σ_{wmx}	maximum value of the residual vertical mechanical turbulence (m-s^{-1})
σ_{wT}	total vertical turbulence (m-s^{-1})
σ_{y}	total lateral dispersion for the direct & indirect sources (m)
$\sigma_{ya,zaj}$	ambient turbulence induced dispersion for the direct & indirect sources (m)
$\sigma_{yap,zap}$	ambient dispersion for penetrated source (m)
$\sigma_{yas,zas}$	ambient dispersion for the stable source (m)
$\sigma_{yd,zd}$	downwash induced dispersion for all sources (m)
σ_{yl}	lateral spread from combined effects of ambient turbulence and building downwash (m)
$\sigma_{yp,zp}$	total dispersion for the penetrated source (m)
$\sigma_{ys,zs}$	total dispersion for the stable source (m)
σ_{zaj}	ambient vertical dispersion for the updraft & downdrafts plumes (j = 1,2), respectively, for both the direct & indirect sources (m)
σ_{zej}	elevated portion of σ_{zaj} (m)
σ_{zes}	elevated portion of σ_{zas} (m)
σ_{zj}	total vertical dispersion for the updrafts and downdrafts (j=1,2 respectively), for both the direct and indirect sources
σ_{zl}	combined effects of ambient turbulence and building downwash
σ_{zs}	surface portion of σ_{zaj} (m)
σ_{zss}	surface portion of σ_{zas} (m)
σ_{θ}	standard deviation of the horizontal component of the wind (degrees)
τ	time constant controlling the temporal interpolation of z_{im} (sec)
ϕ	solar elevation angle
ϕ_{p}	fraction of plume mass below H_c (dimensionless)
Ψ_{dj}	total height of the direct source plume (i.e. release height + buoyancy + convection) (m)
Ψ_{rj}	total height of the indirect source plume (m)
ψ_{m}	similarity function for momentum (stability correction) - eq. **(7)** for the CBL and eq. **(29)** for the SBL (dimensionless)

8 APPENDIX: Input / Output Needs and Data Usage

8.1 *AERMET Input Data Needs*

Besides defining surface characteristics, the user provides several files of hourly meteorological data for processing by AERMET. At the present time AERMET is designed to accept data from any for the following sources: 1) standard hourly National Weather Service (NWS) data from the most representative site; 2) morning soundings of winds, temperature, and dew point from the nearest NWS upper air station; and 3) on-site wind, temperature, turbulence, pressure, and radiation measurements (if available).

The minimum measured and/or derived data needed to run the AERMOD modeling system are as follows:

8.1.1 METEOROLOGY

wind speed (u); wind direction; cloud cover - opaque first then total (n); ambient temperature (t)

8.1.2 DIRECTIONALLY AND/OR MONTHLY VARYING SURFACE CHARACTERISTICS

noon time albedo (r'); Bowen ratio (B_o); roughness length (z_o) - For AERMET, the user can specify monthly variations of three surface characteristics for up to 12 upwind direction sectors. These include: the albedo (r), which is the fraction of radiation reflected by the surface; the Bowen ratio (B_o), which is the ratio of the sensible heat flux to the evaporation heat flux; and the surface roughness length (z_o) , which is the height above the ground at which the horizontal wind velocity is typically zero. The user will be guided by look-up tables (in the AERMET user's guide) of typical values for these three variables for a variety of seasons and land use types.

8.1.3 OTHER

Latitude; longitude; time zone; wind speed instrument threshold for each data set (u_{Th}).

8.1.4 OPTIONAL

solar radiation; net radiation *(r_n)*; profile of vertical turbulence *(σ_w)*; profile of lateral turbulence *(σ_v)*

8.2 *Estimation of solar insolation for small solar elevation angles*

If the sun is above the horizon but the elevation is less than about *2 °*,eq.**(5)** estimates the clear sky insolation, R_o, to be negative. To avoid this situation, R_o is approximated for solar elevations less than *10 °* by linearly interpolating between *0.0 W* m^{-2} (ϕ*=0 °*) and *141.91* W *m-2* (ϕ*=10 °*).

8.3 *Selection and Use of Measured Winds, Temperature and Turbulence in AERMET*

8.3.1 THRESHOLD WIND SPEED

The user is required to define a threshold wind speed (u_{TH}). Although the current version of AERMOD can not accept a separate u_{TH} for offsite data, we believe that a separate u_{TH} should be selected for each data set being used.

8.3.2 REFERENCE TEMPERATURE AND HEIGHT

The reference height for temperature (z_{Tref}), and thus the reference temperature, is selected as the lowest level of data which is available between z_o & 100m.

8.3.3 REFERENCE WIND SPEED AND HEIGHT

The reference height for winds (z_{ref}), and thus the reference wind speed (u_{ref}), is selected as the lowest level of data which is available between $7z_o$ & 100m. Although the current version of AERMOD can not accept a separate z_{ref} for offsite data, we believe that a separate z_{ref} should be selected for each data set being used.

If no valid observation of the reference wind speed or direction exists between these limits the hour is considered missing and a message is written to the AERMET message file. For the wind speed to be valid its value must be greater than or equal to the threshold wind speed. AERMOD processes hours of invalid wind speed, e.g. calms, in the same manner as ISC (EPA calms policy).

All observed wind speeds in a measured profile that are less than u_{TH} are set to missing

and are therefore not used in the construction of the wind speed profile (profiling of winds is accomplished in AERMOD).

8.3.4 CALCULATING *THE POTENTIAL TEMPERATURE GRADIENT* ABOVE THE MIXING HEIGHT FROM SOUNDING DATA

AERMET calculates $d\theta/dz$ for the layer above z_i as follows:

- If the sounding extends at least 500m above z_i the first 500 meters above z_i is used to determine $d\theta/dz$ above z_i.
- If the sounding extends at least 250 meters above z_i (but not 500m) then the available sounding above z_i is used to determine $d\theta/dz$ above z_i.
- AERMET limits $d\theta/dz$ above z_i to a minimum of 0.005.
- If the sounding extends less than 250m above z_i then set $d\theta/dz = 0.005$ (a default value).

8.3.5 MEASURED TURBULENCE

All measured turbulence values are passed to AERMOD if the hour is non-missing. This is true even for those levels where the wind speed is below u_{TH}.

Based on measurements with research grade instruments, reasonable minimum turbulence levels in non-calm conditions for vertical turbulence (σ_w) and lateral turbulence (σ_v) values are set by AERMOD to *0.02 m/s* and *0.2 m/s*, respectively.

Although these lower limits are applied to the measured values of the turbulence the calculated profile values of σ_w & σ_v are not subjected to any lower limits. We do not restrict these estimated profiles because it would bias the calculation of the effective values of turbulence, which are averages through the layer between the receptor and the plume height, in determining the dispersion of the plume.

8.3.6 DATA SUBSTITUTION FOR MISSING ON-SITE DATA

If on-site data are missing for an hour the hour is considered missing unless the user specifies a substitute data set. AERMET does not default to NWS (or any other offsite) data.

8.4 *Information Passed by AERMET to AERMOD*

The following information is passed from AERMET to AERMOD for each hour of the meteorological data record.

- All observations of wind speed *(u);* wind direction*;* ambient temperature *(T);* lateral turbulence *(σ_v); &* vertical turbulence *(σ_w)* with their associated measurement heights.
- Sensible heat flux *(H)*,friction velocity *(u_*)*, Monin Obukhov length *L*, z_{im} (for all hours), z_{ic} & w_* (for convective hours only), z_o , *r{ ϕ}*, & B_o, $d\theta/dz$ (above z_i), u_{ref} , wind direction at the reference height, z_{ref}, ambient temperature at the reference height *(T_{ref}) (not used in AERMOD), &* the reference height for temperature *(z_{Tref})*

8.5 *Restrictions on the Growth of PBL Height*

AERMET restricts the growth of z_i to a reasonable maximum of 4000 meters. This restriction applies to both calculated and measured mixing heights. Although mixing heights in excess of 4000 meters may occur on rare occasions, in desert climates, the additional effect on surface concentration is most likely insignificant.

8.6 *Initializing the Mechanical Mixing Height Smoothing Procedure*

If $\{t+\Delta t\}$, in eq. **(15)**, is the first hour of the data set then no smoothing takes place. Furthermore, if a missing value occurs at time step *t* then smoothing is not performed at time step $\{t+\Delta t\}$.

8.7 *Determining The Mixing Height When the Sounding Is Too Shallow*

The left hand side of eq. **(9)** is determined from the morning temperature sounding and the right hand side from the daytime history of surface heat flux.

When the temperature sounding, obtained from the NWS, does not reach a height which is greater than the convective mixing height, we must assume a profile for the potential temperature gradient in order to estimate z_{ic}. This is accomplished as follows:

- Determine $d\theta/dz$ in the top *500m* layer of the sounding. However, if part of the *500m* layer is within the first *100m*'s of the PBL the layer should be reduced (to a minimum thickness of *250m*) to avoid using the portion of the sounding that is below *100m*. If the above conditions can not be satisfied then z_{ic} is defined as missing.
- Extend the sounding by persisting $d\theta/dz$ up and recomputing z_{ic}.
- Provide warning messages which tell users

- the height of the actual sounding top,
- that $d\theta/dz$ has been extrapolated above the sounding z_{ic}, and
- that z_{ic} has been recomputed.

- Allow the user to reject the "fixed-up" value for z_{ic} by defining it as missing.

8.8 *Input Data Needs for AERMAP*

The following data is required input for AERMAP

- DEM formatted terrain data (x_t , y_t , z_t)
- User provided receptors (x_r, y_r , z_r) and terrain
- Design of receptor grid; AERMAP accepts either polar, Cartesian or discrete receptors

8.9 *Information Passed by AERMAP to AERMOD*

AERMAP passes the following parameters to AERMOD: x_r, y_r, z_r, z_t, & the height scale (h_c) for each receptor.

8.10 *Wind Speed & Turbulence Limits Used in Model Calculations*

At the time of plume rise calculations the turbulence at stack top (or whatever level the meteorology is selected from in the case of iterative plume rise) will be recalculated as

$$\sigma_w\{h_s\} = MAX\,[\,\sigma_w\{h_s\}\ ,\ 0.02\,m/s\,] \qquad \textbf{(136)}$$

$$\sigma_v\{h_s\} = MAX\,[\,\sigma_v\{h_s\},\ 0.05\,u\{h_s\},\ 0.2\ m/s\,]. \qquad \textbf{(137)}$$

Dilution of the plume is determined by the wind that corresponds to average over the magnitudes of the wind vectors during a given time interval. But measurements only give us the vector averaged wind, which can be zero, even though the dilution wind is not zero. We can estimate the dilution wind by assuming that the vector wind, u_v, can be expressed as

$$u_v = \left(\bar{u} + u', v'\right), \qquad \textbf{(138)}$$

where $\bar{u}$ is the mean measured wind, and the primed quantities refer to the turbulent fluctuations. Notice that, as assumed $\overline{u_v} = \bar{u}$. If we assume that the measured velocity fluctuations correspond only to the angular variations of a constant vector, u_v, we can write from eq. **(138)**,

$$u_v^2 = \bar{u}^2 + \sigma_v^2 + \sigma_u^2. \qquad \textbf{(139)}$$

In this simple model, u_v , is the dilution wind. If we take $\sigma_u = \sigma_v$, the dilution wind can be written as

$$u\{h_s\} = \sqrt{u\{h_s\}^2 + 2\sigma_v^2}\,. \qquad \textbf{(140)}$$

This formulation assures that the dilution wind is not zero as long as either '' or σ_v is not zero.

Similarly, at the time of dispersion calculations, the effective turbulence and effective wind speed will be recalculated using eqs. **(136)**, **(137)** & **(140)**, where the stack top values will be replaced with $\underline{\sigma}_w$,$\underline{\sigma}_v$ & $\underline{u}$.

8.11 *Using Profiles for Interpolating Between Observations*

When observations are available AERMOD uses the similarity profile functions to interpolate adjacent measurements. **Figure 17** illustrates how AERMOD's INTERFACE uses the expected shape of a meteorological profile to interpolate between observations.

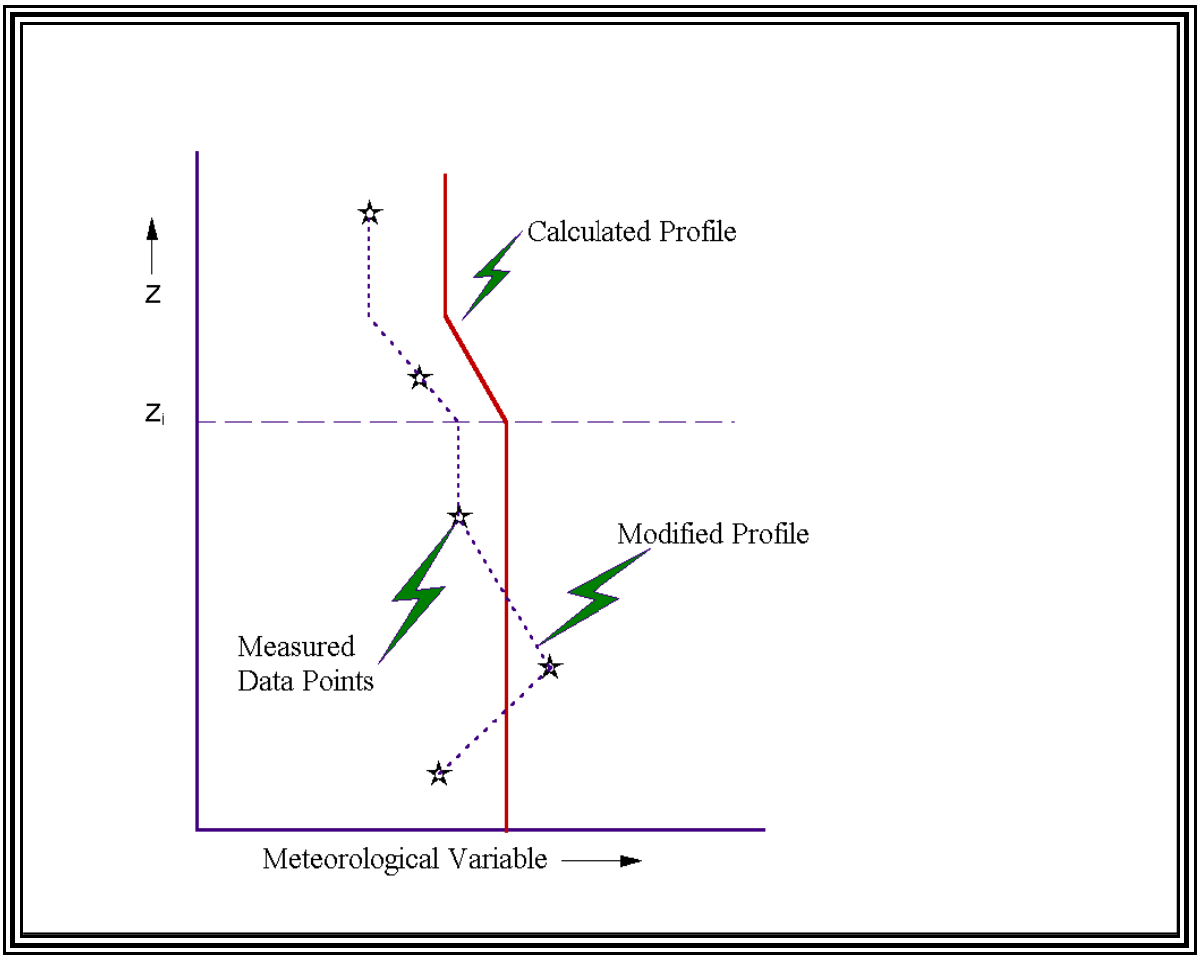

Figure 17: AERMOD's construction of a continuous meteorological profiles by interpolating between observations.

For a gridded profile height between two observed profile heights, the observations are interpolated to the gridded height while maintaining the shape of the similarity profile. This is accomplished as follows:

1. the observations are linearly interpolated to the gridded profile height;
2. the similarity function is evaluated at the gridded profile height;
3. the similarity function is evaluated at the observed profile heights immediately above and below the grid height and linearly interpolated to the grid height;

4. the ratio of the value obtained in 2 to the value obtained in 3 is applied to the value obtained in 1.

For a gridded profile height above the highest observation, the procedure is modified slightly:

1. the observation at the highest observed profile height is extrapolated by persisting the value upward;
2. the similarity function is evaluated at the grid height;
3. the similarity function is evaluated at the highest height in the observed profile;
4. the ratio of the value obtained in 2 to the value obtained in 3 is applied to the value obtained in 1.

A similar procedure for extrapolating to heights above the observed profile is applied to heights below the lowest observed profile height.

8.12 *Using Measured Mixing Heights*

If measured mixing heights are available, then they are treated in the following manner: If $L>0$ (SBL) the measured mixing height is defined as z_{ie} and it is treated the same as a calculated mechanical mixing height (smoothing, etc). If $L<0$ (CBL) the measured mixing height is defined as z_{ic}, and z_{ie} is calculated from eq.**(12)** then proceed as if both z_{ic} and z_{im} had been calculated values.

If a user has "measured" mixing heights available (and chooses to use them), the model defaults to substituting calculated mixing heights for missing measurements and a message is written that a substitution has occurred. If the user elects to substitute calculations for missing measurements, the model will print out a message to the message file for each hour that a substitution has occurred.

9 **References**

AERMIC, 1995, Formulation of the AERMIC MODEL (AERMOD) (Draft), Regulatory Docket AQM-95-01, AMS/EPA Regulatory Model Improvement Committee (AERMIC).

Andre, J.C. and L. Mahrt, 1982, “The nocturnal surface inversion and influence of clean-air radiative cooling,” J. Atmos. Sci., 39:864-878.

Baerentsen, J.H., and R. Berkowicz, 1984 “Monte Carlo simulation of plume dispersion in the convective boundary layer,” Atmos. Environ., 18:701-712.

Barad, M.L, (Ed.)., 1958, Project Prairie Grass, A Field Program in Diffusion, Geophysical Research Papers, No. 59, Vols. I and II, Report AFCRC-TR-58-235, Air Force Cambridge Research Center, 439pp.

Berkowicz, R., J. R. Olesen, and U. Torp, 1986, "The Danish Gaussian air pollution model (OLM): Description, test and sensitivity analysis, in view of regulatory applications," Air Pollution Modeling and Its Application, V. C. De Wispelaire, F. A. Schiermeier, and N. V. Gillani, Eds. Plemum, New York, 453-481pp.

Bornstein, R.D., 1968, “Observations of urban heat island effect in New York city,” J. Appl. Meteor., 7:575-582.

Brett, A.C. and S.E. Tuller, 1991, “Autocorrelation of hourly wind speed observations,” J. Appl. Meteorol., 30:823-833.

Briggs, G. A., 1971, "Some recent analyses of plume rise observations", in Proceedings of the Second International Clean Air Congress, H. M. Englund and W. T. Berry, Eds., Academic Press, New York, 1029-1032.

Briggs, G. A., 1975, “Plume rise predictions” in Lectures on Air Pollution and Environmental Impact Analysis, D. A. Haugen, ed., American Meteorological Society, Boston (59-111).

Briggs, G.A., 1984, "Plume rise and buoyancy effects," in Atmospheric Science and Power Production, D. Randerson, Ed., DOE/TIC-27601, U.S. Dept. of Energy, 327-366.

Briggs, G.A., 1988, “Analysis of diffusion field experiments,” Lectures on Air Pollution

Modeling, A. Venkatram and J.C. Wyngaard, Eds., Amer. Meteor. Soc., Boston, 63--117.

Briggs G.A., 1993, "Plume dispersion in the convective boundary layer. PartII: Analyses of CONDORS field experiment data," J. Applied Meterol., 32:1388-1425.

Brost, R.A., J.C. Wyngaard, and D.H. Lenschow, 1982, "Marine stratocumulus layers: Part II: Turbulence budgets," J.Atmos. Sci., 39:818-836.

Carruthers, D.J., R.J. Holroyd, J.C.R. Hunt, W.S. Weng, A.G. Robins, D.D. Apsley, D.J. Thomson, and F.B. Smith, 1992, "UK-ADMS – a New Approach to Modelling Dispersion in the Earth's Atmospheric Boundary Layer," In Proceedings of the Workshop: Objectives for Next Generation of Practical Short-Range Atmospheric Dispersion Models, May 6-8, 1992, Riso, Denmark, pp. 143-146.

Carruthers, D.J., Holroyd, R.J., Hunt, J.C.R., Weng, W.-S., Robins, A.G., Apsley, D.D., Smith, F.B., Thomson, D.J., and Hudson, B., 1992, "UK atmospheric dispersion modelling system," Air Pollution Modeling and Its Application, H. van Dop and G. Kallos, Eds., Plenum Press, New York.

Carson, D. J., 1973, "The development of a dry inversion-capped convectively unstable boundary layer," Quart. J. Roy. Meteor. Soc., 99:450-467.

Caughey, S.J., and S.G. Palmer, 1979, "Some aspects of turbulence structure through the depth of the convective boundary layer" Quart. J. Roy. Meteor. Soc., 105, 811-827.

Cimorelli, A.J., S.G. Perry, R.F. Lee, R.J. Paine, A. Venkatram, J.C. Weil and R.B. Wilson, 1996, "Current Progress in the AERMIC Model Development Program," in Proceedings 89TH Annual Meeting Air and Waste Management Association, 96-TP24B.04, Air and Waste Management Association, Pittsburgh, PA.

Code of Federal Regulations, July 1, 1997, 40CFR, Part 51, App. W, Guideline on Air Quality Models, pp. 346-438 .

Collier, L. R., and J. G. Lockwood, 1975, "Reply to Comment," Quart. J. Roy. Meteor. Soc.., 101, 390-392.

Deardorff, J.W. 1972, "Numerical investigation of neutral and unstable planetary boundary layers," J. Atmos. Sci., 29: 91--115.

Deardorff, J.W., 1980, Progress in Understanding Entrainment at the Top of a Mixed Layer, in Workshop on the Planetary Boundary Layer, J.C. Wyngaard, Ed., American Meteorological Society, Boston, MA.

Garratt, F.R., 1992, The Atmospheric Boundary Layer, Cambridge University Press, New York, New York, 334pp.

Gifford, F.A., 1975, “Atmospheric dispersion models for environmental pollution applications,” Lectures on Air pollution and Environmental Impact Analyses, D.A. Haugen, Ed., Amer. Meteor. Soc., Boston, 35-58.

Gifford, F.A., 1959, "Statistical properties of a fluctuating plume dispersion model," Advances in Geophysics, Academic Press, 6:117-138.

Hanna, S.R., 1983, “Lateral turbulence intensity and plume meandering during stable conditions,” J. Appl. Meteorol, 22:1424-1430.

Hanna, S.R., J.C. Weil, and R.J. Paine, 1986, Plume Model Development and Evaluation - Hybrid Approach, EPRI Contract No. RP-1616-27, prepared for the Electric Power Research Institute, Palo Alto, CA.

Hanna, S.R., and R.J. Paine, 1989, "Hybrid Plume Dispersion Model (HPDM) development and evaluation," J. Appl. Meteor., 28:206-224.

Hanna, S.R. and J.S. Chang, 1991, “Modification of the Hybrid Plume Dispersion Model (HPDM) for urban conditions and its evaluation using the Indianapolis data set, Volume III: Analysis of urban boundary layer data,” Report for EPRI, Palo Alto, CA, EPRI Project No. RP-02736-1.

Hanna, S.R., and J. C. Chang, 1993, “Hybrid Plume Dispersion Model (HPDM), improvements and testing at three field sites,” Atmos.. Environ., 27A:1491-1508.

Hayes, S.R., and G.E. Moore, 1986, “Air quality model performance: a comparative analysis of 15 model evaluation studies,” Atmos. Environ., 20: 1897--1911.

Hicks, B.B., 1985, “Behavior of turbulent statistics in the convective boundary layer,” J. Climate Appl. Meteor., 24:607-614.

Holtslag, A.A.M., and A.P. Van ulden, 1983, “A simple scheme for daytime estimates for the surface fluxes from routine weather data,” J.Climate Appl. Meteor., 22:517-529.

Huber, A.H., and W.H. Snyder, 1976, “Building Wake Effects on Short Stack Effluents,” Preprint Volume for the Third Symposium on Atmospheric Diffusion and Air Quality, American Meteorological Society, Boston, MA.

Huber, A.H., and W.H. Snyder, 1982, “Wind tunnel investigations of the effects of a rectangular-shaped building on dispersion of effluents from short adjacent stacks,” Atmos. Environ., 176:2837-2848.

Irwin, J. S,, J. O. Paumier, and R. W. Brode, 1988, Meteorological Processor for Regulatory Models (MPRM) User's Guide, EPA-600/3-88-043, U. S. Environmental Protection Agency, Research Triangle Park, North Carolina.

Kaimal, J.C., J.C. Wyngaard, D.A. Heugen, O.R. Cote’, Y. Izumi, S.J. Caughey, and C.J. Readings, 1976, “Turbulence structure in the convective boundary layer,” J. Atmos. Sci., 33, 2152-2169.

Kasten, F. and G. Czeplak, 1980, “Solar and terrestial radiation dependent on the amount and type of cloud.” Solar Energy, 24:177-189.

Lee, R.F., S.G. Perry, A.J. Cimorelli, R.J. Paine, A. Venkatram, J.C. Weil and R.B. Wilson, 1995, “AERMOD - the developmental evaluation,” Preprints of the Twenty-First NATO/CCMS International Technical Meeting on Air Pollution Modeling and Its Application, Baltimore, MD, U.S.A.

Lamb, R.G., 1982, “Diffusion in the convective boundary layer,” Atmospheric Turbulence and Air Pollution Modelling, F.T.M. Nieuwstadt and H. van Dop, Eds., Reidel, 159--229.

Lee, R.F., R.J. Paine , S.G. Perry, A.J. Cimorelli, J.C. Weil, A. Venkatram, and R.B. Wilson, 1998a, “Developmental Evaluation of the AERMOD Dispersion Model”, Tenth Joint AMS/AWMA Conference on Application of Air Pollution Meteorology, January 11-16, 1998, Phoenix, AZ, American Meteorological Society, Boston.

Lee, R.F., R.J. Paine , S.G. Perry, A.J. Cimorelli, J.C. Weil, A. Venkatram, and R.B. Wilson, 1998b, “Developmental Evaluation of the AERMOD Dispersion Model” Draft document (included in peer review package)

Misra, P.K., 1982, "Dispersion of non-buoyant particles inside a convective boundary layer," Atmos. Environ., 16:239-243.

Nieuwstadt, F.T.M., and H. van Dop, 1982, Atmospheric Turbulence and Air Pollution Modelling, Reidel, 358 pp.

Oke, T.R., 1973, “City size and the urban heat island,” Atmos. Environ., 7:769-779.

Oke, T.R., 1978, Boundary Layer Climates, John Wiley and Sons, New York, New York, 372pp.

Oke, T.R., 1982, “The energetic basis of the urban heat island,” J. R. Met. Soc., 108, pp.1-24.

Olesen, H.R., P. Lofstrom, R. Berkowicz, and A.B. Jensen, 1991, “An Improved Dispersion Model for Regulatory Use – the OML Model,” In Proceedings of the 19th International Technical Meeting on Air Pollution Modeling and its Applications, Ierapetra, Crete, Greece. 29 September – 4 October 1991.

Paine, R. J. and B. A. Egan, 1987, User's guide to the Rough Terrain Diffusion Model (RTDM)-Rev. 3.20 ERT Document PD-535-585, ENSR, Acton, MA, 260 pp.

Paine, R.J., and S.B. Kendall, 1993, “Comparison of Observed Profiles of Winds, Temperature, and Turbulence with Theoretical Results,” from Proceedings of an International Specialty Conference on the Role of Meteorology in Managing the Environment in the 90s, pp.395-413.

Panofsky, H.A., J.A.Dutton, 1984, Atmospheric Turbulence: Models and Methods for Engineering Applications, John Wiley and Sons, NY, 417 pp.

Panofsky, H.A., H. Tennekes, D.H. Lenschow, and J.C. Wyngaard, 1977, “The characteristics of turbulent velocity components in the surface layer under convective conditions,” Bound.-Layer Meteor., 11:355-361.

Pasquill, F., F.R. Smith, 1983, Atmospheric Diffusion, third edition, John Wiley & Sons Inc., New York, pp.440.

Perry, S.G., D.J. Burns, L.H. Adams, R.J. Paine, M.G. Dennis, M.T. Mills, D.G. Strimaitis, R.J. Yamartino, E.M. Insley, 1989, User’s Guide to the Complex Terrain Dispersion Model Plus Algorithms for Unstable Situations (CTDMPLUS) Volume 1: Model Description and User

Instructions, EPA/600/8-89/041, U.S. Environmental Protection Agency, Research Triangle Park, NC, 196pp.

Perry, S. G., 1992, "CTDMPLUS: A dispersion model for sources in complex topography. Part I: Technical formulations," J. Appl. Meteor., 31:633-645.

Perry, S.G., A.J. Cimorelli, R.F. Lee, R.J. Paine, A. Venkatram, J.C. Weil, and R.B. Wilson, 1994, "AERMOD: A dispersion model for industrial source applications," in Proceedings 87TH Annual Meeting Air and Waste Management Association, 94-TA23.04, Air and Waste Management Association, Pittsburgh, PA.

PES, 1998, "Performance (Phase II) Evaluation of the AERMOD Dispersion Model (Draft)", U.S. Environmental Protection Agency Report, Pacific Environmental Services under EPA Contract No. 68D70069, Work Assignment No. 01-04.

Reading, C.J., D.A. Haugen, and J.C. Kaimal, 1974, "The 1973 Minnesota atmospheric boundary layer experiment," Weather, 29: 309-312.

Schulman, L.L., J.S. Scire, 1980, Buoyant Line and Point Source (BLP) Dispersion Model User's Guide., Document P-7304B, Envireomental Research and Technology, Inc., Concord, MA.

Sheppard, P. A., 1956, "Airflow over mountains," Quart. J. Roy. Meteor. Soc., 82:528-529.

Smith, M.E., 1984, "Review of the attributes and performances of 10 rural diffusion models," Bull. Amer. Soc., 65, 554-558.

Snyder, W. H., R. S. Thompson, R. E. Eskridge, R. E. Lawson, I. P. Castro, J. T. Lee, J. C. R. Hunt, and Y. Ogawa, 1985, "The structure of the strongly stratified flow over hills: Dividing streamline concept," J. Fluid Mech., 152:249-288.

Sykes, R.I., D.S. Henn, S.F. Parker, and R.S. Gabruk, 1996, "SCIPUFF - A generalized hazard dispersion model," Preprints Ninth Joint Conference on Applications of Air Pollution Meteorology with A&WMA, Amer. Meteor. Soc., Boston, 184--188.

Taylor, G.I., 1921, "Diffusion by continuous movements," Proc. London Math. Soc., Ser.2(20):196-211.

Turner, D.B., T. Chico and J. Catalano, 1986, TUPOS—A Multiple Source Gaussian Dispersion Algorithm Using On-site Turbulence Data, EPA/600/8-86/010. US EPA, Research Triangle Park, NC, 39 pp.

U.S. Environmental Protection Agency, 1992, Protocol for Determining the Best Performing Model[2], EPA-454/R-92-025, U.S. Environmental Protection Agency, Research Triangle Park, NC.

U.S. Environmental Protection Agency, 1995, SCREEN3 User's Guide., EPA-454/B-95-004, U.S. Environmental Protection Agency, Research Triangle Park, NC, (NTIS No. PB 95-222766).

U.S. Environmental Protection Agency, 1995, User's Guide for the Industrial Source Complex (ISC3) Dispersion Models (revised) Volume I - User Instructions EPA-454/b-95-003a, U.S. Environmental Protection Agency, Research Triangle Park, NC.

U.S. Geological Survey, 1994: The 1994 plan for the National Spatial Data Infrastructure - Building the foundation of an information based society. Federal Geographic Data Committee Report, U.S. Geological Survey, Reston VA, Internet World Wide Web HTML ftp://fgdc.er.usgs.gov/gdc/html/fgdc.html

van Ulden, A. P., and A. M. Holtslag, 1983, "The stability of the atmospheric surface layer during nighttime", Sixth Symposium on Turbulence and Diffusion, American Meteorological Society, Boston, 257-260.

van Ulden, A. P., and A. M. Holtslag, 1985, "Estimation of atmospheric boundary layer parameters for diffusion applications," J. Clim. and Appl. Meteor., 24:1196-1207.

Venkatram, A., 1980, "Estimating the Monin-Obukhov length in the stable boundary layer for dispersion calculations," Bound. Layer Meteor., 19:481-485.

Venkatram, A., 1983, "On dispersion in the convective boundary layer," Atmos. Environ., 17:529-533.

Venkatram, A., 1988, "Dispersion in the stable boundary layer," Lectures on Air Pollution Modeling, A. Venkatram and J.C. Wyngaard, Eds., Amer. Meteor. Soc., Boston, pp.229-265.

Venkatram, A., and J.C. Wyngaard, Eds., 1988, Lectures on Air Pollution Modeling, Amer. Meteor. Soc., 390 pp.

Venkatram, A., 1992, “Vertical dispersion of ground-level releases in the surface boundary layer,” Atmos. Environ., 26A:947-949.

Weil, J. C., and R. P. Brower, 1983, Estimating convective boundary layer parameters for diffusion applications, Report No. PPSP-MP-48, Maryland Power Plant Siting Program, Maryland Department of Natural Resources, Baltimore, MD, 45pp.

Weil, J.C. and R.P. Brower, 1984, “An updated gaussian plume model for tall stacks,.” J. Air Poll.. Control Assoc., 34: 818-827.

Weil J.C., 1985, “Updating applied diffusion models,” J. Clim. and App. Meteor., 24(11):1111-1130 .

Weil, J.C., L.A. Corio, and R.P. Brower, 1986,"Dispersion of buoyant plumes in the convective boundary layer," Preprints 5th Joint Conference on Applications of Air Pollution Meteorology, Amer. Meteor. Soc., Boston, 335-338.

Weil, J.C., 1988a, "Dispersion in the convective boundary layer," in Lectures on Air Pollution Modeling, A. Venkatram and J.C. Wyngaard, Eds., Amer. Meteor. Soc., Boston, 167-227.

Weil, J.C., 1988b, "Plume rise" in Lectures on Air Pollution Modeling, A. Venkatram and J.C. Wyngaard, Eds., Amer. Meteor. Soc., Boston, 167-227.

Weil, J.C., 1990, "A diagnosis of the asymmetry in top-down and bottom-up diffusion using a Lagrangian stochastic model," J. Atmos. Sci., 47:501-515.

Weil J.C., 1992, "Updating the ISC model through AERMIC," in Proceedings 85th Annual Meeting of Air and Waste Management Association, 92-100.11, Air and Waste Management Association, Pittsburgh.

Weil, J.C., L.A. Corio, and R.P. Brower, 1997, “A PDF dispersion model for buoyant plumes in the convective boundary layer,” J. Appl. Meteor., 36:982-1003.

Willis, G.E., and J.W. Deardorff, 1981, “A Laboratory study of dispersion in the middle of the convectively mixed layer,” Atmos. Env., 15: 109-117.

Wyngaard, J.C., 1988, Structure of the PBL, in Lectures on Air Pollution Modeling, A. Venkatram, and J.C. Wyngaard, Eds, American Meteorological Society, Boston, MA, pp.402.

Zilitinkevich, S.S., 1972, "On the determination of the height of the ekman boundary layer," Bound. Lay. Meteor., 3:141-145.